

**Experimental Investigation of Polyvinyl Alcohol Degradation
in UV/H₂O₂ Photochemical Reactors Using Different Hydrogen
Peroxide Feeding Strategies**

By

Dina Hamad

**BSc, Cairo University, Egypt, 2001
MSc, Kuwait University, Kuwait, 2008**

A Dissertation

Presented to Ryerson University
in Partial Fulfillment of the Requirements for the Degree of
Doctor of Philosophy
in the Program of Chemical Engineering

Toronto, Ontario, Canada, 2015

© Dina Hamad, 2015

Author's Declaration

I hereby declare that I am the sole author of this dissertation.

I authorize Ryerson University to lend this dissertation to other institutions or individuals for the purpose of scholarly research.

I further authorize Ryerson University to reproduce this dissertation by photocopying or by other means, in total or in part, at the request of other institutions or individuals for the purpose of scholarly research.

I understand that my dissertation may be made electronically available to the public.

Author's Signature

Dina Hamad

Abstract

Experimental Investigation of Polyvinyl Alcohol Degradation in UV/H₂O₂ Photochemical Reactors Using Different Hydrogen Peroxide Feeding Strategies

Dina Hamad

Doctor of Philosophy, Chemical Engineering Department
Ryerson University, Toronto, 2015

Synthetic water-soluble polymers are popular in industry and they are produced in large scale owing to their wide spectrum of applications. In particular, the polyvinyl alcohol polymer (PVA), a well-known refractory pollutant, is abundant in wastewater effluents since it is heavily used in industry as paper coating and polarization layer in liquid crystal displays (LCDs). These polymers are non-biodegradable and contaminant to water resources. Alternatively, they can be effectively removed by advanced oxidation processes (AOPs).

This study investigates the photo-oxidative degradation of aqueous PVA solutions in UV/H₂O₂ photoreactors and the effect of hydrogen peroxide feeding strategies on the photoreactor performance. The research covers thoroughly the impact of operating conditions on the polymer number average molecular weight (Mn), TOC content, and H₂O₂ residual under batch, fed-batch and continuous modes of operation. The experimental results show that the performance of the fed-batch photoreactor was higher than the batch system for similar experimental conditions revealing that the way H₂O₂ is fed into the system has a considerable effect on the PVA degradation.

The experimental result of batch system was used as a guide to develop a photochemical kinetic model of the PVA degradation in UV/H₂O₂ batch process that describes the disintegration

of the polymer chains in which the statistical moment approach was considered. The model predictions are in good agreement with data.

Realizing the limitations of batch and fed-batch UV/H₂O₂ processes, an innovative continuous treatment technique was devised to enhance the process performance and to minimize UV dosage. Response surface methodology (RSM), based on Box-Behnken method, was adopted for design set of experiments required to determine the impact of operating variables and their interaction on the process performance.

Finally, the results show that Mn was reduced from 130 kg/mol to 24.9, 20.3, and 2.2 kg/mol, corresponding to percent TOC removal of 41.5, 64.2 and 94.4 and H₂O₂ residual of 17, 3 and 1% were achieved in batch, fed-batch (120-min), and continuous (30-min) UV/H₂O₂ photoreactors, respectively. In addition, the overall power consumption of the process was assessed to determine the economic incentive for continuous feeding strategy and ensure the possibility of the process scale-up.

Acknowledgment

I would like to express my deepest gratitude to my supervisors, Professor Ramdhane Dhib and Professor Mehrab Mehrvar for their valuable guidance and support throughout the creation of this thesis. I have been given unique opportunities to work on this research area under their expert guidance and mentorship. To each of them, I owe a great debt of gratitude for their patience and inspiration.

My sincere thanks is also extended to Professor Ramin Farnood (Department of Chemical Engineering, University of Toronto), the external member of my Ph.D. thesis committee. I would also like to express my gratitude to my thesis committee members: Professor Ginette Turcotte and Professor Yaser Dahman (Department of Chemical Engineering, Ryerson University), and Professor Russell Viirre (Department of Chemistry and Biology, Ryerson University).

I would like to thank Professor Alexander Penlidis and Professor Neil McManus (University of Waterloo) as well as Professor Daniel Foucher (Department of Chemistry, Ryerson University) for their help. I acknowledge the assistance of the engineering staff, Mr. Ali Hemmati, Mr. Daniel Boothe, and Mr. Tondar Tajrobekar, and also the help of the administration staff in the Department of Chemical Engineering at Ryerson University.

Finally and most importantly, this thesis is dedicated to my loving wonderful husband, Mohamed, my dearest daughters Nour, Mariam, and Mallak, my parents and my brother for their continuous encouragement, patience, and understanding during the realization of this thesis.

Dedication

This thesis is dedicated to:

my beloved husband, Mohamed

my father, Professor Hamad,

my mother, Eng. Ebtesam,

my brother, Dr. Ahmad,

and my daughters, Nour, Mariam, and Mallak.

Table of Contents

ABSTRACT	iii
ACKNOWLEDGMENT	v
LIST OF TABLES.....	xi
LIST OF FIGURES	xiii
NOMENCLATURE	xix
CHAPTER 1: INTRODUCTION	1
CHAPTER 2: LITERATURE REVIEW	7
2.1. WATER-SOLUBLE POLYMERS	7
2.1.1. Principle and Applications	7
2.1.2. Disposal of Water-Soluble Polymers	7
2.1.3. Polyvinyl Alcohol (PVA) as a Model Compound for the Present Study	10
2.1.4. Recent Studies on the Most Popular Water-Soluble Polymers	12
2.1.5. Environmental Fate of Polyvinyl Alcohol Polymer and Its Physical Properties.....	14
2.2. ADVANCED OXIDATION PROCESSES (AOPs).....	17
2.2.1. Principles and Applications	17
2.2.2. General Description of Advanced Oxidation Processes	18
2.3. UV/H ₂ O ₂ PROCESS AND ITS FUNDAMENTAL CONCEPTS	21
2.3.1. Effect of Hydrogen Peroxide Residual.....	24
2.3.2. Photolysis Rate	25
2.4. FREE RADICAL-INDUCED DEGRADATION OF POLYMERS	28
2.4.1. Polymer Molecular Weight Distribution and Polydispersity	30
2.4.2. Polymer Population Balance Technique	31
2.4.3. Recent Studies on the Degradation Water-Soluble Polymers by AOPs	32
2.5. RESEARCH OBJECTIVES	35

CHAPTER 3: MATERIALS AND METHODS	38
3.1. MATERIALS	38
3.2. EXPERIMENTAL SETUP.....	40
3.3. EXPERIMENTAL PROCEDURE FOR BATCH AND FED-BATCH EXPERIMENTS	43
3.4. CONTINUOUS PHOTOREACTOR SETUP	45
3.5. EXPERIMENTAL PROCEDURE FOR CONTINUOUS EXPERIMENTS.....	47
3.6. ANALYTICAL TECHNIQUES	48
3.7. ERROR ANALYSIS.....	54
3.8. EXPERIMENTAL DESIGN AND STATISTICAL METHOD	55
CHAPTER 4: POLYVINYL ALCOHOL DEGRADATION IN BATCH AND FED-BATCH	
 UV/ H₂O₂ PHOTOREACTORS	60
4.1. Introduction.....	60
4.2. Experimental Procedure	61
4.3. Effect of Hydrogen Peroxide Concentration on TOC Removal in the Fed-Batch Photoreactors.....	63
4.4. Effect of Hydrogen Peroxide Feeding Strategies on TOC Removal	67
4.5. PVA Degradation Efficiency	68
4.6. pH Variations during the PVA Degradation Process	75
4.7. Polydispersity Variations and Molecular Weight Distribution	77
4.8. Concluding Remarks	83
CHAPTER 5: PHOTOCHEMICAL KINETIC MODELING OF PVA DEGRADATION IN	
 BATCH RECIRCULATING UV/H₂O₂ PHOTOREACTOR	84
5.1. Introduction.....	84
5.2. Reaction Mechanism of Photodegradation	86
5.3. Kinetic Modeling of PVA Degradation Using Batch Recirculating Photoreactor	90
5.3.1. Photolysis rate and molar balance	90
5.3.2. Polymer breakage population balance.....	94

5.4. Experimental Approach for Model Verification	97
5.5. Selection of Parameter Estimation	97
5.6. Model Validation	99
5.7. Prediction of PVA Molecular Weights Reduction	101
5.8. Predictions of Hydrogen Peroxide Consumption	106
For instant, Figure 5.5 shows the variation of the hydrogen peroxide concentration versus time for both experimental data and model predictions as it indicates a successful model validation. The high coefficient of determination R^2 value of 0.9907 as shown in Figure 5.2a, and low RMSE value of 0.022 confirmed a good agreement between experimental data and model predictions.....	106
5.9. Predictions of the Acidity of the Treated Polymer Solution.....	107
5.10. Concluding Remarks	110

CHAPTER 6: A NOVEL CONTINUOUS PHOTOREACTOR.....112

6.1. Introduction.....	112
6.2. Photoreactor Design and Operation	113
6.3. Experimental Design Using Box-Behnken Design (BBD).....	115
6.4. Response Surface Methodology for Model Development.....	117
6.5. Statistical Data Analysis	121
6.6. Model Predictions for the Individual Effect of Process Parameters	122
6.7. Interactions of Process Parameters	130
6.8. Optimal Operating Conditions and Experimental Validation	134
6.9. Concluding Remarks	135

CHAPTER 7: COMPARATIVE STUDY OF PVA PHOTODEGRADATION IN BATCH, FED-BATCH, AND CONTINUOUS PHOTOREACTORS.....143

7.1. Introduction.....	143
7.2. Experimental Setups and Procedures	144
7.3. Preliminary Experimental Testing.....	145
7.4. H_2O_2 Feeding Strategies for TOC Removal	146

7.5. Variation of PVA molecular weight distribution with hydrogen peroxide feeding strategies	152
7.6. Power Consumption of PVA Degradation by UV/H ₂ O ₂ Process.....	161
7.7. Concluding Remarks	162
CHAPTER 8: CONCLUSIONS AND RECOMMENDATIONS	166
8.1. CONCLUSIONS	166
8.2. RECOMMENDATIONS FOR FUTURE WORK.....	170
REFERENCES	172
LIST OF APPENDICES	184

List of Tables

Table 2.1.	Molecular weight and application of water-soluble polymers.....	9
Table 2.2.	Applications of the most widely used water-soluble polymers.....	10
Table 2.3.	Physical and chemical properties of vinyl alcohol and polyvinyl alcohol.....	15
Table 3.1.	Photoreactor specifications and UV lamp characterizations.....	42
Table 3.2.	Experimental conditions of the batch and fed-batch photoreactor systems.....	44
Table 4.1.	Experimental conditions of the photoreactor system with recirculation.....	62
Table 4.2.	Experimental design for the photochemical PVA (130 kg/mol) degradation in batch and fed-batch photoreactor.....	64
Table 4.3.	Variation of PDI of PVA in fed-batch photoreactor.....	79
Table 5.1.	Photolysis reactions of hydrogen peroxide and the rate constants	87
Table 5.2.	Physical parameters of the UV/H ₂ O ₂ process.....	99
Table 5.3.	New estimates of reaction rate constants for PVA degradation in the UV/H ₂ O ₂ photoreactor.....	99
Table 6.1.	Experimental ranges and coded levels of the independent variables employed in Box-Behnken design	117
Table 6.2.	Three-factor three-level experimental design generated by Box-Behnken design....	118
Table 6.3.	Experimental results of the measured responses of PVA degradation in continuous	120

UV/H ₂ O ₂ process	
Table 6.4. Regression coefficients and probability values of statistical analysis for the prediction of the responses by the continuous UV/H ₂ O ₂ process.....	124
Table 6.5. Randomized experimental runs formulated for RSM model verification for continuous UV/H ₂ O ₂ process.....	124
Table 7.1. Operating condition of the PVA in UV/H ₂ O ₂ photoreactors.....	145
Table 7.2. Technical conditions for the UV/H ₂ O ₂ processes.....	164
Table 7.3. Electric power consumption for the UV/H ₂ O ₂ process.....	164

List of Figures

Figure 2.1.	World consumption of water-soluble polymers.....	8
Figure 3.1.	Schematic diagram of batch and fed-batch recirculating photoreactor system.....	41
Figure 3.2.	Schematic diagram of the continuous UV/H ₂ O ₂ system.....	46
Figure 4.1.	TOC removal versus reaction time in fed-batch photoreactor. [PVA] _o = 500 mg/L; [H ₂ O ₂]/[PVA] mass ratios: 0.1,5,10, and 15.....	66
Figure 4.2.	TOC removal for batch and fed-batch photoreactors. [PVA] _o = 500 mg/L; [H ₂ O ₂]/[PVA] mass ratios: 0.2,1,5,10, and 15.....	69
Figure 4.3.	TOC removal versus reaction time in fed-batch photoreactor. [PVA] _o = 50 mg/L; [H ₂ O ₂]/[PVA] mass ratios: 1, 5 and 10.....	70
Figure 4.4.	TOC removal versus reaction time in batch photoreactor. [PVA] _o = 50 mg/L; [H ₂ O ₂]/[PVA] mass ratios: 1, 5 and 10.....	71
Figure 4.5.	H ₂ O ₂ variation versus reaction time in batch photoreactor, [PVA] _o =50 mg/L; for [H ₂ O ₂ /PVA] mass ratio: 1 and 5.....	72
Figure 4.6.	H ₂ O ₂ variations versus reaction time in fed-batch photoreactor, [PVA] _o = 50 mg/L; [H ₂ O ₂]/[PVA] mass ratio of 5, addition of H ₂ O ₂ every 30 min.....	73
Figure 4.7.	PVA degradation and TOC removal efficiencies versus [H ₂ O ₂]/[PVA] mass ratio in fed-batch photoreactor. [PVA] _o = 500 mg/L.....	74

Figure 4.8. pH variations of PVA solutions versus reaction time. Batch and fed-batch photoreactors, $[H_2O_2]/[PVA]$ mass ratio of 10.....	76
Figure 4.9. Number average molecular weights (M_n) versus UV exposure time in the fed-batch photoreactor, $[PVA]_o=500$ mg/L, $[H_2O_2/PVA]$ mass ratio: 1, 5 and 10.....	80
Figure 4.10. MWD of the untreated PVA, $[PVA]_o=500$ mg/L.....	81
Figure 4.11. Variations of MWD of PVA in the fed-batch photoreactor, $[PVA]_o=500$ mg/L at $[H_2O_2]/[PVA]$ mass ratio of 10.....	82
Figure 5.1. Model verification plots for PVA (a) number and (b) weight averages molecular weights in a batch UV/ H_2O_2 photoreactor, $[PVA]_o=500$ mg/L at H_2O_2/PVA mass ratios of 0.2, 1, and 5.....	103
Figure 5.2. Model verification plots for (a) H_2O_2 residual and (b) solution pH in a batch UV/ H_2O_2 photoreactor, $[PVA]_o=500$ mg/L at $[H_2O_2]/[PVA]$ mass ratios of 0.2, 1, and 5.....	104
Figure 5.3. Variation of the number average molecular weight M_n of PVA in a batch UV/ H_2O_2 photoreactor, $[PVA]_o=500$ mg/L at $[H_2O_2]/[PVA]$ mass ratios of 0.2, 1, and 5.....	105
Figure 5.4. Variation of the weight average molecular weight M_w of PVA in a batch UV/ H_2O_2 photoreactor, $[PVA]_o=500$ mg/L at $[H_2O_2]/[PVA]$ mass ratios of 0.2, 1, and 5.....	105

Figure 5.5. Model prediction versus experimental data for H ₂ O ₂ consumption during the degradation of PVA in a batch UV/H ₂ O ₂ photoreactor, [PVA] _o =500 mg/L at [H ₂ O ₂]/[PVA] mass ratios of 0.2, 1, and 5.....	108
Figure 5.6. Variation of pH during PVA degradation in a batch UV/H ₂ O ₂ photoreactor, [PVA] _o =500 mg/L at [H ₂ O ₂]/[PVA] mass ratios of 0.2, 1, and 5.....	109
Figure 6.1. RSM model verification plots for percent TOC removal response in the continuous UV/H ₂ O ₂ process.....	125
Figure 6.2. RSM model verification plots for PVA molecular weight (kg/mol) response in the continuous UV/H ₂ O ₂ process.....	125
Figure 6.3. RSM model verification plot for percent H ₂ O ₂ residual as an output response in the continuous UV/H ₂ O ₂ process	126
Figure 6.4. Individual effects of operating parameters of the continuous system on the percent of TOC removal.....	129
Figure 6.5. Individual effects of operating parameters of the continuous system on PVA molecular weight (kg/mol).....	129
Figure 6.6. Individual effects of operating parameters of the continuous system on percent of hydrogen peroxide residual.....	131
Figure 6.7. Interaction of operating parameters for PVA degradation by continuous UV/H ₂ O ₂ process and their effects on the TOC removal %.....	132
Figure 6.8. Interaction of operating parameters for PVA degradation by continuous	132

UV/H ₂ O ₂ process and their effects on the polymer molecular weight (kg/mol).....	
Figure 6.9 Interaction of operating parameters for PVA degradation by continuous UV/H ₂ O ₂ process and their effects on the H ₂ O ₂ residual %.....	133
Figure 6.10. Response surface plots of operating parameters for continuous UV/H ₂ O ₂ process, interaction effects of a) PVA and H ₂ O ₂ inlet concentrations (mg/L), b) H ₂ O ₂ inlet concentrations (mg/L) and feed flow rate mL/min, c) PVA inlet concentrations (mg/L) and feed flow rate mL/min, on PVA molecular weight (kg/mol).....	137
Figure 6.11. Response surface plots of operating parameters for continuous UV/H ₂ O ₂ process, interaction effects of a) PVA and H ₂ O ₂ inlet concentrations (mg/L), b) H ₂ O ₂ inlet concentrations (mg/L) and feed flow rate mL/min, c) PVA inlet concentrations (mg/L) and feed flow rate mL/min, on the TOC Removal %.....	139
Figure 6.12. Response surface plots of operating parameters for continuous UV/H ₂ O ₂ process, interaction effects of a) PVA and H ₂ O ₂ inlet concentrations (mg/L), b) H ₂ O ₂ inlet concentrations (mg/L) and feed flow rate (mL/min), c) PVA inlet concentrations (mg/L) and feed flow rate mL/min, on the percent H ₂ O ₂ residual.....	141
Figure 7.1. Comparison of TOC removal in batch and fed-batch (2 h) and continuous (30.6 min. residence time) UV/H ₂ O ₂ photoreactors; [PVA] ₀ =500 mg/L,	147

different $[H_2O_2]$ /[PVA] mass ratios.....	
Figure 7.2. Hydrogen peroxide residual versus reaction time PVA degradation in UV/ H_2O_2 batch and fed-batch photoreactors; $[PVA]_o= 500$ mg/L, $[H_2O_2]/[PVA]$ mass ratio of 1.....	150
Figure 7.3. Hydrogen peroxide residual in each UV/ H_2O_2 photoreactor; batch, fed-batch (2 h), continuous (residence time of 30.6 min); $[PVA]_o=500$ mg/L; $[H_2O_2]/[PVA]$ mass ratio of 1.....	151
Figure 7.4. Variation of number average molecular weights (M_n) of PVA degradation by UV/ H_2O_2 operated at different H_2O_2 feeding strategies, $[PVA]_o= 500$ mg/L, $Mn_o=130$ kg/mol, $[H_2O_2]/[PVA]$ mass ratio of 1, 2 h reaction for batch and fed-batch, 30.6 min residence time for continuous system.....	153
Figure 7.5. The molecular weight distribution of initial untreated PVA polymer sample; $Mn_o=130$ kg/mol, $Mw_o=148$ kg/mol, PDI=1.14.....	155
Figure 7.6. Time evolution of MWD of PVA degradation in a batch reactor; $[PVA]_o=500$ mg/L, exposure time: a) 30 min, b) 60 min, c) 90 min, and d) 120 min.....	156
Figure 7.7. Time evolution of MWD of PVA degradation in a fed-batch reactor; $[PVA]_o=500$ mg/L, $[H_2O_2]/[PVA]$ mass ratio of 1, exposure time: a) 30 min, b) 60 min, c) 90 min, and d) 120 min.....	159
Figure 7.8. Time evolution of MWD of PVA degradation in a continuous reactor; $[PVA]_o=500$ mg/L, $[H_2O_2]/[PVA]$ mass ratio of 0.78 and 1 for plots a-c,	160

and d, respectively at residence time a) 9.2 min, b) 18.4 min, c) 30.6 min.,
and d) 30.6 min.....

Figure 7.9. Operation costs per kilogram of TOC removed in batch and fed-batch (2 h)
and continuous (30.6 min. residence time) UV/H₂O₂ photoreactors;

[PVA]₀=500 mg/L..... 165

Nomenclature

A	Absorbance of light
A'	Optical density, dimensionless
A_{254}	UV absorbance at 254 nm
b	UV path length in the photoreactor, cm
b'	UV path length in the spectrophotometer, cm
b_i	regression coefficients for the linear term
b_{ii}	regression coefficients for the quadratic term
b_{ij}	regression coefficients for the interaction term
b_o	regression coefficient at the intercept
C	Concentration, mol/L
C	Speed of light, m/s
C_f	TOC concentration in the effluent, mg C/L
C_i	TOC concentration in the influent, mg C/L
E_r	Energy rate, \$/kWh
f_i	Fraction of radiation that is absorbed by i
h	Planck's constant, J.s
i	Number of species
I_a	Absorbed light intensity, Einstein/L.s
q_o	Incident light intensity, Einstein/L.s
I_λ	Specific light intensity, Einstein/L.s
J_r	Electricity cost, \$/kg TOC removed
J	Objective function
j	Order of polymer moment
k	Rate constant, L/mol.s, 1/s
k_{d1}	Rate constant of monomer decomposition by primary radical, L/mol. S
k_{d2}	Rate constant of monomer decomposition by secondary radical , L/mol.s
k_p	Rate constant of depropagation reaction, L/mol.s
k_{tc}	Rate constant of termination by coupling, L/mol.s
p_1	Monomer
M_n	Number average molecular weights of the polymer, kg/mol
M_{n_0}	Initial number average molecular weights of the polymer, kg/mol
M_w	Weight average molecular weights of the polymer, kg/mol
M_o	Monomer molecular weight, g/mol
M_{w_0}	Initial weight average molecular weight, kg/mol
n	number of variables
n'	Number of data points
N	Number of compounds
N_{exp}	Number of experiments
P	Power rating of system, W
p_r	Dead polymer of chain length r, $r \geq 1$

p_r^{\bullet}	Live radical of chain length r, $r \geq 1$
p_s	Dead polymer of chain length s, $s \geq 1$
p_r^{\bullet}	Live radical of chain length s, $s \geq 1$
p -value	Probability value
R	Polymer chain length
r_p	Number of replicates at center point
R	Rate of reaction, mol/L.s
R^2	Coefficient of determination
R^2_{adj}	Adjusted regression coefficient
t	time, min, h
V	Reactor volume, L
V'	Volume of treated wastewater, L
x_1	PVA polymer inlet concentration, mg/L
x_2	Hydrogen peroxide inlet concentration, mg/L
x_3	Feed flow rate, mL/min
y	Dependant variable or predicted response
y_1	TOC removal, %
y_2	PVA molecular weight, kg/mol
y_3	Hydrogen peroxide residual, %

Greek Letters

e_{λ}	Local volumetric rate of photon absorption, Einstein/m ² . s
η	Degradation efficiency, %
λ	Wavelength, nm
λ_0	Zero moment of live temporary polymer radical
λ_1	First moment of live temporary polymer radical
λ_2	Second moment of live temporary polymer radical
μ_0	Zeroth moment of dead polymer
μ_1	First moment of dead polymer
μ_2	Second moment of dead polymer
Φ_i	Quantum yield, mol/Einstein
Ω	stoichiometric kernel
ϵ	Molar extinction or molar absorptivity, L/mol.cm

Acronyms

2D	Two dimensional
3D	Three dimensional
ANOVA	Analysis of variance
AOP	Advanced Oxidation Process
ATRP	Atom Transfer Radical Polymerization
BBD	Box-Behnken Design
CCD	Central Composite Design

GPC	Gel Permeation Chromatography
HPLC	High Pressure Liquid Chromatograph
LVREA	Local volumetric rate of energy absorption (Einstein L/s)
MWD	Molecular Weight Distribution
NACL	Number average chain length
NDIR	Non-Dispersive Infra-Red
PAA	Polyacryliacid
PAA _{lmw}	Low molecular weight Polyacrylic acid
PAM	Polyacrylamide
PASP	Polyaspartic Acid
PBEs	Population Balance Equations
PDI	Polydispersity Index
PEG	Polyethylene glycol
PEO	Polyethylene oxide
PMA	Polymethacrylic acid
PVA	Polyvinyl alcohol
PVP	Polyvinyl pyrrolidone
RMSE	root mean square error
QP	Quadratic programming
RSM	Response Surface Methodology
SEC	Size Exclusion Chromatography
TOC	Total Organic Carbon
US	Ultrasound
UV	Ultraviolet
WACL	Weight average chain length

Chapter 1

INTRODUCTION

Water-soluble synthetic polymers are organic substances that can dissolve, disperse, or swell in aqueous medium. They are popular in industry and are manufactured in considerable quantity owing to their versatility in a wide spectrum of applications (Swift, 1997). In fact, water-soluble polymers are usually employed in a variety of interesting commodity and industrial applications; especially in textile industry, water treatment, oil field products, detergent-based industry and cosmetics (Aarthi et al., 2007). Consequently, the growing turnover and consumption of synthetic water-soluble polymers generate a huge amount of wastes during production, use, and disposal. After usage, they likely end up in rivers, lakes, oceans and even in wastewater treatment plants, thus creating a potential pollution hazard. In contrast to biopolymers, water-soluble polymers are resistant to microorganisms-mediated biodegradation (Shonberger et al., 1997; Solaro et al., 2000). One of the concerns is the accumulation of such non-biodegradable water-soluble polymers in the environment. Water-soluble polymers cover a wide range of highly varied families of products and have numerous interesting applications.

Polyvinyl alcohol (PVA), polyethylene glycol (PEG), polyvinyl pyrrolidone (PVP), polyacrylic acid (PAA), polymethacrylic acid (PMA), polyamines, polyacrylamide (PAM), and polyaspartic acid (PASP) are examples of water-soluble polymers made from synthetic raw materials (Swift, 1997; Swift et al., 1998).

Particularly, polyvinyl alcohol (PVA), a well-known refractory pollutant, is one of the most commercially important water-soluble synthetic polymers with an annual world-wide production of 650,000 tons. The PVA polymers are used in industry as paper and textile coatings, and also as packing materials. Its iodine complexes are widely used as polarization layers in liquid crystal displays (LCDs) (Zhang et al., 2011). Because of its suitable mechanical and chemical properties, it can be used as a carrier for enzyme or whole-cell immobilization in biotechnology, for example in ethanol and pharmaceutical productions. Due to its solubility in water, PVA is also utilized as a wrapping material for laundry packaging or fishing lures (Sun et al., 2012). As the production of PVA finds new markets, its consumption grows and the volume of wastewater containing PVA increases during its production and consumption. Besides, PVA is highly soluble in water (up to 100 g/L) and it leaches readily from soil into groundwater creating environmental issues due to increasing the mobilization of heavy metals from sediments of lakes and oceans which results in accumulation of hazardous materials (Ciner et al., 2003; Zhang et al., 2011; Sun et al., 2012). Therefore, the removal of PVA from wastewater systems is essential.

Conventional biological technologies are not efficient to breakdown PVA polymer chains since the degradation capacity of most microorganisms towards PVA is very limited and requires specially adapted bacteria strains (Shonberger et al., 1997). In addition, wastewaters containing PVA can foam formation in biological equipment which inhibits the activity of aerobic microorganisms due to oxygen absence that results in unstable operation with low performance (Zhang and Yu, 2004). Therefore, alternative treatment techniques are considered in order to remove PVA from wastewater systems. For instance, advanced oxidation processes (AOPs) are relatively novel technologies that have been proven to be effective in treating industrial polymeric wastewater.

The AOP technique involves two stages of oxidation reactions; the formation of strong free radicals during the photolysis of hydrogen peroxide or ozone followed by the reaction of these particular radicals with organic contaminants in wastewater. In general, the oxidation of pollutants can occur by either direct or indirect photolysis. In direct photolysis, upon absorption of UV light, organic contaminants of relatively low molecular weights are quickly brought to electronically excited state, thus causing them to react and eventually break up into other chemical compounds. However, in indirect photolysis, pollutants may be degraded by hydroxyl radicals that are produced when an oxidant (ozone or hydrogen peroxide) streams into wastewater either prior to or during UV irradiation. Recent studies on the removal of PVA have focused on processes that are radiation induced oxidation process such as photocatalytic processes (Chen et al., 2011; Zhang et al., 2011), UV/H₂O₂ process (Kazmarek et al., 1998; Zhang and Yu, 2004; Aarthi et al., 2007; Chen et al., 2011), photo-Fenton (Zhang et al., 2011), and radiation-induced electrochemical process (Kim et al., 2003). In photocatalytic processes, a pre-treatment is required to avoid fouling of the active sites and destructive inhibition of the catalyst (Mohajerani et al., 2010). In addition, an eventual rapid loss of photocatalytic activity may require catalytic regeneration process. The main drawbacks of photo-Fenton process are the production of a significant amount of ferric hydroxide sludge that needs further separation and also the necessity of a very low pH environment to keep iron in the solution (Poyatos et al., 2010). Therefore, it is imperative to apply an effective technique to remove PVA contained in wastewater systems. In fact, the UV/H₂O₂ process seems to be the most promising technique to transfer biorefractory organics containing high concentration of PVA into more biologically oxidizable products. Hydrogen peroxide and ultraviolet light are combined in a synergistic effect to degrade organic chemicals in aqueous solutions operating at ambient temperature and

pressure. The effectiveness of the UV/H₂O₂ process strongly depends on several synergistic oxidation mechanisms to breakdown water-soluble polymer chains. The generation of hydroxyl radicals is fundamental to the UV/H₂O₂ process as these hydroxyl radicals are largely responsible for the success of this process (Getoff, 1996). Even though the degradation of a polymer component must be assessed by the reduction and analysis of its molecular weights, there are only few studies in open literature on the devolution of the molecular weight size distributions of water-soluble polymers (Zhang et al., 2004; Hamad et al., 2014). Also, the residual hydrogen peroxide is still a challenging issue in the UV/H₂O₂ process which has been overlooked in some studies. In fact, maintaining optimum concentration of hydrogen peroxide during the photodegradation process is important in order to guarantee an effective degradation of the water-soluble polymers and a significant reduction in the TOC. Nevertheless, high residual of hydrogen peroxide in the effluent affects negatively the post biological treatment due to the risk of hydrogen peroxide toxicity of the microorganisms (Bustillo-LeCompte et al., 2015). Therefore, a post-treatment stage is required for the removal of hydrogen peroxide residuals, which is a costly process, prior to a biological treatment.

Furthermore, there is little information on the photochemical mechanism of the photo-oxidative degradation of PVA polymer solutions in a UV/H₂O₂ process. Recently, several attempts have been made to comprehend the chemical kinetics dominating thermal degradation of water-soluble polymers and assuming constant pH (McCoy and Madras, 1997; Tayal and Khan, 2000; Sonntag, 2003). Besides, no data is available on the distribution of the molecular weights of the polymer being degraded.

The majority of the experimental studies have been carried out in a conventional design which is based on a batch operation for wastewater treatment (Ranby, 1989; Kaczmarek et al. 1998;

Zhang et al. 2004; 2011; Santos et al. 2009). The elimination of PVA from aqueous solutions in batch photoreactors achieves limited success due to the scavenging effect of hydrogen peroxide. The limitation of this process has been overlooked in literature. Exploiting the advantages of studying the effect of hydrogen peroxide feeding strategy is scarce in the open literature. However, according to the literature, the UV/H₂O₂ process has some limitation. The objective of this study is to effectively identify and address the common shortcomings of previous studies, and to account for the effect of operating parameters on the process performance. A comprehensive experimental study for the photo-oxidative degradation of the PVA polymer by UV/H₂O₂ processes in laboratory scale photochemical reactors operated under batch, fed-batch and continuous feeding strategies is carried out. A novel experimental technique that investigates the desirable dosage level of the oxidant to increase the process efficiency is investigated using experimental design and statistical data analysis. A new approach of a photochemical kinetic model describing the degradation of PVA polymer under UV irradiation along with hydrogen peroxide is developed to investigate the change in polymer molecular weights.

Chapter 2 is organized in two sections. The first part is devoted to the background and a thorough literature review of water soluble polymers, advanced oxidation processes, photochemical degradation of polymers, and hydrogen peroxide photolysis. In the second part, the research objective is presented. In Chapter 3, the laboratory-scale experimental setups (batch, fed-batch, and continuous), analytical techniques, experimental procedures, experimental design using response surface methodology are described.

Chapter 4 to 7 discuss in detail the theoretical and experimental investigations carried out on the degradation of the polyvinyl alcohol (PVA) polymer in different UV/ H₂O₂ photoreactors. Chapter 4 is dedicated to studying the effect of hydrogen peroxide feeding strategies in

recirculating batch and fed-batch photoreactors on the PVA molecular weight, TOC removal, pH of the solution and hydrogen peroxide residual. Chapter 5 is devoted to the development of a photochemical kinetic model. It stems from population balance of all chemical species. Taking into account the probabilistic nature of the polymer fragments, the statistical moment approach is considered to model the molar population balance of live and dead polymer chains, which allows estimating the number and weight average molecular weights of PVA as a function of radiation time. The model also considered the impact of hydrogen peroxide concentration on the PVA molecular weight reduction, acidity of the solution, and hydrogen peroxide residual.

Chapter 6 presents an innovative treatment technique with hydrogen peroxide feeding strategies that enhance the process performance, minimize UV dosage and hydrogen peroxide consumption and residual. Response surface methodology employing the Box-Behnken method was employed the design of experiments. Chapter 7 provides a thorough comparative discussion on the performance of each photoreactor (batch, fed-batch, continuous) used for the treatment of aqueous polyvinyl alcohol (PVA) solutions. In addition, the operational cost of PVA degradation by UV/H₂O₂ process per kg TOC removed incorporating UV dosage and hydrogen peroxide consumption was also evaluated. Finally, Chapter 8 presents the major conclusions drawn from this study and provides recommendations for future work.

Chapter 2

LITERATURE REVIEW

2.1. WATER-SOLUBLE POLYMERS

2.1.1. Principle and Applications

Water-soluble polymers, by definition, include soluble polymers and hydrogels that can dissolve, disperse, or swell in aqueous medium. They may be classified in a number of different ways; molecular weight, functional group, structure (linear, branched, or cross-linked), synthetic or natural origin, which often reflect their applications. World consumption of synthetic water-soluble polymers was valued at \$8.2 billion in 2014 based on an average cost of \$2,900/ton (IHS Inc., 2014). The United States, Canada, and China accounted for 73% of the world consumption on a volume basis. Figure 2.1 shows the world consumption of water-soluble polymers (SRI Consulting, 2012). Tables 2.1 and 2.2 show different applications of the most widely used industrial water-soluble polymers of potential environmental concern based on the range of molecular weight and the functional group, respectively (Swift, 1998).

2.1.2. Disposal of Water-Soluble Polymers

There are several pathways for the disposal of water-soluble polymers after their useful life is complete, either into wastewater treatment systems or directly into the aqueous environment.

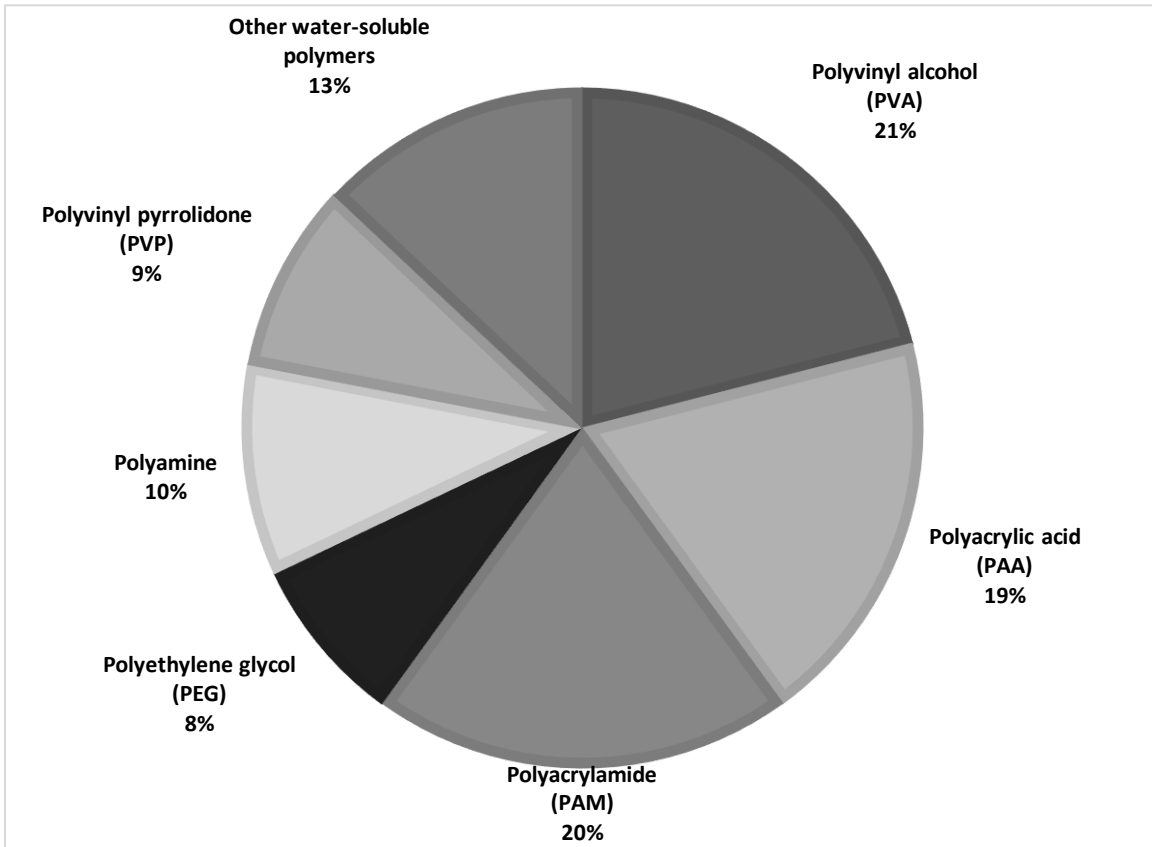


Figure 2.1. World consumption of water-soluble polymers.
(Adapted from SRI Consulting, 2013)

Water-soluble polymers enter the environment in a less obvious manner as they are ultimately dissolved in wastewater after being used as detergents and unlike plastics they cannot be readily recovered for recycle or destruction; hence their degradation is their fate.

It is clear, therefore, from the disposal methods currently adopted, that complete destruction of these polymers would impose a large measure of protection in avoiding potentially widespread environmental contamination with polymers of uncertain fate and effects. A complete degradation (removal of the original polymer from the environment) is advisable to ensure that no toxic or harmful products are produced at any time during the treatment process.

Table 2.1. Molecular weight and application of water-soluble polymers.
(Adapted from Swift, 1997)

Molecular Weight Range	Applications
< 10,000	Detergents, pigment dispersants, emulsifiers, paper additives and polymeric surfactants.
10,000 - 100,000	Rheological modifier and corrosion and scale inhibitor.
100,000 - 1,000,000	Thickeners, flocculants and cosmetics.
> 1,000,000	Superabsorbent, controlled release for fertilizers and gelling agents.

2.1.3. Polyvinyl Alcohol (PVA) as a Model Compound for the Present Study

In the field of water-soluble polymers, PVA is known to be an important class of materials. It represents almost 21% of the total world consumption of synthetic water-soluble polymers due to its use in various industrial applications (IHS Inc., 2014). Polymers with alcohol groups are amongst the most important water-soluble polymers. However, they are non-biodegradable, except for their oligomers, which will possibly produce much damage since they are directly released into the environment. Polyvinyl alcohol (PVA) is the archetype of such polymers.

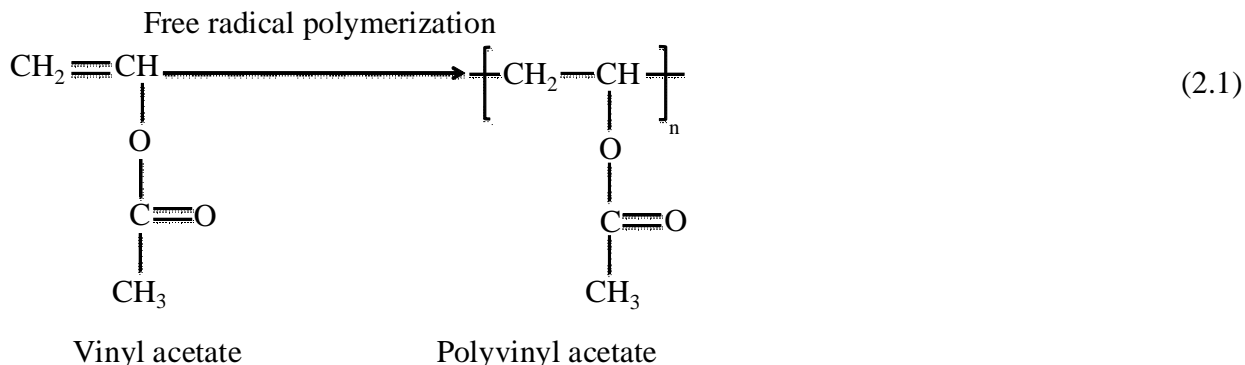
Table 2.2. Applications of the most widely used water-soluble polymers
(Adapted from Swift, 1997)

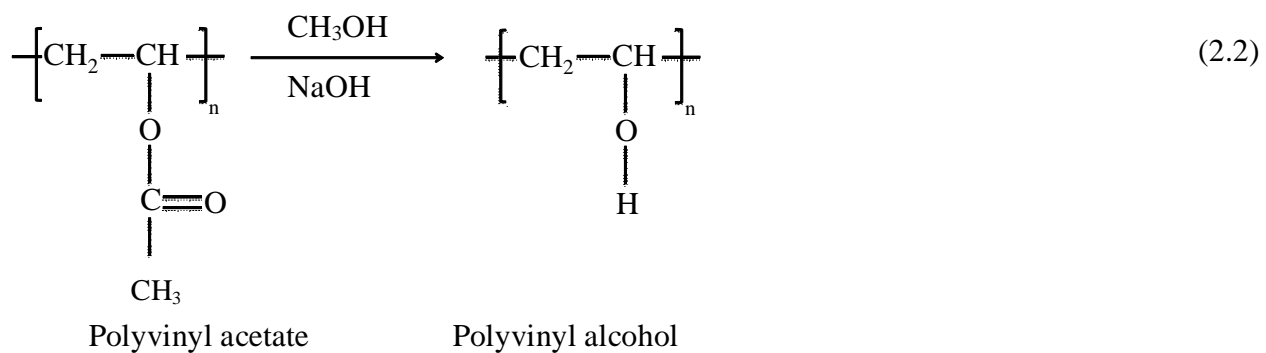
Synthetic Water-Soluble Polymer	Applications
Polyacrylamide (PAM)	Flocculants, adhesive, lubricant, paint and pigment dispersant.
Polyvinylalcohol (PVA)	Detergent, dissolvable laundry packages, paper and textile coatings.
Polyacrylic acid (PAA)	Detergent, thickener, super absorbent.
Polyaspartic acid (PASP)	Detergent, paint, fertilizer, cosmetics, biomedical (drug delivery, artificial skin, dialysis membranes).
Polyethylene glycol (PEG)	Tissue engineering, drug delivery, cosmetic.
Polyethylne oxide (PEO)	Tissue engineering, drug delivery, cosmetic.
Polycarboxylates (PAA-PMA)	Pharmaceutical compound (vaccine).
Gulactomannan (Guar)	Food additives, Rheology modifier.
Polyethyleneimines (PEI)	Detergent, lubricant, binder.
Polyvinylpyrrolidone (PVP)	Pharmaceutical compound (disinfectant), emulsifier, adhesive.

It is used as adhesives, sealants, coating, textiles sizing agent, binder for pigments, ceramics and cements emulsifying agent. Polyvinyl alcohol also offers a combination of excellent film forming and binder characteristics for dissolvable unit packages and hospital laundry.

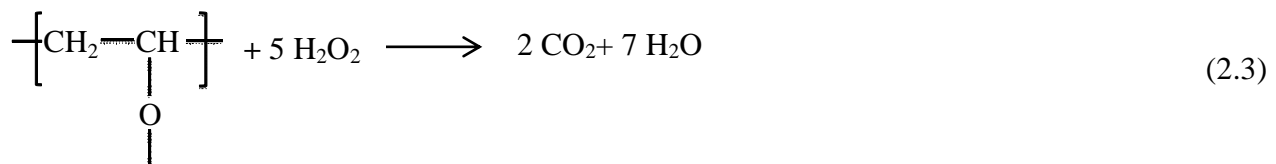
2.1.3.1. Synthesis of commercial viable polyvinyl alcohol

Since vinyl alcohol monomer is not a stable compound, polyvinyl alcohol with an average molecular weight ranged from 80,000-130,000 is synthetically produced from vinyl acetate monomer by free radical polymerization process followed by subsequent hydrolysis. The process of hydrolysis is based on the replacement of ester group in vinyl acetate with the hydroxyl group to produce PVA $[C_2H_4O]_n$ and sodium acetate (CH_3COONa) as a by-product (Odian, 1991; Won et al., 2003).





The stoichiometric molar ratio of H_2O_2 /[VA] required for the total oxidation of PVA-unit ($\text{C}_2\text{H}_4\text{O}$) is 5 according to Equation 2.3. This is actually the maximum amount that would be needed if only H_2O_2 would be involved in the mineralization process.



2.1.4. Recent Studies on the Most Popular Water-Soluble Polymers

Malik (2009) established a mechanism of degradation of PVA as permanganate oxidation followed by hydrolysis. The proposed mechanism is based on the experimental findings. The progress of PVA oxidation was monitored spectrophotometrically by measuring the absorbance of the PVA solution at different time intervals at 525 nm.

In another study, Benard (2010) first synthesized polyacrylic acid (PAA) by atomic transfer radical polymerization (ATRP). Then measured the rate of biodegradation using a

laboratory scale bioreactor and the percentage of remaining PAA versus incubation time was studied. For PAA with initial molecular weight (1.7 kg/mol) and initial concentration of 80 mg/L, the results showed 30% decrease in polymer concentration after 48 h. The synthesis of high molecular weight PAA by traditional free radical polymerization has been extensively studied (Uhniat, 1979; Ng, 1982; Rangaraj, 1997; Fung, 2008). Ito (2005) tested the biodegradability of PAA by treating it with manganese peroxidase (MnP) prepared from the culture of lignin-degrading white rot fungi. No change in the molecular weight of PAA was observed after a 24-h MnP treatment.

Polyvinyloxyacetic acid is demonstrably biodegradable over a wide range of molecular weight by hydrolysis to glyoxylic acid and polyvinyl alcohol. Polyhydroxy-carboxylic acids are prepared from poly chloroacrylic acid by hydrolysis. Maximum 30% biodegradation can be achieved for the low molecular weight versions. These polymers have not been widely accepted as biodegradable. Polyethers are widely used as chemical intermediates and as surfactants in the detergent industry. Hydrophobic polyethers are a combination of low molecular weight hydrocarbon and polyether. As such, they are biodegradable based on the biodegradability of these components. The rates of polyether biodegradation are in the following order: alkyl phenol > polyethylene glycol > polypropylene glycol (Premraj and Mukesh, 2004).

Poly carboxylic acids such as polyacrylic acid (PAA), polymethacrylic acid (PMAA), and polymethyl methacrylate (PMMA) are non-biodegradable to any extent and most of the industrial research attention is focused in this area, particularly for detergents. Polymalic and polyglyoxylic acids have been demonstrated as biodegradable detergent polymers equivalent for polyacrylic acid, however, cost consideration and synthesis difficulties preclude both of them.

Polyaspartic acid (PASP) has proven to be fully biodegradable water-soluble polymer, which is a key factor in determining its usefulness as a polymeric detergent component. PASP has been accepted as technical and functional equivalent for polyacrylic acid, however, it has cost/performance disadvantages. Its performance is poorer than polyacrylic acid in most applications and its cost is slightly higher than polyacrylic acid. Polyaspartic acid, with a molecular weight in the range of 2000 to 5000 g/mol, is a biodegradable water-soluble polymer having several unique characteristics that can be exploited for a range of industrial applications such as detergents and other cleaning products, scale and corrosion inhibitor, green water treatment agent, and as a nutrient absorption intensifier in agriculture. Polyaspartic acid is produced synthetically by thermal condensation step growth polymerization from starting material that may be produced by fermentation of fumaric acid or from purely synthetic materials; ammonia and maleic anhydride (Nita, 2006). Chemical modification of polyacrylic acid (PAA) by benzo-quinone and tetramethyl-hydroquinone has also been studied (Nakamiya, 1997; Moulay, 2005). PAA underwent severe degradation due to sharp decrease in molecular weight. Nakamiya (1997) studied the effect of polymer molecular weight and structure on the degradation time for PAM, PAA, PEG, and PVA polymers. The synthesis of low molecular weight PAA using metal activated redox initiation was studied (Hughes et al., 1986). They succeeded to produce PAA with molecular weight as low as 2500 g/mol which enhance its biodegradability.

2.1.5. Environmental Fate of Polyvinyl Alcohol Polymer and Its Physical Properties

Polyvinyl alcohol is a versatile polymer for providing performance characteristics to hundreds of applications owing to varying degrees of durability, hardness, and glass transition

temperatures which promote consumption in many end-use materials. Polyvinyl alcohol is a white granule or powder at room temperature. Physical and chemical properties of vinyl alcohol and polyvinyl alcohol are given in Table 2.3. Polyvinyl alcohol (PVA) has been the interest of several studies because of its widespread usage in textile and paper industries, which generate considerable amounts of PVA in wastewater streams.

PVA leaches readily into groundwater from soils as a result of its high water solubility. Therefore, it creates environmental issues as it facilitates the mobilization of heavy metals from sediments of lakes and oceans which results in accumulation of hazardous materials (Ciner et al., 2003; Zhang et al., 2011; Sun et al., 2012).

Table 2.3. Physical and chemical properties of vinyl alcohol and polyvinyl alcohol.

Property	Values	References
Vinyl alcohol		
Molecular weight	44.0 g/mol	Brandrup et al., 2005.
Molecular formula	C ₂ H ₄ O	Brandrup et al., 2005.
Polyvinyl alcohol		
Molecular weight	22,000–154,000 g/mole	Odian, 1991.
Molecular formula	(C ₂ H ₄ O) _n	Odian, 1991.
Normal boiling point	228°C	Othmer, 1984.
Normal melting point	150 – 190°C	Weast and Astle, 1985.
Density (at 25 °C)	1.19-1.31 g/mL	Othmer, 1984.
Viscosity (at 25°C), 6 g/L solution	0.9 mPa.s	Modarress et al., 2004.

Water-soluble polymers used in various processes resist conventional chemical and biological wastewater treatment methods. The elimination or destruction of the most toxic or recalcitrant polymers cannot be handled by conventional chemical and biological treatment methods. Water solubility does not necessarily confer biodegradability of synthetic polymers. These polymers are not easily biodegradable because their high molecular weight. The PVA polymer with average molecular weights over 100,000 g/mol, is known to be a non-biodegradable synthetic polymer (Santos et al., 2009; Benard and Darcos, 2010).

The elimination of PVA from aqueous solutions has been investigated using microbial and chemical processes with limiting success. Some microorganisms and symbiotic mixed cultures so far identified are able to degrade only PVA with low molecular weight in the range of 800 - 2000 g/mol (Paik and Swift, 1996; Baumann, 1997; Solaro et al., 2000; Watanabe et al., 2003). The overall number of PVA-degrading microorganisms is rather limited in comparison to the large number of species able to degrade biodegradable polymers. In addition, their presence seems to be restricted to rather peculiar environments, such as PVA-polluted textile or paper mill effluents. Insufficient treatment of PVA-pollutant wastewaters as well as direct release of PVA into the environment may lead to the penetration of PVA into natural aquatic ecosystems. For this reason, other processes such as alternative treatment technologies to other conventional methods are considered. Advanced oxidation processes are considered as promising techniques that have the advantages of complete mineralization of recalcitrant compounds, producing by-products with little hazard to the environment (Oppenländer, 2003; Tabrizi et al., 2004; Edalatmanesh et al., 2008a; 2008b; Cao and Mehrvar, 2011; Mohajerani et al., 2012).

2.2. ADVANCED OXIDATION PROCESSES (AOPs)

2.2.1. Principles and Applications

Advanced oxidation processes are the novel technologies for treating industrial and domestic wastewaters containing organic components such as polymers. AOPs are known as powerful and complete transformation of organic contaminants into harmless end products such as water and carbon dioxide. AOPs are those in which the oxidation of organic contaminants occurs primarily through reactions with hydroxyl radicals. These radicals tend to be highly unstable and, therefore, highly reactive because one of their electrons is unpaired. Oxidation reactions that produce radicals tend to be followed by additional oxidation reactions between the radical oxidants and other reactants until stable oxidation products are formed.

The ability of an oxidant to initiate chemical reactions is measured in terms of its oxidation potential. The most powerful oxidants commonly used in AOPs are hydroxyl radicals, atomic oxygen, hydrogen peroxide, and chlorine with oxidation potentials of 2.85, 2.45, 2.07, 1.77, and 1.49 volt, respectively (Tarr, 2003). The end products of complete oxidation (mineralization) of organic compounds are basically carbon dioxide and water. To summarize, AOPs involve two stages of oxidation as follows:

- 1) The formation of strong oxidants (e.g., hydroxyl radicals)
- 2) The reaction of these oxidants with organic contaminants in water.

One of the most important features in advanced oxidation processes in wastewater treatment is that there is not generation of waste sludge or volatile organic compounds associated with most conventional treatment processes. In addition, they can be applied at ambient pressure

and temperature. Therefore, much research during the past thirty years has been carried out based on the AOPs for water and wastewater treatment. However, the major drawback of AOPs is that the capital and operating costs are usually much higher when compared to conventional biological treatment process. Therefore, AOPs are typically used as a pre-treatment process to enhance the biodegradability of the polymeric wastewater before the biological treatment process (Tabrizi and Mehrvar, 2004).

2.2.2. General Description of Advanced Oxidation Processes

In wastewater treatment applications, AOPs usually refer to a specific subset of processes that involve O_3 , H_2O_2 , TiO_2 catalysis, Fenton's reaction and/or US, UV and E-beam irradiation. All of these processes can produce hydroxyl radicals, which can react with and destroy a wide range of organic contaminants. Although different AOPs have different mechanisms for destroying organic contaminants, in general, the effectiveness of an AOP is proportional to its ability to generate hydroxyl radicals.

Heterogeneous advanced oxidation processes generally use catalysts such as TiO_2 , Al_2O_3 , and ZrO_2 for the degradation of organic compounds. Unlike homogeneous processes, such heterogeneous catalysis has the advantage of separating the products with greater ease. On the other hand, during photocatalysis, some toxic intermediates may form. Moreover, the most common problem in photocatalytic oxidation is the reduction of the process performance of the semiconductor due to the adsorption of pollutants on the photocatalyst surface as well as the deactivation of sites (Mehrvar et al., 2000; Mohajerani et al., 2010). TiO_2 is the most effective catalyst of those used in AOPs. TiO_2 assisted photocatalysis can be performed at higher

wavelengths (300 to 380 nm) than the other UV oxidation processes. When TiO₂, a solid metal oxide catalyst, is irradiated by UV light, valence band electrons are excited to the conduction band and electron vacancies, or holes are created (Crittenden et al., 1996). This combination of excited electrons is capable of initiating a wide range of chemical reactions. Pre-treatment is required to avoid fouling of TiO₂ active sites and destructive inhibition of the TiO₂ catalyst. When TiO₂ is attached to a support substrate (e.g., silica-based material, cobalt [II]-based material), a post-treatment separation system is not needed. In fact, TiO₂ catalyzed UV oxidation is a process recommended for treating waters with low contaminant concentrations (Kavanaugh et al., 2004; Poyatos et al., 2010).

Homogeneous processes such as Fenton process can be carried out either with or without energy. In Fenton process, hydrogen peroxide reacts with iron (II) as a catalyst to form Fenton's reagent, an unstable iron-oxide complex; that subsequently reacts to form hydroxyl radicals (Fenton, 1894). Because of its simplicity and low energy consumption compared to other oxidation technologies that utilize O₃ or UV, Fenton reaction can be effectively applied to remove recalcitrant compounds. But due to production of iron sludge waste, an iron extraction system is needed to remove residual iron from the treated water, which may increase the costs of the system (Poyatos et al., 2010; Zhang, 2011).

In photo-Fenton process (Fe²⁺/UV/H₂O₂), the degradation of the contaminants can be enhanced by introducing UV irradiation into the original Fenton system. Employing UV light reduces the formation of the sludge waste. It is important to emphasize that the pH range of the photo-Fenton process should be between 2.6 and 3 for the best process performance (Aarthi et al., 2007; Poyatos et al., 2010).

The combined O_3/H_2O_2 process has been demonstrated to be more effective at removing natural and synthetic organic contaminant of low concentration than O_3 alone. In addition, using a combination of O_3 and H_2O_2 to produce hydroxyl radicals allows a lower dosage of O_3 to be used. Ozone is unstable in an aqueous medium. It participates in a complex chain of reactions that result in the formation of radicals such as the hydroxyl radical (HO^\bullet) and the superoxide radical (O_2^\bullet). The degradation of the compound occurs through the action of the ozone itself as well as through the radicals (HO^\bullet and O_2^\bullet) generated at alkaline medium. During the use of AOPs that employ ozone, bromate can be formed if bromide is present in the source water. However, in any ozone-based AOPs, specifically O_3/H_2O_2 systems, varying the chemical ratio of O_3 to H_2O_2 is effective at minimizing bromate formation.

On the other hand, conventional ozone or hydrogen peroxide oxidation of organic compounds does not completely oxidize organics to CO_2 and H_2O in most cases. In some reactions, the intermediate oxidation products remaining in the solution may be more toxic than the initial compound. Completion of oxidation reactions, as well as oxidative destruction of compounds can be achieved by supplementing the reaction with ultraviolet radiation or ultrasound energy. The removal efficiency of the combined UV/O_3 process is typically higher than the removal efficiencies of ozone and UV alone. The UV/O_3 process is less energetically efficient than UV/H_2O_2 or H_2O_2/O_3 for generating large quantities of hydroxyl radicals due to the low solubility of O_3 in water compared to that of H_2O_2 . Thus, operational costs of UV/O_3 are expected to be much higher than these comparative processes. Besides, a combined UV/O_3 process may not be cost effective for treating waters with high TOC contents. $UV/O_3/H_2O_2$ process is a combination of two systems, UV/O_3 and UV/H_2O_2 . In spite, the additional cost of using hydrogen peroxide in a UV/O_3 process, it can still accelerate the decomposition of ozone

and increase the generation of hydroxyl radicals according to the following reaction (Kavanaugh et al., 2004; Poyatos et al., 2010).



Furthermore, E-beam treatment as a new technology refers to the use of ionizing radiation from an electron beam source to initiate chemical changes in aqueous contaminants. In contrast to other forms of radiation, such as UV, ionizing radiation from an E-beam is absorbed almost completely by the target compounds. It has minimum potential for inorganic by-product formation (e.g., bromate) compared to other AOPs due to the large number of radicals produced. E-beam systems are energy intensive and may prove to be cost prohibitive and they also are widely used in food and drug industry for disinfection application (Kavanaugh et al., 2004; Poyatos et al., 2010).

Homogeneous Processes using ultrasound (US) energy such as US/O₃, US /H₂O₂, US /O₃/H₂O₂ are also applied extensively in variety of wastewater treatment applications. Ultrasonic irradiation or sonication is a method of producing hydroxyl radicals using cavitation which is described as the formation of microbubbles in solutions that implode violently after reaching a critical resonance size (Shukla et al., 1990; Mohajerani et al., 2010; Poyatos et al., 2010; Koda et al., 2011).

2.3. UV/H₂O₂ PROCESS AND ITS FUNDAMENTAL CONCEPTS

The UV spectrum can be divided according to the wavelength into three bands; UV-A (315 to 400 nm), UV-B (280 to 315 nm), and UV-C (100 to 280 nm). The spectral output generally used in environmental applications and purposes is mostly at 254 nm, to take

advantage of the high energy associated with the shorter wavelength (one mole of photons at 254 nm equals 471 kJ). Many organic contaminants absorb UV energy in the range of 200–400 nm and decompose due to direct photolysis or become excited and more reactive with chemical oxidants.

The hydroxyl radical highest yields are obtained when short-wave UV lights (200–280 nm) are used because of the stronger absorption by hydrogen peroxide at lower wavelengths. UV light is in the high-energy end of the light spectrum with wavelengths less than that of visible light (400 nm) but greater than that of x-rays (100 nm). UV radiation can destroy organic contaminants through direct and indirect photolysis. In direct photolysis, the absorption of UV light by organic contaminants of low molecular weight places it in an electronically excited state, causing it to react with other compounds, and eventually degrade. In contrast, indirect photolysis of pollutants (e.g. polymers) is mediated by hydroxyl radicals that are produced when an oxidant (ozone or hydrogen peroxide) is added.

The most common sources of UV light are low pressure mercury vapor lamps (LP-UV) (monochromatic emission at 254nm operating at 30-60°C), and medium pressure mercury vapor lamps (MP-UV) (polychromatic emission at 200-400nm operating at 500-800°C). Furthermore, while an LP-UV lamp is more electrically efficient than an MP-UV lamp, the latter produces a greater UV output per lamp.

The direct photolysis of hydrogen peroxide leads to the formation of $\cdot HO^\bullet$ radicals. Hydrogen peroxide is photo-reactive over the 185-400 nm wavelength range. The UV absorption of H_2O_2 is wavelength dependent since the absorbance at 220 nm is five times greater than 254 nm.

The effectiveness of the UV/ H_2O_2 process relies on several synergistic oxidation

mechanisms for the degradation of polymers. The oxidation of organics can occur by either direct photolysis or indirect photolysis by reacting with hydroxyl HO^\bullet radicals. The degradation of polymers is primarily due to the oxidation reactions initiated by the highly reactive hydroxyl radicals as shown in the following reactions:



The UV/ H_2O_2 process has been proven to be effective in oxidizing a wide range of organic compounds (Ng, 1982; Tabrizi and Mehrvar, 2004; Mehrvar et al., 2005; Johnson and Mehrvar, 2008; Mohajerani et al., 2009; Santos et al., 2009; Ghafoori et al., 2012; Lu et al., 2012). The parameters affecting UV/ H_2O_2 process are the H_2O_2 dose, the UV lamp, and the UV dose (Kavanaugh et al., 2004). The UV/ H_2O_2 process has several advantages over other oxidizing sources used for polymer degradation. Its advantages are commercial availability, minimal capital investment, thermal stability, and on-site storage, which make it very cost-effective system. Physical properties such as hydrogen peroxide infinite solubility in water, the lack of mass transfer problems associated with gases, and the readiness of the reactions of the HO^\bullet radicals with most organic contaminants, also contribute to make hydrogen peroxide system very useful.

2.3.1. Effect of Hydrogen Peroxide Residual

Hydrogen peroxide is utilized in most advanced oxidation processes which have been applied for the treatment of polymeric wastewater such as UV/H₂O₂ process (Aarthi et al., 2007; Santos et al., 2009; Vinu et al., 2008; Ghafoori et al., 2012; Lu et al., 2012; De Sena et al., 2013), O₃/H₂O₂ process (Suzuki et al., 1978; Poyatos et al., 2010), Fenton process (Zhang, 2011; Lu et al., 2012), photo-Fenton process, (Zhang et al., 2011; Lu et al., 2012; De Sena et al., 2013), US/H₂O₂ process (Koda et al., 1993; Aarthi et al., 2007; Koda et al., 2011), and UV/US/H₂O₂ process (Aarthi et al., 2007), due to its high oxidation potential compared to other oxidizing agents. Increasing the hydrogen peroxide dosage is not a solution as it has two opposing competing effects on the degradation: although it increases the production of hydroxyl radicals, it will also increase the scavenging effect. Increasing hydrogen peroxide dosage, beyond an optimal concentration, results in a decrease in the degradation rate due to the consumption of hydroxyl radicals by hydrogen peroxide which acts as free radical scavenger according to reaction (2.4). In fact, it is known that H₂O₂ can trap hydroxyl radicals (HO^{\bullet}) to form hydroperoxyl radicals (HO_2^{\bullet}) and thus causing the concentration of free HO^{\bullet} radicals to decrease in the solution. Since HO_2^{\bullet} radicals ($E^o = 1.7$ V) are much less reactive than HO^{\bullet} radicals ($E^o = 2.8$ V), the TOC removal decreases (Mehrvar et al., 2001).

The high residual of hydrogen peroxide in the effluent negatively affects the post biological treatment by killing the micro-organisms, therefore additional post-treatment step will be required for the removal of hydrogen peroxide residual remaining in the treated wastewater. Quenching one milligram of hydrogen peroxide residual in one liter of the treated wastewater can be done by adding some reagents (to act as scavengers of H₂O₂ residual) such as sodium

hypochlorite (2.09 mg), sodium thiosulfate (9.29 mg), or sodium sulfite (3.7 mg) according to the following reactions:



High residual concentrations of hydrogen peroxide are inhibitory to the indigenous microorganisms and can also be detrimental to the bioculture, but relatively low concentrations (up to 7.5 mg/L) do not pose a serious problem for microorganisms (Laera et al., 2012). Hydrogen peroxide and the hydroxyl radical are collectively known as reactive oxygen species (ROS). In general, ROS are toxic to cells because of their tendency to cause macromolecule damage. Although H_2O_2 is a mild oxidant, it has to be removed or eliminated before entering the biological treatment step that is usually preceded by a pre-treated UV/ H_2O_2 process because H_2O_2 is readily converted to the highly reactive hydroxyl radical. Therefore, measures have to be taken to prevent the introduction of chemical oxidants into subsequent biological processes (Scott and Ollis, 1995).

2.3.2. Photolysis Rate

Radiant energy is a form of energy emitted and absorbed by particles which exhibits wave-like behavior as it travels through the space. These waves are assumed to stand in a fixed ratio of intensity to each other, oscillate with frequency ν , and propagates at speed of light c . Frequency of radiation ν (1/s) is inversely proportional to light wavelength λ , according to the following equation:

$$\lambda = \frac{c}{\nu} \quad (2.12)$$

A quantum is the amount of energy E of absorbed light, called photons ($h\nu$) and it is given in the following equation:

$$E = h\nu = \frac{hc}{\lambda} \quad (2.13)$$

Where, λ is wavelength (m), c is speed light (m/s), and h is Planck's constant (J.s).

The absorption of the ultraviolet energy activates the chemical species and generates radiolytic reactions. Therefore, photo-oxidative chemical reactions are characterized the interaction of photons of a proper energy level with molecules of the targeted chemical species which produce free reactive radicals. Hence, the absorption of the UV light by hydrogen peroxide is essential in the UV photolysis process for the generation of hydroxyl radicals. The radiation transfer equation can be obtained from the following photon balance:

$$\frac{dI_\lambda}{ds} + k_\lambda I_\lambda = 0 \quad (2.14)$$

With the boundary condition: $I_\lambda = I_o$ at $s=0$.

Where I_λ is the specific monochromatic intensity of the light with a wavelength λ , s is the distance traveled by the radiation ray and k_λ is the absorption coefficient of radiation being absorbed by chemical species at wavelength λ . Since k_λ is a function of the radiation absorbed and chemical species concentration, it can be modeled as $\varepsilon \cdot C$, in which ε is the molar absorptivity and C is the concentration of all chemical species. Taking $k_\lambda = \varepsilon \cdot C$ and integrating Equation (2.14), one obtains:

$$I_\lambda = I_o \exp \left(- \int_0^b \varepsilon \cdot C \, ds \right) \quad (2.15)$$

Where I_o is the incident light intensity emitted at the radiation source, I_λ is the reflected light intensity, and b is the path length of the ray through the medium (Weinstein and Bielski, 1979).

Alternatively, Beer–Lambert law relates the absorption of the light to the properties of the material through which the light is travelling:

$$\frac{I_\lambda}{I_o} = 10^{-A} \quad (2.16)$$

Where the absorbance $A = b \sum_{i=1}^N \varepsilon_i \cdot C_i$ (2.17)

The light absorbance A is a dimensionless parameter that quantifies the total amount of radiant power absorbed by a component i ($i = 1, 2, \dots, N$) and it depends on the effective path length of the ray through the medium b inside the photochemical reactor, the molar absorptivity ε and the species concentration C_i . However, the absorbed light intensity is only a fraction of the difference between incident and reflected light intensities. Therefore, absorbed light intensity I_a is given by:

$$I_a = I_o - I_\lambda \quad (2.18)$$

For chemical component i , the absorbed light intensity is expressed:

$$I_{a_i} = f_i I_o \left(1 - \exp(-2.303 b \sum_{i=1}^N \varepsilon_i \cdot C_i) \right) \quad (2.19)$$

Where C_i is the concentration of chemical species i and f_i is the fraction of the UV irradiation absorbed by species i defined as follows (Jacob and Dranoff, 1966):

$$f_i = \frac{\varepsilon_i \cdot C_i}{\sum_{i=1}^N \varepsilon_i \cdot C_i} \quad (2.20)$$

According to a fundamental law of photochemistry which postulates that only the light absorbed by a molecule can be effective in producing variations in that particular molecule, the quantum yield ϕ_i is defined as follows:

$$\phi_i = \frac{\text{number of moles of pollutants transformed}}{\text{number of photons of wavelength } \lambda \text{ absorbed by pollutant}} \quad (2.21)$$

The irradiation balance must be coupled with other equations of change for the modeling of photoreactors and the local volumetric rate of energy absorption (LVREA) must be estimated. The rate of organic degradation by direct photolysis is proportional to the LVREA. It is also a ratio of the change in concentration of the pollutant with time over the intensity of light absorbed (Koppenol et al., 1978):

$$\phi_i = \frac{-dC_i}{dt} \equiv \frac{R_{UV,i}}{I_{a_i}} \quad (2.22)$$

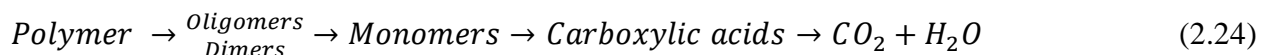
The rate of radiation is proportional to the absorbed energy and the amount of photons that are absorbed per unit time per unit volume. Therefore, the local volumetric rate of absorption (LVRPA) by component i is expressed as (Weinstein and Bielski, 1979):

$$R_{UV,i} = -\phi_i f_i I_o \left(1 - \exp(-2.303 b \sum_{i=1}^N \varepsilon_i \cdot C_i) \right) \quad (2.23)$$

This equation of the radiation rate is fundamental to model the photochemical reactors, as discussed further.

2.4. FREE RADICAL-INDUCED DEGRADATION OF POLYMERS

This study investigates the degradation of PVA polymers in aqueous solution under UV light intensity and in presence of hydrogen peroxide. Polymers such as PVA can break down into shorter monomeric or oligomeric components, as shown below, due to the cleavable chemical bonds.



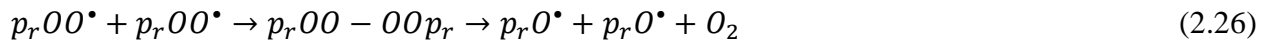
Furthermore, the degradation of polymers mainly occurs by free-radical-induced chain scission. The chain scission reaction is a chemical reaction between the macromolecular compounds (polymers) and end / mid-chain radicals. Chain scission is a bond scission from the backbone of a polymer chain, proceeding either with random or chain-end scission. under UV light, hydrogen peroxide breaks into hydroxyl radicals (HO^\bullet) reacts with the polymer P via H-abstraction giving live polymer radical P_r^\bullet in the presence of oxygen, subsequently the live radical P_r^\bullet converts to peroxy radical P_rOO^\bullet . The mechanism of the photo-oxidative degradation is attributed to the HO^\bullet radicals attacking the α - or β -carbon atom of the polymer, thus, enabling the oxidative scission of the macroradical (Kostoglou 2000). The random chain scission and chain-end scission (release of monomer) mechanisms explain the concept of polymer degradation. Binary fragmentation is also considered to explain kinetics fragmentation in which a polymer of chain length r splits into two polymer units of chain $r-s$ and s such that $1 \leq s < r$. Therefore, the mechanism of degradation polymer solution by means of UV irradiation using hydrogen peroxide as an oxidant results in the generation of polymeric hydroxyl radicals, which undergo degradation reactions. As mentioned above, hydroxyl radicals (HO^\bullet) are generated when hydrogen peroxide is irradiated with UV light. The electron pathway proceeds with the formation of superoxide radicals, which react to form hydrogen peroxide and hydroxyl radicals.

Hydroxyl radicals can react with the polymer which gives off a hydrogen by abstraction at the α or β positions to the hydroxyl group, thus, forming live polymer radicals (Sonntag, 1999).

The polymer radicals p_r^\bullet are the precursor of subsequent polymer chain breakage. In the presence of oxygen, the formation of polymer peroxy radicals p_rOO^\bullet is possible via the reaction of p_r^\bullet with oxygen as stated below:



The polymer peroxy radical may combine with another polymer radical to form a new compound $p_rOO - OOp_r$ which results in the formation of polymer oxy-radical $p_rO \cdot$.



The latter compound, likely unstable, breaks down further by giving off oxygen. The final step in the photo-oxidative degradation is the formation of scission products from the polymer radicals. Termination reactions of peroxy radicals of polymers eventually lead to the chain scission. The scission products are radical and non-radical fragments (monomer or polymer with lower molecular weight).

2.4.1. Polymer Molecular Weight Distribution and Polydispersity

Polymers consist of repeat units (monomers) chemically bonded into long chains. Chain length is often expressed in terms of the molecular weight of the polymer chain, related to the relative molecular mass of the monomers and the number of monomers connected in the chain. Actually, all synthetic polymers are polydisperse since they contain polymer chains of unequal lengths. Hence the molecular weight of a polymer is not a single value; therefore, it is expressed as a distribution of chain lengths. The molecular weight of a polymer can, therefore, be described as some average molecular weight calculated from the molecular weights of all the chains in the sample. The molecular weight distribution (MWD) is the distribution of sizes in a polymer sample while the polydispersity index (PDI) represents the breadth of the distribution curve. Thus, the polydispersity index is used as a measure of the broadness of a molecular weight distribution of a polymer sample.

The larger the polydispersity index, the broader the molecular weight distribution. A monodisperse polymer is a polymer where all the chain lengths almost are equal and usually used as a standard. The PDI is also the ratio of weight average molecular weight (M_w) to the number average molecular weights (M_n). Polymer molecules, even those of the same type, come in different sizes, so the average molecular weight depends on the method of averaging. The number average molecular weight is the ordinary arithmetic average of the molecular weights of the polymer. The weight average molecular weight M_w is determined by measuring the weight of each species in the sample, rather than the number of molecules of each size.

2.4.2. Polymer Population Balance Technique

Under UV radiation, polymer chains are broken down into oligomers (short-chain polymers), dimers and monomers. Enhanced photo-degradation of polymer can lead to a wider distribution of molecular weights, indicating that the degraded polymer becomes less and less uniform. This behavior is expected for degraded polymers, as irradiation promotes an increase in the number of polymer chains, lowering the molecular weight, and consequently increasing the polydispersity. Hence, polymer degradation is a fragmentation process in which population balance concepts is often applied in fragmentation models to describe how the distributions of different size entities evolve over the time of reaction.

The degradation of high molecular weight polydisperse materials results in the formation of large number of polymeric chains with different chain lengths and various chemical compositions, i.e., the number of branches. Population balance based models have been developed to study molecular weight decrease of polymers in a fragmentation process (Madras et

al., 1995; Wang et al., 1995; Kodera and McCoy, 1997; McCoy and Madras, 1997; Sezgi et al., 1998). Population balance approach is generally employed to model the size distribution of the macromolecular compound during polymerization, depolymerization, and chain breakage. The population balance model is a balance equation of species of different sizes and it is similar to the mass, energy, and momentum balances, to track the changes in the size distribution. Earlier, Randolph and Larson (1971) proposed a solution for the population balance equation (PBE) in a well-mixed batch system. They used the concept of moment transform to convert the population balance equations into ordinary differential equations.

Most mathematical methods of polymer degradation, however, have considered only average properties of the polymer chain-length distribution or molecular-weight distribution (MWD). The advantage of the population models is that they provide a straightforward procedure to derive expressions for the moments of the polymer distributions during the degradation reaction.

2.4.3. Recent Studies on the Degradation Water-Soluble Polymers by AOPs

Few studies have been reported in open literature on the degradation of water-soluble polymer by AOPs. These processes are particularly useful in treating waste streams contaminated with compounds that are very difficult to oxidize. For instance, Kang et al., 2000 conducted an experimental study in which a PVA solution of 100 mg/L was treated by photo-Fenton process and showed an optimum pH ranging from 3-5 for PVA removal. Also, a photocatalytic degradation of 30 mg/L aqueous PVA solutions was carried out by Chen et al. (2001) who showed that 55% TOC removal was achieved in 1 hour of reaction. In another

attempt, Zhang et al. (2011) investigated the degradation of PVA by a photocatalytic-Fenton process and obtained 94% decrease in the PVA original molecular weight. However, AOPs have limitations in practical applications. For instance, the UV/O₃ process has a relatively high operational and capital (Poyatos et al., 2010). In photocatalytic processes, a pre-treatment is required to avoid fouling of the active sites and destructive inhibition of the catalyst (Mohajerani et al., 2010). In addition, an eventual rapid loss of photocatalytic activity may require catalytic regeneration process. The main drawbacks of Fenton process are the production of a significant amount of ferric hydroxide sludge that needs further separation of sludge from wastewater and also a very low pH environment which is necessary to keep the iron in the solution (Poyatos et al., 2010). Therefore, it is imperative to apply another more effective technique to remove PVA in wastewater. In fact, the UV/H₂O₂ process seems to be the most promising technique to transfer biorefractory organics containing high concentration of PVA into more biologically oxidizable products.

The UV/H₂O₂ process has been successfully applied for the degradation of water-soluble polymers (Santos et al., 2009; De Sena et al., 2013). The UV/H₂O₂ process ranges from medium to high level of reliability, flexibility, adaptability, energy efficiency, ease of implementation, and potential for modification. The effectiveness of the UV/H₂O₂ process depends strongly on several synergistic oxidation mechanisms to breakdown water-soluble polymer chains. Previous studies have successfully demonstrated the benefit of employing the UV/H₂O₂ process to reduce the harmful effect of PVA polymers in wastewater (Santos et al., 2009; Ghafoori et al., 2012). Therefore, the UV/H₂O₂ process has been selected, as a treatment method of PVA aqueous solution in this study. The UV/H₂O₂ process is applied for the treatment of polymeric wastewater since it shows a good efficiency and facility in operation. The major

advantages of this process are as follows: (a) high rates of pollutant oxidation (most organic contaminants are eventually completely mineralized to harmless chemicals, such as carbon dioxide and water); (b) large range of applicability regardless of water quality and (c) convenient dimensions of the equipment. Some concerns, such as high operating costs (in some cases) and special safety requirements due to the use of very reactive chemicals (hydrogen peroxide) and high-energy sources (UV lamps) must be assessed. Nevertheless, these concerns can be dealt with by properly designing reliable UV/H₂O₂ industrial process.

2.5. RESEARCH OBJECTIVES

The H₂O₂ residuals are found to be toxic to microorganisms. This challenging issue in the UV/H₂O₂ process still has been not been tackled to the required extent. Therefore, there is a need to determine the amount H₂O₂ to maximize the removal and minimize the H₂O₂ residuals.

According to the literature review, the main findings and conclusions of past studies on the degradation of PVA are as follows:

- Most of the past investigations discussed thermal degradation of polymers with maximum of 50% weight loss after approximately 5 h at elevated temperatures (260-300°C). Nevertheless, it is important to highlight that studies on the photodegradation of PVA by AOPs are quite limited.
- The majority of experimental investigations on the treatment of polymeric wastewater by AOP have been realized in batch reactor processes. The limitation of the batch photo reactor process is mainly due to the scavenging effect of hydrogen peroxide.
- Even though the degradation of a polymer component must be assessed by the characterization of its molecular weight distribution, there are hardly no experimental data of molecular weights of the degraded PVA polymer
- Besides, monitoring the amount of hydrogen peroxide is crucial for maintaining consistent quality of the treated wastewater.
- Furthermore, the information on the mechanism of photo oxidative degradation of PVA polymers as macromolecule compounds by the UV/H₂O₂ process in literature is insufficient and need to be explored further for a better understanding and characterization of the UV/H₂O₂ process.

Objectives of this study:

- To perform an experimental study in batch and fed-batch photoreactors by varying the most influential parameters affecting the photo-oxidative degradation of PVA polymer in order to determine the feasibility and limitations of the existing UV/H₂O₂ photoreactor when operated in batch and fed-batch modes.
- To explore experimentally the procedure of multiple feeding strategies of H₂O₂ into the photoreactor processes.
- To use the batch experimental data as a guide to develop a photochemical kinetic mechanism and model for a better understanding of the cracking of the PVA macromolecules by UV/H₂O₂ process. The model should in principles be a tool to elucidate the scavenging effect of hydrogen peroxide, describe the solution pH variations and evolution of the polymer molecular weights distribution. Data from the batch to be employed to update the reaction rate constants and validate the photochemical kinetic model.
- To design and test an efficient continuous UV/H₂O₂ photoreactor which main purpose is to enhance the PVA photodegradation and overcome the limitations of the UV/H₂O₂ process when operated in batch mode
- To investigate the effectiveness of the continuous photoreactors in series using response surface methodology (Box-Behnken Design) combined with quadratic programming for experimental design, statistical analysis and determination of optimal process operation conditions.

- To assess and compare the performance of batch, fed-batch, and continuous photoreactors for different hydrogen peroxide feeding strategies and investigate their impact on the polymer molecular weight distribution, TOC content of the polymer being degraded and residual hydrogen peroxide.

Chapter 3

MATERIALS AND METHODS

In this chapter, materials and methods used in this study are explained in details. The experimental setup for the batch and fed-batch photoreactor, the continuous photoreactor, the feeding strategies, and the analytical techniques are also explained. Two experimental set ups are utilized in this study. They are shown in Figures 3.1 and 3.2.

3.1. MATERIALS

The following materials were used in this study.

3.1.1. Reaction Reagents

The photodegradation reaction mixture consists of three components:

PVA

Commercial-grade polyvinyl alcohol (PVA) (an odorless and tasteless, translucent, white granular powder) having a number average molecular weight of 130 kg/mol, and a weight average molecular weight of 148 kg/mol, polydispersity index (PDI) of 1.14 was purchased from Sigma-Aldrich (Oakville, Ontario). PVA (hydrolysis degree (% OH group) of 99+ %) was stored in tightly closed plastic container in a cool well-ventilated area. The PVA polymer was used as received.

Water

Distilled water was used for all experimental runs.

Hydrogen Peroxide

Hydrogen peroxide used in all of the experiments was purchased from Aldrich. It was 30% (wt) with molecular weight of 34.04 g/mol, and density of 1.11 g/cm³. It was stored in opaque glass bottle at 2 - 8°C to retain its quality.

3.1.2. Reagents for Hydrogen Peroxide Analysis

DMP (2,9-dimethyl-1,10-phenanthroline) ((CH₃)₂C₁₂H₆N₂) reagent (98+%) was purchased from Alfa Aesar. Ethanol (98%) and copper (II) sulphate pentahydrate (99.3%) were purchased from Fisher Scientific Chemicals. Potassium phosphate dibasic (K₂HPO₄) (ACS grade) and sodium phosphate monobasic (99+ %) (NaH₂PO₄) were purchased from EMD Chemicals.

3.1.3. Reagents for TOC Analysis and Calibration

KHP (potassium hydrogen phthalate) (KC₈H₅O₄) is used as a standard for total organic carbon (TOC) calibration as recommended by the TOC analyzer supplier company. Sodium persulfate (Na₂S₂O₈) supplied by Sigma Aldrich and phosphoric acid solution (H₃PO₄) supplied by VWR (Mississauga, Ontario) were used as eluents for TOC analysis.

3.1.4. Reagents for Gel Permeation Chromatograph Analysis (GPC) and Calibration

Sodium nitrate (NaNO₃) (0.2 M), monosodium phosphate (NaH₂PO₄), and disodium phosphate (Na₂HPO₄) were used as an eluent which is a carrier portion of the mobile phase that moves the sample through the chromatograph for GPC analysis. They were purchased from Sigma Aldrich (Oakville, Ontario).

3.2. EXPERIMENTAL SETUP

The schematic diagram of the experimental setup is shown in Figure 3.1. An annular steel photoreactor is connected to a holding tank. The photoreactor is equipped with an internal quartz glass in which placed a 14-W low pressure mercury lamp is placed. A quartz sleeve envelops the lamps from fouling formation that may negatively affects the UV radiation emission. The whole system equipped with a heat exchanger to keep the temperature constant at $25 \pm 2^\circ\text{C}$ during the experiment. The reactor is continuously cooled down by the circulating cold water. The holding tank is provided with a thermometer and holes made at the top of the tank for feeding the reactants and a probe to take samples. The circulation rate of the feed of the polymer solution was adjustable using an acrylic in-line flow meter (model R-32477-00, Cole-Parmer) with a flow-rate range between 0.1 and 1 L/min and a centrifugal pump with a maximum capacity of 17.4 L/min and maximum head of 12 m (Model RK-72012-10, Cole-Parmer). The water solution circulates around at a rate of 1 L/min. The volume of polymer solution feed in the tank for operation was 2 L. The photoreactor specifications and UV lamp characterizations are given in Table 3.1. To investigate the effect of hydrogen peroxide feeding strategies on the performance of the UV/H₂O₂ process, a conventional photoreactor was used. In addition, a kinetic study was carried out in a batch reactor, which is a recirculating annular laboratory scale batch photoreactor. A first set of experimental runs have been performed in order to investigate the effect hydrogen peroxide injection strategy on the degradation of aqueous PVA solutions. A second set of experimental runs was done to validate the developed kinetic model for the PVA degradation by UV/H₂O₂ process.

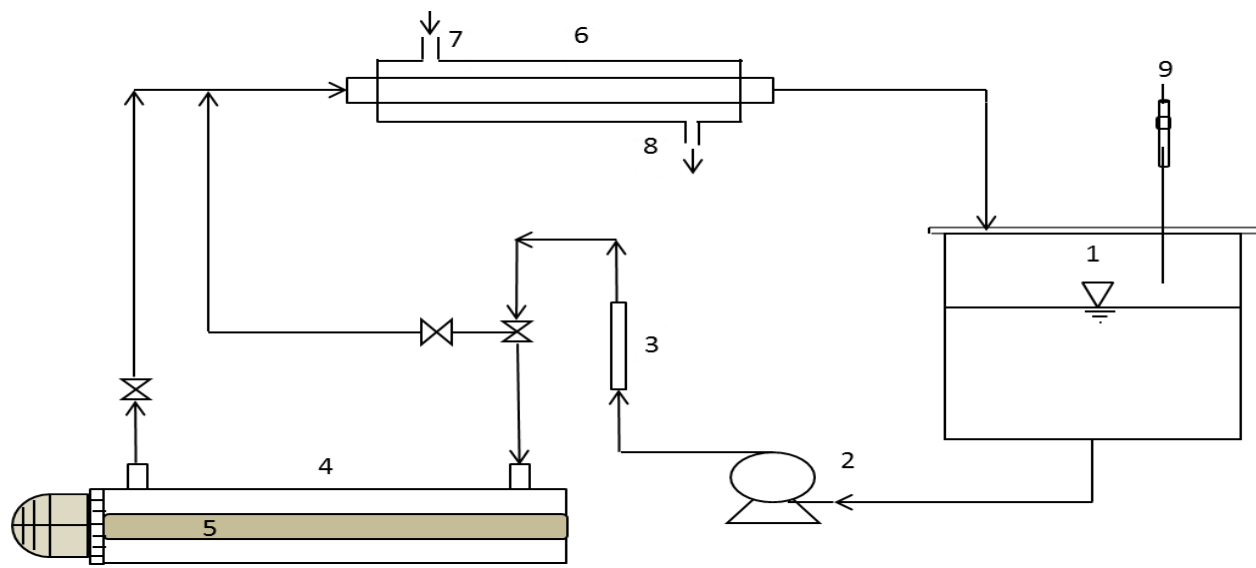


Figure 3.1. Schematic diagram of batch and fed-batch recirculating photoreactor system.

1. Holding tank
2. Centrifugal pump
3. Flow meter
4. Annular metal photoreactor
5. UV-C lamp
6. Heat exchanger
7. Cooling water inlet
8. Cooling water outlet
9. Syringe for H_2O_2 injection.

Table 3.1. Photoreactor specifications and UV lamp characterizations.

UV Reactor Specifications	
Geometry	Cylindrical with annular shape
Installation direction	Horizontal
Model	SL-LAB 2 (Siemens Inc.)
Material	304 SST
Dimensions	
Chamber length	30.5 cm
Inner diameter	5.11 cm
Thickness	3.18 mm
Effective volume	0.46 L
Quartz sleeve	
Inner diameter	2.62 cm
Thickness	1.0 mm
UV Lamp Specifications	
Type	Germicidal
Model	Siemens LP4130
Wavelength	254 nm
Input power	14 W
Output power	3.6 W
Diameter	2 cm
Length	28.5 cm

3.3. EXPERIMENTAL PROCEDURE FOR BATCH AND FED-BATCH EXPERIMENTS

First, the experimental procedure involved the preparation of the aqueous solution of PVA with the required concentrations. For all experimental tests, a stock of PVA solution was prepared by gradually dissolving a 10 g of solid commercial-grade PVA in 1 liter-beaker of distilled water using magnetic stirring, at about 50°C in order to prevent foam formation. The concentrated solution was diluted in distilled water in order to obtain the specified PVA concentration. Distilled water was used for all stock solution preparations. Prior to each experimental run, the photoreactor was cleaned by circulating through distilled water. Also, after each run, distilled water was recirculated through the photoreactor for about 30 min.

Before operating the recirculating mixture, the UV lamp was switched on for 30 min to ensure that the lamp has reached its operating temperature and efficiency for maximum UV output. After feeding the solution into the holding tank, the centrifugal pump for circulation was started. Then, H₂O₂ feeding (0.3- 14 mL) and time measurements were started, with collection of the first sample. Subsequent hydrogen peroxide amounts were added afterwards as required for the fed-batch photoreactor operations.

Hence, for the experimental runs discussed in Sections 4.1, 4.2, and 4.4, a specific quantity of the hydrogen peroxide was introduced into the process by either the pour method (batch system) or the drip method (fed-batch system). For the batch system, a predetermined amount of hydrogen peroxide was added to an aqueous polymer solution prior to the UV reactor. The hydrogen peroxide and the polymer solution were thoroughly mixed in the holding tank. The mixture was pumped through the photoreactor and irradiated under UV light. For the fed-batch

system, drip method was used where a predetermined amount of hydrogen peroxide was delivered evenly into the holding tank in a stepwise manner. In both experimental procedures, the entire hydrogen peroxide charge was introduced directly into the holding tank containing recirculating polymer solution and then the solution was allowed to pass through the UV irradiation field. The objective of the drip experiments was to deliver a specified amount of H₂O₂ evenly over irradiation time period. At the end of each experiment, hydrogen peroxide feeding was stopped 30 min before the end of the reaction. Thus, during the last 30 min in each experiment, the H₂O₂ concentration was allowed to decrease gradually. The operating conditions are summarized in Table 3.2.

Table 3.2. Experimental conditions of the batch and fed-batch photoreactor systems.

Parameter	Value
Holding tank volume	2 L
Reaction volume	0.46 L
Reaction time	120 min
Solution temperature	25 °C
Operating pressure	1 atm
Circulation flow rate	100, 1000 mL/min
PVA initial concentration	50 mg/L, 500 mg/L
[H ₂ O ₂]/[PVA] mass ratio	0, 0.2, 0.78, 1, 5, 10, 15

3.4. CONTINUOUS PHOTOREACTOR SETUP

As the research in the relatively new area of feeding strategies is progressing, there have been issues in conventional batch photoreactor. Although, the degradation of various organic pollutants by UV/H₂O₂ process in batch reactor has been extensively studied, the feeding strategies remain issue and still need to be addressed. The results obtained from the degradation of PVA using the previous setup (Figure 3.1) and that are discussed in Chapter 4 have demonstrated that the feeding strategies of hydrogen peroxide have a considerable impact on the performance of a UV photoreactor operated in batch and fed-batch manner to degrade PVA polymer in aqueous solutions. The experimental results concluded that the photoreactor must be operated in stepwise (fed-batch) manner. Hence, the degradation of PVA by UV/H₂O₂ process requires a continuous or stepwise operation for a better degradation of the polymer chains with noticeable reduction in the consumption and residual of hydrogen peroxide. However, there is little information available in the open literature on PVA degradation in continuous photochemical reactors. Consequently, the degradation of PVA in continuous photochemical reactors was examined. Degradation results in the new continuous photoreactor are discussed in chapters 6 and 7. The experimental setup consists of two photoreactors in series. The way of introducing hydrogen peroxide into the system was modified by some changes to the piping system. Necessary peristaltic pumps were utilized for this purpose. A multi-channel peristaltic pump (model FH100M, Thermo Scientific) delivering flow rates from 0.001 up to 60 mL/min of hydrogen peroxide was utilized in the new experimental setup. An acrylic in-line flow meter (model FR2000, VWR), with a flow rate range of 20-250 mL/min, was used to measure the feed flow rate.

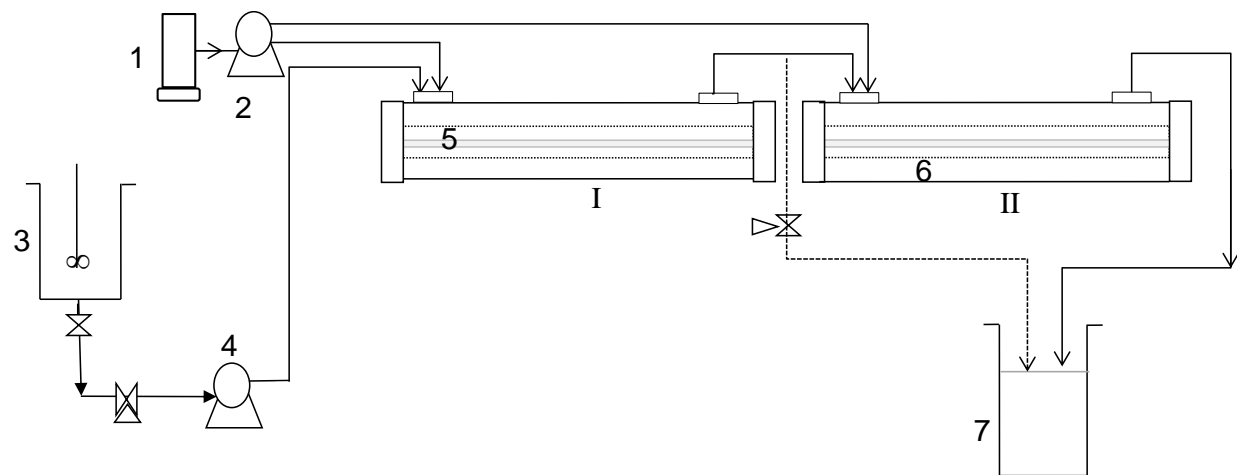


Figure 3.2. Schematic diagram of the continuous UV/H₂O₂ system.
 I,II Photoreactors, 1. H₂O₂ storage 2. Multichannel peristaltic pumps 3. Feed tank 4. Feed peristaltic pump 5. UV lamp 6. Reaction zone 7. Effluent tank.

The photoreactor system is also equipped with a second peristaltic pump (model A-100N FLEXFLO, Blue-White) with maximum flow capacity of 600 mL/min to pump the wastewater solution from the feed tank into and through the photoreactor.

3.5. EXPERIMENTAL PROCEDURE FOR CONTINUOUS EXPERIMENTS

In this section, the photoreactor operation under the continuous feeding strategies is explained. The feed of polymer solution was introduced to the photochemical processes according to the volumetric flow ranged from 30 to 100 mL/min providing the system with a hydraulic residence time of 9.2- 30.4 min. The photoreactor was operated at room temperature (25°C). Reactants (polymer solution and hydrogen peroxide) were continuously fed into the reactor system at a flow rate controlled by means of peristaltic pumps. A constant volumetric flow rate of fresh hydrogen peroxide was fed into a separate stream by a multichannel peristaltic pump (model FH100M, Thermo Scientific) delivering flow rate ranges from 0.001 to 60 mL/min under UV irradiation zone inside the photoreactor as shown in the experimental set up (Figure 3.2). This feeding strategy will ensure the consistency of the hydrogen peroxide dosage throughout the degradation process and maximize the benefit of hydrogen peroxide photolysis which results in high PVA degradation and TOC removals, as discussed in Chapters 6 and 7.

The experimental procedure includes preparing a stock solution using solid PVA as previously described in Section 3.3, then delivering the solution with a known PVA concentration into the photoreactor by the peristaltic pump (model A-100N FLEXFLO, Blue-White) with a flow capacity of 600 mL/min and simultaneously introducing the required amount

of hydrogen peroxide into the inlet of each photoreactor. Basically, hydrogen peroxide stream was merged into the untreated polymer solution immediately before the exposure to UV irradiation zone. After a specified residence time, samples of the treated solution were withdrawn from the effluent tank, and then analyzed for TOC content, hydrogen peroxide residuals, and characterization of the PVA molecular weight distributions.

3.6. ANALYTICAL TECHNIQUES

3.6.1. Polymer Molecular Weight Characterization

The samples of the treated PVA polymer were taken at various times and analyzed by gel permeation chromatography (GPC) for the characterization of the polymer molecular weights. A sample of untreated PVA polymer was analyzed before each run. All analyses were performed by Agilent GPC (model PL-GPC 50) at the Department of Chemical Engineering, University of Waterloo. A solution of 0.1 N NaNO₃ in double distilled water was used as eluent. The eluent (mobile phase) must be a good solvent for the polymer. It should permit high detector response from the polymer, and wet the packing surface. The eluent was pumped at a flow rate of 1mL/min using an isocratic pump (Waters 515 HPLC pump). The column used was Waters Ultra hydrogel Linear SEC column (7.8 mm × 300 mm). Aliquot of 500 µL were injected in a Rheodyne injector. The refractive index of the sample was measured continuously with a Waters 401 differential refractometer. Molecular weights (MW) of the samples were determined using a polyvinyl alcohol calibration standard. The GPC works on the principle of size exclusion, therefore, when a polymer solution is passed through a column of porous particles, large

molecules cannot enter the pores of the packing and hence, they elute first. But, smaller molecules that can penetrate or diffuse into the pores are retained for a while in the column and then elute at a later time. Thus, a sample is fractionated by molecular hydrodynamic volume and the resulting profile describes the molecular weight distribution. A concentration detector (e.g., differential refractometer (RI) or UV detector) is placed downstream of the columns to measure the concentration of each fraction as a function of time. The actual method for determining the molecular weight averages and the MWD depends upon the attached detectors.

3.6.2. TOC Analysis

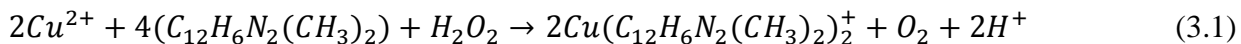
Total organic carbon (TOC) is the amount of carbon in the degraded polymer sample that was measured by Teledyne Tekmar Apollo 9000 Combustion TOC Analyzer. The extent of PVA solution degradation reaction to CO₂ was monitored by measuring the TOC of the samples. TOC analyzer is based on the oxidation of organic compounds to carbon dioxide and water, with subsequent quantities of the carbon dioxide. The TOC analyzer subtracts the inorganic carbon (CO and CO₂) and reports the total organic carbon, which is a close approximation of organic content. The analytical range of TOC measurement is between 0.04-25,000 mg carbon/L. A 15 mL-sample is filled in a sampling vial and placed in the auto sampler. The TOC standard calibration analysis was carried out using the working standard solutions. A 50 µL of the sample is injected into the furnace for oxidation by combustion at temperature of 680-1000°C. The oxidation step carried out at high temperatures to achieve complete oxidation of carbon compounds. The carbon dioxide generated by oxidation of the organic carbon in the sample is directly and specifically measured by the Non-Dispersive Infra-Red (NDIR) detector which is sensitive for low levels of carbon dioxide. The TOC analyzer was equipped with an automatic

sampler. A computer attached to the analyzer integrated the results using TOC Talk, the Apollo 9000 software package supplied by Tekmar Company. The eluent was prepared from 1.5 M sodium persulfate solution and 1.0 M phosphoric acid solution. TOC analyzer was calibrated to ensure consistent response over time and verify the efficiency of the process. The TOC calibration curve for the range of 1-1000 mg carbon/L was obtained for analyzing TOC concentrations. Measurement of each sample was repeated in triplicate and an average value was reported as the TOC reading. A response factor of the instrument correlates the raw counts to a known amount of organic carbon in the standard. The calibration of the TOC was done on 3 months basis. The TOC standards employed for TOC calibration was KPH. The TOC standard calibration analysis was carried out using the working standard solutions (10, 25, 50, 100, 250, 500, 750, 1000 ppm). The calibration curve is shown in Figure A.1 in Appendix A.

3.6.3. Hydrogen Peroxide Measurement

The variation of hydrogen peroxide concentration during the degradation reaction was determined by means of spectrophotometer method using DMP (2, 9-dimethyl-1, 10-phenanthroline) ($C_{12}H_6N_2(CH_3)_2$) and copper as previously mentioned in Section 2.1. DMP method provides a precise determination of hydrogen peroxide concentration. This method can be used for a wide range of concentrations since the detection limit for this method is 0.034-3400 mg/L.

The principle of this measuring method is based on the chemical reduction of copper (II) by hydrogen peroxide in presence of DMP, thus forming a copper (I) – DMP complex according to the following reaction:



The Cu(DMP)₂⁺ is a bright yellow cationic complex with maximum absorbance at 454 nm; it possesses a molar extinction coefficient of 15x10³ L/mol.cm. The color is stable in the visible range and not sensitive to light. The concentration of the complex was directly determined by UV-visible spectrophotometer (Ultrospec 1100 pro, Amersham Biosciences) at 454 nm (Kosaka et al., 1998). The Cu(DMP)₂⁺ is stable in saturated solutions of air and oxygen. The DMP method appears to be simple, robust, and rather insensitive to interference. Intermediate compounds such as acetic and formic acids, formaldehyde, and acetaldehyde, which are formed by the decomposition of organic matter exposed to AOPs, do not interfere with the DMP method.

The test procedure is as follows: One gram of DMP was dissolved in 100 mL of ethanol and stored in a dark bottle at 4°C. Copper (II) sulphate solution (0.01 M) was made by dissolving copper (II) sulphate into distilled water. Moreover, a phosphate buffer solution (0.1 M) was prepared from 13.5 g K₂HPO₄ and 12 g NaH₂PO₄. The pH of this solution was adjusted to 7 by H₂SO₄ (1N) and NaOH (1N) (Kosaka et al., 1998). One mL of each of the reagent solutions of DMP solution, Copper (II) sulphate solution, and phosphate buffer were added to a 10 mL volumetric flask and mixed well. Three mL of sample were added to the flask and diluted with distilled water to 10 mL. After mixing, the absorbance of the sample was measured at 454 nm. Blank solution was prepared in the same way with distilled water instead of sample. To make a calibration curve, different standards with different concentrations of H₂O₂ were prepared and their absorbance was measured at 454 nm. Therefore, the concentration of the samples could be read directly from the calibration curve (Figure A.2, Appendix A). Calibration curve was prepared on a monthly basis to avoid the aging effect of the reagents. Before each run two samples of known concentration of hydrogen peroxide were measured by the spectrophotometer

using DMP method. If the measured concentration deviated significantly from the 95% confidence interval, another calibration curve was prepared.

3.6.4. pH Measurement

pH measurements and the control of its level are important in water treatment systems. In advance oxidation processes, measurements of pH can show that the reaction is moving toward production of acid, which is the expected pathway. The pH of the reaction mixture was monitored using a glass gel filled pH probe (Thermo Orion Model 9107BN) combined with a Thermo Orion Meter model 230Aplus. pH meter with relative accuracy of 0.02 was calibrated every time prior to each measurement using buffers of pH 3 and pH 7.

3.6.5. Molar extinction of PVA measurement

The light absorption by the polymer solution to find the extinction coefficient was measured using a UV-visible spectrophotometer. The spectrophotometer used was Ultrospec 1100 pro, Amersham Biosciences with the ability to measure the absorbance, percent transmission, and concentration values. It can measure the absorbance of samples based on the amount of light that has passed through a sample relative to a blank. The spectrophotometer can wavelength range is within 200-900 nm with the accuracy of ± 2 nm. The light sources are tungsten halogen and deuterium arc. The instrument has a one cell compartment. The 3-mL cell used for the experiments was a standard rectangular quartz cell (optical glass). Thus, the molar extinction of PVA was determined by measuring the absorbance of several concentrations of the PVA in distilled water by means of a spectrophotometer.

The absorbance (A) at wavelength of 254 nm is then related to the extinction coefficient ε as follows:

$$A_{254} = \varepsilon_{PVA} \cdot C_{PVA} \cdot b' \quad (3.2)$$

Where C is the concentration of the PVA (mol/L) and b' is the effective path length of the UV radiation in the spectrophotometer (1 cm). The extinction coefficient (ε) was estimated from the slope of the plot shown in Figure A.3 in Appendix A.

3.6.6. Measurement of UV Lamp Intensity

For the PVA photodegradation experiments, a tubular low-pressure mercury-vapor fluorescent lamps emitting short-wave ultraviolet radiation model LP4130 (Siemens Water Technologies Limited) with a nominal wavelength of 254 nm lamp was used as the UV-C light source. According to the manufacturer information, the UV lamp is 28.7 cm in length and 32 mm in diameter with 95% UV transmittance (UVT), a nominal wattage of 14 watts, and a current of 0.3 Ampere having an effective surface area of 200 cm². UV dosage calculations are provided in Appendix B. To ensure a constant light intensity during the experiments, the intensity of each UV lamp used was measured by means of a digital radiometer and recorded on a monthly basis.

The UV efficiency has to be monitored to maintain the same process performance since the UV lamp ages and the intensity of the light and effective UV dose decreases. The UV dose is a function of the UV intensity at 254 nm wavelength and exposure time. The lower the lamp intensity, the longer the tubes must be illuminated to accomplish the same removal efficiency. The light intensity was measured using a Spectroline Digital Radiometer (DRC-100X). UV irradiance measurement is sensitive in the 254 nm region of the ultraviolet spectrum. It is capable of measuring sensitivity ranges of 0-19999 $\mu\text{W}/\text{cm}^2$. There are several parameters including

calibration, spectral response and sensor field of view that should be taken into consideration to ensure accurate measurements. Prior to each measurement, the radiometer should be set to zero to ensure the best accuracy. This is done by first covering the sensor so that no UV light strikes the sensor window. After setting the zero, ultraviolet intensity reading was taken by placing the sensor close to the UV lamp.

3.7. ERROR ANALYSIS

Experimental work might involve different sources of errors such as measurements, preparation of solutions, and device accuracy. Errors should be minimized to the confidence about the data accuracy by the following:

- The TOC analyzer was calibrated in the range of interest every three months upon the supplier guidelines.
- Prior to each batch of samples, two KHP standards of known TOC concentrations were measured for calibration verification. If the measured concentration deviated significantly from the 95% confidence interval, another calibration curve was prepared.
- The background TOC content of two distilled water samples (blank samples) was measured before measuring the treated polymer samples.
- For the spectrometric analysis, the UV-vis spectrophotometer was auto-calibrated every day and three samples for each measurement were tested.
- Most of the experiments were conducted at least twice with three replicates in measurements.

Standard deviation for the light absorption analysis was insignificant. For the TOC measurement,

the standard deviation was calculated (sample of calculation is provided in Appendix C) and the error bars were provided based on its value. Low standard deviation of the experimental results revealed a good repeatability and reproducibility of the experiments.

3.8. EXPERIMENTAL DESIGN AND STATISTICAL METHOD

In this section, the experimental design, modeling, and optimization of PVA degradation using the UV/H₂O₂ process are introduced.

3.8.1. Response Surface Methodology

The classical approach of changing one variable at a time to study the effects of variables on the objective or response functions is a time-consuming procedure for multivariable systems and in particular, for processes with more than one output response. The statistical design of experiments can help reducing the number of experiments and take into account interactions among the process variables (Schulze-Hennings and Pinnekamp, 2013).

For instance, the response surface methodology (RSM) is a statistical technique, well-known for high caliber performance and efficiency to design experiments, to develop mathematical models, and determine optimum conditions for systems with several variables. RSM originally developed by Box and Wilson (Box and Wilson, 1951) to improve the yield of reaction for some industrial process. RSM has been applied in several water and wastewater treatment applications (Nair et al., 2014; Rezaee et al., 2014). In fact, response surface methodology is a global approximation to system behavior based on the experimental data where the sensitivity of a response to the

factors of interest can be analyzed. The RSM method has five consecutive computation phases which are:

- Selection of process parameters and their ranges,
- The design of experiments and conducting the experiments,
- Generation of a modeling scheme using non-linear regression based on the experimental results,
- Testing the accuracy of the developed kinetic model,
- An optimization approach to determine the best process operating conditions.

3.8.1.1. Selection of process parameters

According to a previous knowledge of the process, the process independent parameters to be varied during the experimental design should be selected. The number of experiments increases with the number of independent variables. The experimental tests can be performed at three levels; low, high, and center levels. Center level is taken midway level between the low and high level of the variable. This procedure is applied to each variable independently.

3.8.1.2. Experimental design

Various experimental designs are available for conducting the experiments. These designs differ from one another with respect to their selection of experimental points and number of runs. Some of the extensively used experimental designs are central composite design (CCD), Box-Behnken design (BBD) and full factorial design (Montgomery, 2010). The BBD is

considered as one of the most successful and economical factorial design for a three-factor system with a limited number of planned experiments (Khuri and Cornell, 1996).

In particular, BBD is of interest due to its simplicity and robustness. BBD was first proposed by Box and Behnken in 1960. In BBD, the main effects of variables and interaction effects between the variables on the response can be obtained from a small number of experiments.

In fact, the BBD is a modified central composite experimental design where the variable combinations are at the midpoints of the variable space edges. In BBD, all experimental points lie on a sphere of radius $\sqrt{2}$ where the number of experiments (N_{exp}) to be conducted is determined by the following equation

$$N_{exp} = 2n(n - 1) + r_p \quad (3.3)$$

where n is the number of variables and r_p is the number of replicates at the central point (Nair et al., 2014). The BBDs consist of a set of runs in which each pair of factors is varied between their low and high levels, while the other experimental factors are held at the center level.

3.8.1.3. Selection of the model

Once the experiments have been conducted, the experimental results should be employed to develop an adequate functional relationship between the key variable and response variables of the process. The statistical model, upon which the analysis of response surface designs is based, expresses the process response as a function of the experimental variables, interactions between the variables, and quadratic terms. First-order model is commonly used for representing the main effects only. However, for the UV/H₂O₂ process, the interaction between

variables has a high impact on the process efficiency. Therefore, the experimental data should be fitted to a second-order equation that contains terms representing main effects, second-order interactions, and quadratic effects as follows:

$$y = b_o + \sum_{i=1}^n b_i x_i + \sum_{i=1}^n b_{ii} x_i^2 + \sum_{i=1}^{n-1} \sum_{j=2}^n b_{ij} x_i x_j \quad (3.4)$$

Where y represents the process outputs, n is the number of factors or variables, b_o is the regression coefficient at the intercept, and b_i , b_{ii} , and b_{ij} are the regression coefficients for the linear, quadratic, and interaction of each factor x_i , respectively. The model prediction results are generally presented graphically as 2-D and 3-D plots. The graphical illustration helps in visual interpretation of the functional relationship between the response and the independent variables. Besides, the model can provide information about the system behavior at different conditions but cannot explain the mechanism of the process.

3.8.1.4. Statistical method for confirmation of the model accuracy

The developed RSM model has to be tested to ensure that the model provides an adequate prediction of the system behavior. The statistical validation is determined by the analysis of variance (ANOVA) test at 95% confidence level. The quality of the fit polynomial model is generally explained by coefficient of determination (R^2) which measures the total variation of predicted values from the mean. For a model with good prediction efficiency, the value of R^2 should be close to 1. However, the model should not be assessed by R^2 alone since R^2 increases with the increase in the number of terms in the model equation. R^2 value should be compared with adjusted R^2 which reflects the number of factors in the experiment (Montgomery, 2010). R^2_{adjusted} value decreases if statistically insignificant process variables are selected. The closer the values of R^2 and R^2_{adjusted} are, the more adequate the model is. Also, the residuals which

are the difference between the predicted and actual values are important to confirm the model adequacy.

3.8.1.5. Response surface optimization

The RSM scheme can be also utilized to determine the optimum operating conditions of a process at the target responses incorporating the effects of process variable interactions. The mathematical model developed from Equation (3.4) will then be used as an objective function to maximize or minimize the response and obtaining the associated optimal level of the process parameters. When several responses suggest different optimal operating conditions, a balance between the responses is achieved using desirability method by finding operating conditions that provide simultaneously the most desirable response variables (Costa and Lourenço, 2014). The sensitivity of all responses is set to medium, which means that the desirability of each response increases in a linear fashion throughout the specified range.

Desirability function is multi-criteria methodology in which each response is converted into an individual desirability function that varies over the range of 0 to 1. If the response is at its target, then desirability function is 1, and if a response is outside the specified range, then the desirability functions is zero.

Chapter 4

POLYVINYL ALCOHOL DEGRADATION IN BATCH AND FED-BATCH UV/ H₂O₂ PHOTOREACTORS

4.1. Introduction

The polyvinyl alcohol polymer (PVA) is a well-known refractory pollutant. Recent studies on the removal of PVA focused on processes that are radiation induced oxidation process such as photocatalytic processes (Chen et al., 2001), and photo-Fenton (Xei et al., 1998; Zhang et al., 2011; Kang et al., 2000). However, these processes are reported to have limitations in practical applications. Therefore, it is essential to design an effective technique for a better removal of PVA from wastewater systems. In instance, the UV/H₂O₂ process seems to be one of the most promising techniques to transform biorefractory organics containing high concentration of PVA into more biologically oxidizable products. Comparatively, the UV/H₂O₂ process for its simple operation has distinct advantages over other advanced oxidation processes. In particular, the physico-chemical properties of hydrogen peroxide such as its high solubility in water and the fast hydroxyl radical reactions with the water-soluble polymers help to select the UV/H₂O₂ process as a promising candidate. However, according to open literature, the UV/H₂O₂ process has also some limitations. The primary objective of this study is to investigate and design an efficient UV/H₂O₂ process that can disintegrate PVA and remove it from water streams.

The study begins with an experimental investigation on the photo-oxidative degradation of PVA aqueous solution in a laboratory scale UV/H₂O₂ photochemical reactor operated in batch and fed-batch with a recycle. For the latter reactor, a feeding strategy of hydrogen peroxide was

performed to improve the degradation of PVA polymer. Total organic carbon (TOC) removal and polymer chain degradation were evaluated for different initial polymer and hydrogen peroxide concentrations.

4.2. Experimental Procedure

Two experimental procedures were adopted; batch and stepwise strategies for introducing H₂O₂ into the photoreactor. The batch or pour method consists of introducing the desired quantity of hydrogen peroxide in one single shot into the aqueous waste stream at a point immediately before the solution enters the UV photoreactor. The second experimental procedure called the fed-batch or stepwise mode consists of introducing the hydrogen peroxide in an intermittent manner into the photoreactor. A predetermined initial amount of hydrogen peroxide was dripped into the holding tank. Then, the PVA aqueous solution was pumped into the UV photoreactor. Three more equal amounts of hydrogen peroxide were successively poured into the holding tank at time intervals of 30 min. The purpose of using the stepwise manner testing was to maintain a substantial level of H₂O₂ during the irradiation time period. During the last 30 min of each experiment, hydrogen peroxide was not fed into the system so that the remaining H₂O₂ can be gradually consumed.

To assess the effect of hydrogen peroxide concentration and the way of its injection into the system on the PVA degradation in the UV/H₂O₂ process, a series of experiments were carried out. The schematic diagram of the experimental setup is shown in Figure 3.1.

A detailed description of the UV/H₂O₂ photoreactor system is provided in Sections 3.2 followed by a full description of the experimental procedure in Section 3.3. The hydrogen peroxide to

polymer mass ratio was changed at two levels, low (50 mg/L) and high (500 mg/L) initial polymer concentration. These concentrations were chosen to study the degradation in dilute solution (50 mg/L) and the concentration existing in actual effluents in the textile industrial plants. These runs were repeated twice when introducing all H₂O₂ amount at one shot or dripping it in four equal quantities into the reactor system. The experimental procedure includes preparing a stock solution using solid PVA as described in Section 3.3. The volume of the solution was maintained at 2 L in all runs. Once the PVA solution was poured into the feed tank, the centrifugal pump was started to circulate the solution into the UV photoreactor. At this moment, the hydrogen peroxide feeding and time measurements were started as well as an immediate collection of the first sample. The experimental conditions are given in Table 4.1.

Table 4.1. Experimental conditions of the batch and fed-batch photoreactors with recirculation.

Parameter	Value
Holding tank capacity	2 L
Photoreactor volume	0.46 L
Reaction time	120 min
Circulation flow rate	1000 mL/min
UV lamp radiation wavelength	254 nm
PVA initial concentration	50 mg/L, 500 mg/L
[H ₂ O ₂]/[PVA] mass ratio	0, 0.2, 1, 5, 10, 15

4.3. Effect of Hydrogen Peroxide Concentration on TOC Removal in the Fed-Batch Photoreactors

Referring to Table 4.2, aqueous solutions of PVA were made in order to test the degradation of PVA in the fed-batch photochemical reactor. The generation of free radicals is required for the polymer degradation under UV-light. Hence, the concentration of hydrogen peroxide with respect to the polymer concentration was gradually increased by taking the $[H_2O_2]/[PVA]$ mass ratios of 0, 0.2, 1, 5, 10 and 15 as fractions of stoichiometric amount (mass ratio of 3.9) of H_2O_2 necessary to oxidize vinyl alcohol (C_2H_4O)-units according to the following equation:



Table 4.2 indicates that the system was operated as batch reactor in runs 1 to 9 with initial PVA concentrations of 50 and 500 mg/L. In runs 10 to 18, the photoreactor was operated as a fed-batch reactor using 50 and 500 mg/L of PVA initial concentration and hydrogen peroxide to polymer mass ratios ranging from 0 to 15.

Samples were periodically taken using a 25-mL syringe from the middle of the holding tank, as shown in Figure 3.1, every 30 min for 2 h reaction time. A sample volume of 15 mL is used for TOC measurement by TOC analyzer (Apollo 9000, Teledyne Tekmar, USA). The samples were injected into the analyzer using an automated syringe from the sampling bottle. The sample injection valve automatically selects the appropriate sample volume for the optimum measuring range. A volume of 5 mL was collected in a 5 mL-vial for PVA molecular weight characterization by GPC (PL-GPC 50, Agilent) equipped with a triple detector array.

Table 4.2. Experimental design for the photochemical PVA (130 kg/mol) degradation in batch and fed-batch photoreactor. Feeding of H₂O₂ to the photoreactor: single shot for batch and stepwise for fed-batch systems.

Run	Oxidant feed	[PVA] _o (mg/L)	[H ₂ O ₂]/[PVA] mass ratio
1	No H ₂ O ₂	50	0
2	Batch	50	1
3	Batch	50	5
4	Batch	50	10
5	Batch	500	0.2
6	Batch	500	1
7	Batch	500	5
8	Batch	500	10
9	Batch	500	15
10	Fed-batch	50	1
11	Fed-batch	50	5
12	Fed-batch	50	10
13	No H ₂ O ₂	500	0
14	Fed-batch	500	0.2
15	Fed-batch	500	1
16	Fed-batch	500	5
17	Fed-batch	500	10
18	Fed-batch	500	15

The samples were then analyzed. Also a volume of 3 mL was used to detect the residual hydrogen peroxide through DMP method by means of UV/Visible spectrophotometer (Ultrospec 1100 pro). The analytical techniques are discussed in detail in Section 3.6. Figure 4.1 shows the variation of TOC removal versus reaction time for $[H_2O_2]/[PVA]$ mass ratio varying from 0 to 15. The hydrogen peroxide was injected into the reactor in a stepwise manner for 2 h exposure time. The UV/ H_2O_2 process was able to degrade 500 mg/L of PVA. The percent TOC removal varies from 0 to 87% as the UV/ H_2O_2 ratio was changed from 0 to 10. Therefore, significant enhancement in the PVA degradation rate was observed as the H_2O_2 concentration increases but to a certain limit only. However, the TOC removal dropped to 63% when the $[H_2O_2]/[PVA]$ mass ratio was set to 15. Evidently, it can be concluded that a higher level of hydrogen peroxide has an adverse effect on the TOC removal. This TOC removal threshold can be interpreted by the scavenging effect of H_2O_2 on hydroxyl radicals since the amount of H_2O_2 added to the system is proportionally high. In fact, it is known that H_2O_2 can trap hydroxyl radicals (HO^\bullet) to form hydroperoxyl radicals (HO_2^\bullet) and thus causing the concentration of free HO^\bullet to decrease in the solution. Since HO_2^\bullet radicals are much less reactive than hydroxyl radicals, the TOC removal will decrease (Mehrvar et al., 2001; Mehrvar and Tabrizi, 2006; Mohajerani et al., 2009). Furthermore, in order to assess impacts of ultraviolet light on the degradation of PVA, a test using 500 mg/L of PVA was performed for 2 h under UV irradiation in the absence of hydrogen peroxide.

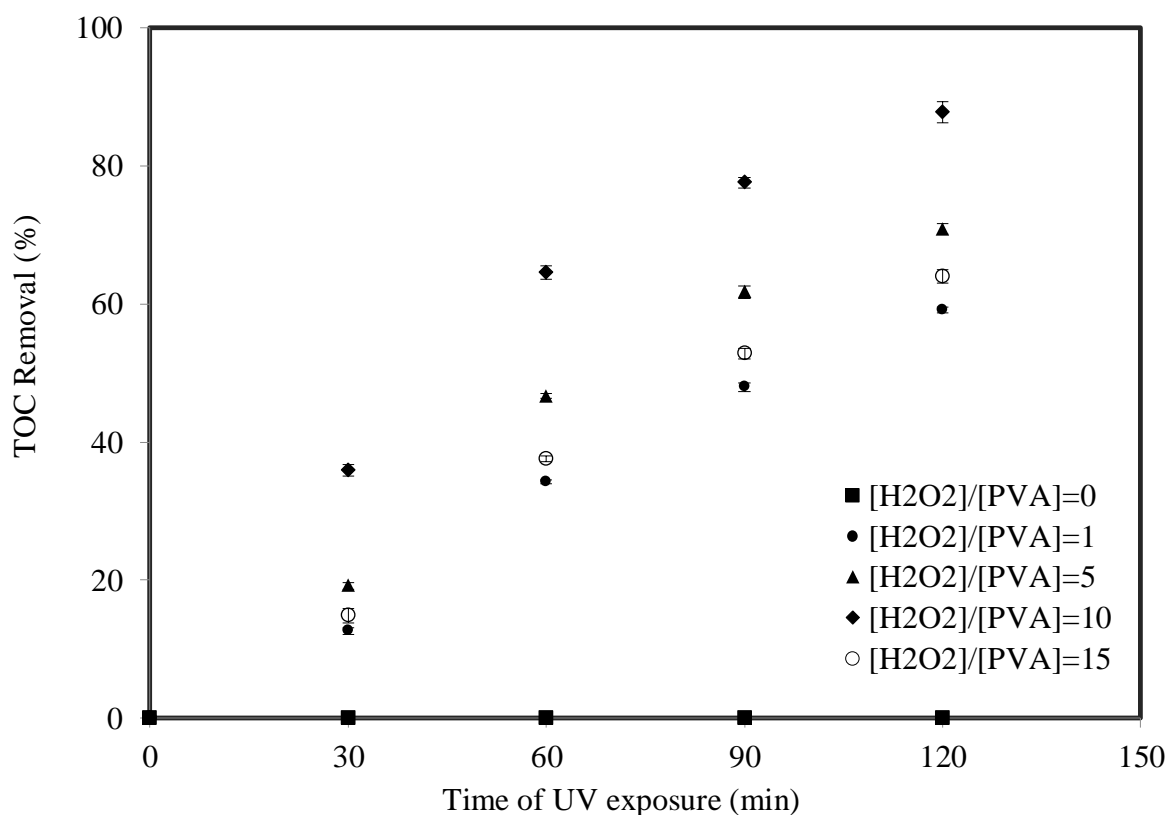


Figure 4.1. TOC removal versus reaction time in fed-batch photoreactor.
[PVA]_o = 500 mg/L; [H₂O₂]/[PVA] mass ratios: 0, 1, 5, 10, and 15.

No significant measurable decrease in PVA concentration was observed after 2 h under UV light alone. Another important observation to record is that hydrogen peroxide is absolutely necessary to initiate the PVA degradation reaction. Direct UV photolysis should in principle require a high UV intensity in order to achieve significant degradation of the macromolecular contaminants such as polymers when there is not enough quantum absorbance of PVA polymers. Hence, adding more H₂O₂ in the solution under UV irradiation generates more active hydroxyl radicals. The outcome of the experimental tests demonstrates that the degradation of PVA polymer requires both UV light and hydrogen peroxide.

4.4. Effect of Hydrogen Peroxide Feeding Strategies on TOC Removal

The PVA degradation was also examined for cases when hydrogen peroxide was introduced in stepwise and single shot manners into the feed tank preceding the photoreactor. The UV/H₂O₂ system was operated for 2 h in each feeding strategy. As shown in Figure 4.2, for an initial PVA concentration of 500 mg/L, the highest TOC removal of 87% was achieved in fed-batch system for [H₂O₂]/[PVA] mass ratio of 10 but only 41% TOC removal was obtained in batch photoreactor for [H₂O₂]/[PVA] mass ratio of 1.

By comparing the TOC removal in Figures 4.3 and 4.4, the results revealed that for an initial polymer concentrations of 50 mg/L and using [H₂O₂]/[PVA] mass ratio of 10, the TOC removal was 10% higher when dripping hydrogen peroxide (Figure 4.3) into the system than pouring it all at once (Figure 4.4) under the same experimental conditions. This is due to the fact that pouring hydrogen peroxide in one single shot into the UV photoreactor system is likely to cause steep local gradient in H₂O₂ concentration along the photoreactor which can quickly

saturate the reaction mixture with hydroxyl radicals and consequently causes the PVA degradation rate to slow down. Figures 4.5 and 4.6 show the consumption of H₂O₂ during the degradation reaction of the PVA polymer in the batch and fed-batch photoreactors, respectively. The falling trend of H₂O₂ content exhibits the rate at which the hydrogen peroxide molecules break down into hydroxyl radicals under UV light effect. One interpretation of the hydrogen peroxide decay is that generated hydroxyl radicals can attack organics, thus generate chemical intermediates species and finally carbon dioxide and water in its final stage.

The experimental results in Figure 4.5 and 4.6 also showed that at [H₂O₂]/[PVA] mass ratio of 5, in case of batch process, a hydrogen peroxide a residual of 17% was observed compared to only 3% residual in case of the fed-batch (stepwise drip) process owing to the fact that introducing small amount of the oxidant (H₂O₂) into the photoreactor efficiently enriches the reaction mixture with hydroxyl radicals.

4.5. PVA Degradation Efficiency

The degradation efficiency η of the PVA polymer is defined as follows:

$$\eta = \frac{[PVA]_o - [PVA]_t}{[PVA]_o} \quad (4.2)$$

Where [PVA]_o and [PVA]_t are the mass concentrations of the polymer prior to and after degradation measured by GPC, respectively. Referring to Figure 4.1, under identical experimental conditions with [H₂O₂]/[PVA] mass ratio of 10, a maximum of 87% TOC removal and 91.6% PVA removal (Figure 4.7) were achieved when H₂O₂ was slowly pumped into the system in a stepwise manner.

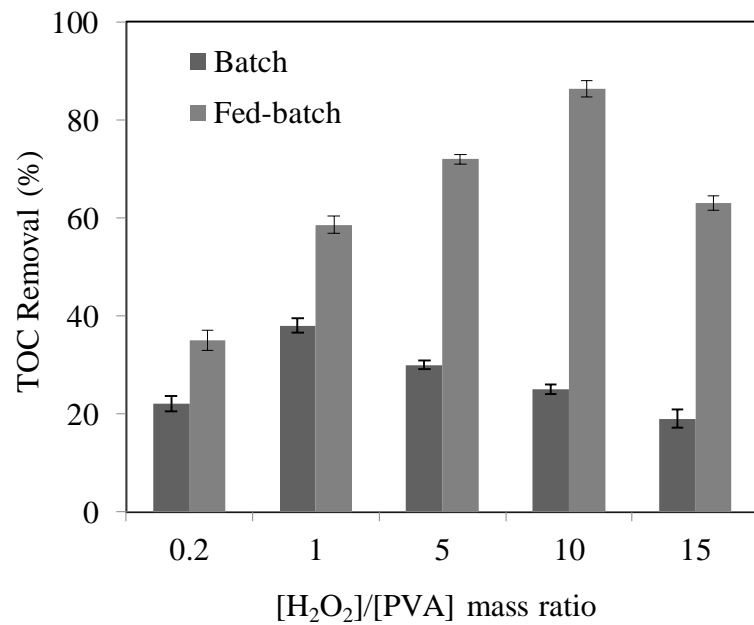


Figure 4.2. TOC removal for batch and fed-batch photoreactors.
[PVA]₀= 500 mg/L; $[H_2O_2]/[PVA]$ mass ratios: 0.2, 1, 5, 10, and 15.

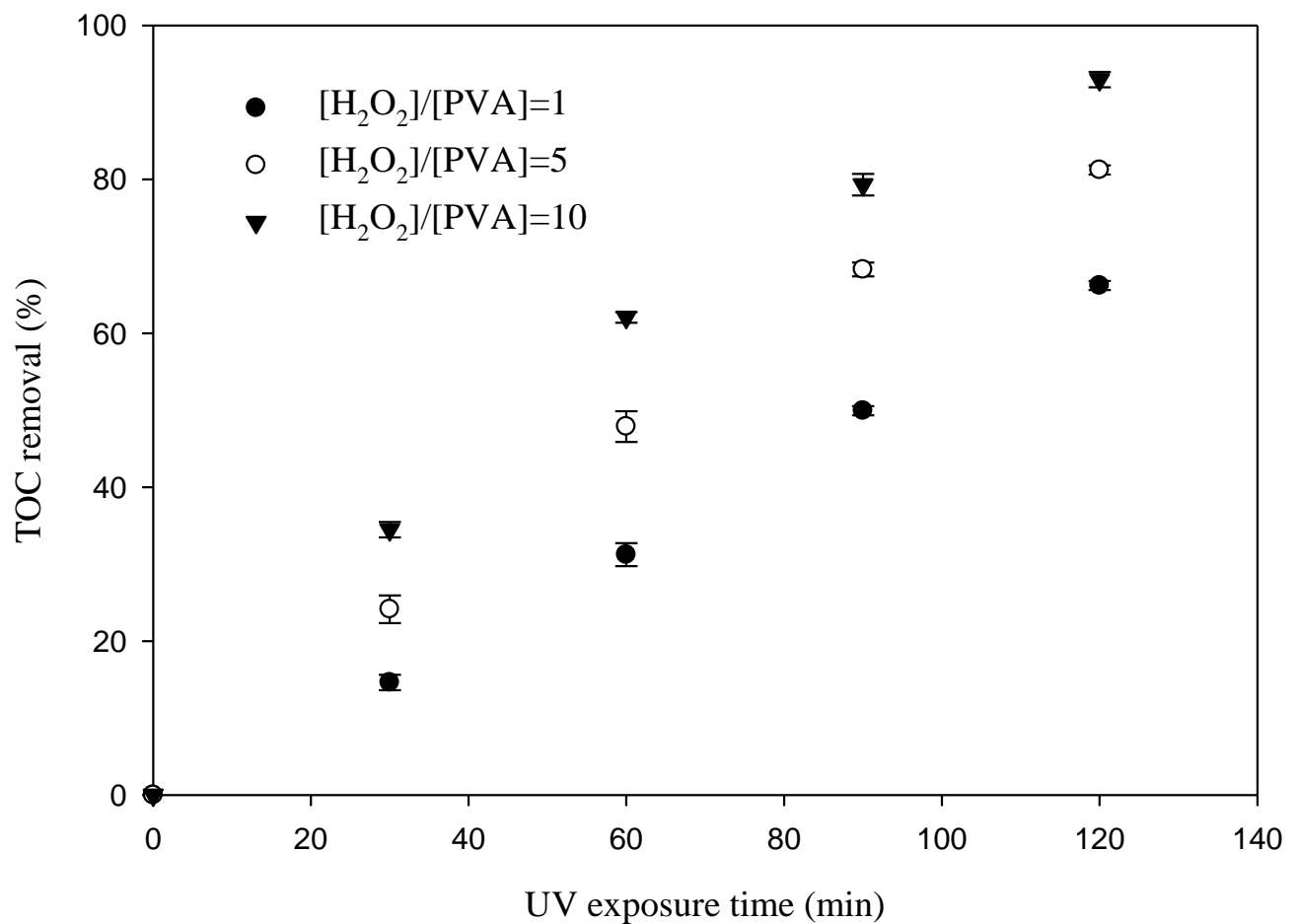


Figure 4.3. TOC removal versus reaction time in fed-batch photoreactor; $[PVA]_o = 50 \text{ mg/L}$.

$[H_2O_2]/[PVA]$ mass ratios: 1, 5 and 10.

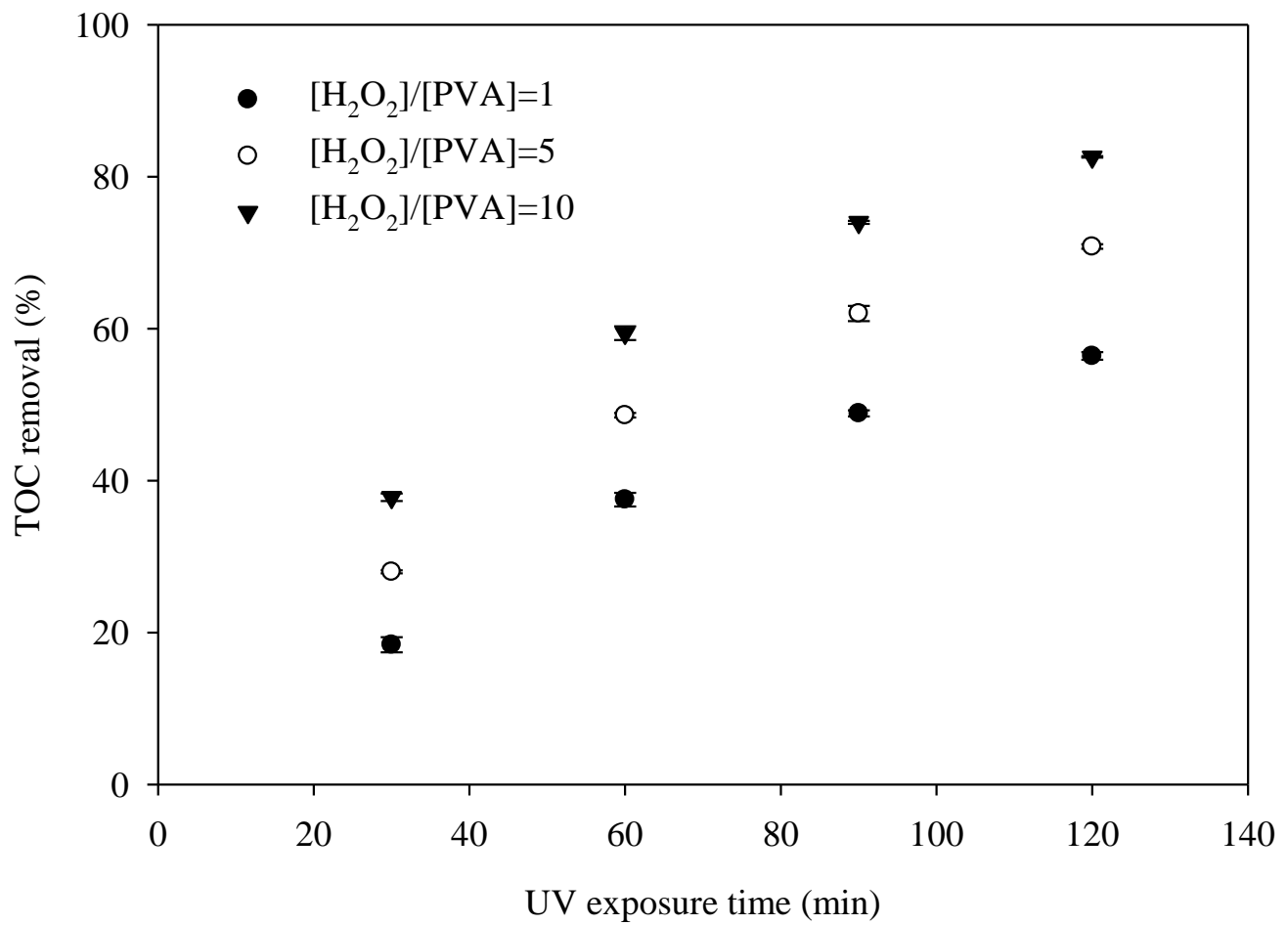


Figure 4.4. TOC removal versus reaction time in batch photoreactor.

$[PVA]_o = 50 \text{ mg/L}$; $[H_2O_2]/[PVA]$ mass ratios: 1, 5 and 10.

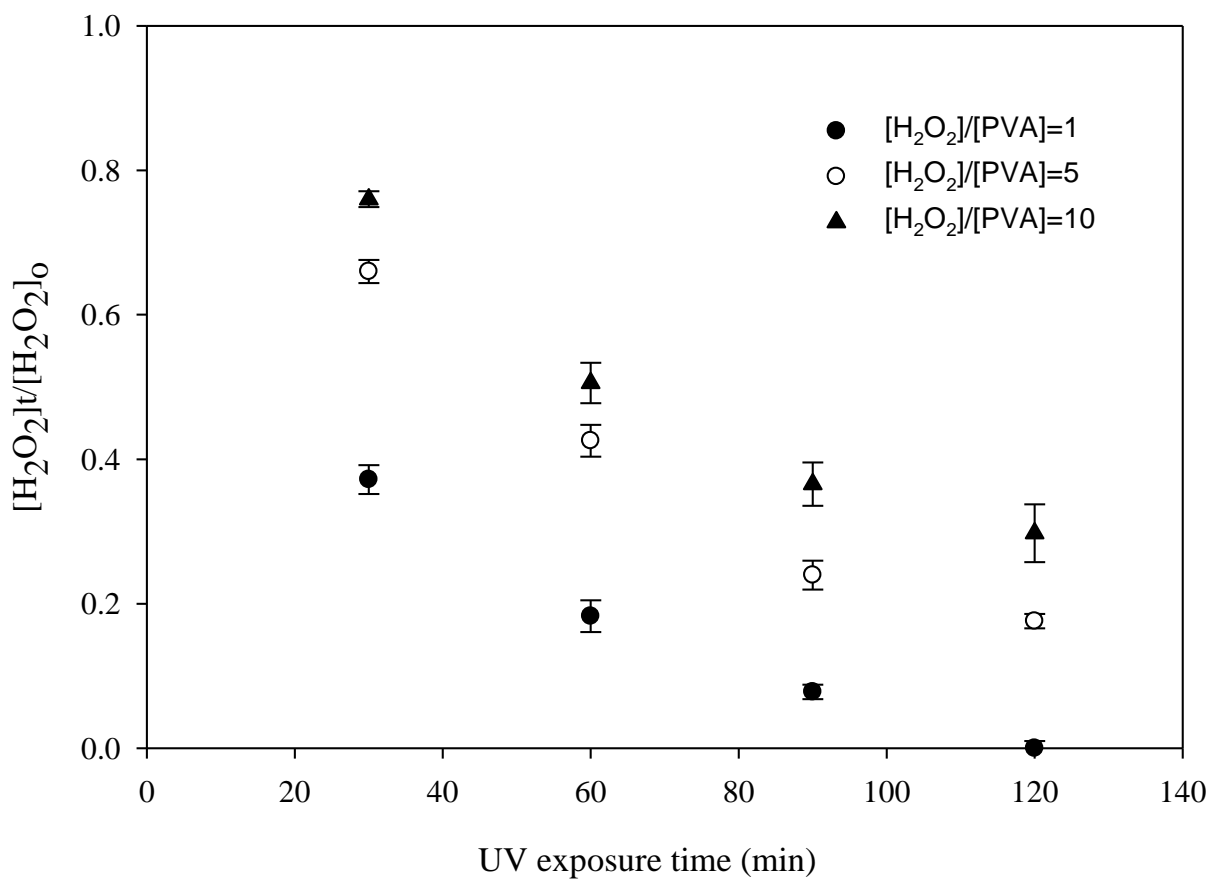


Figure 4.5. H_2O_2 variation versus reaction time in batch photoreactor.

$[PVA]_0 = 50 \text{ mg/L}$; for $[H_2O_2/PVA]$ mass ratio: 1 and 5.

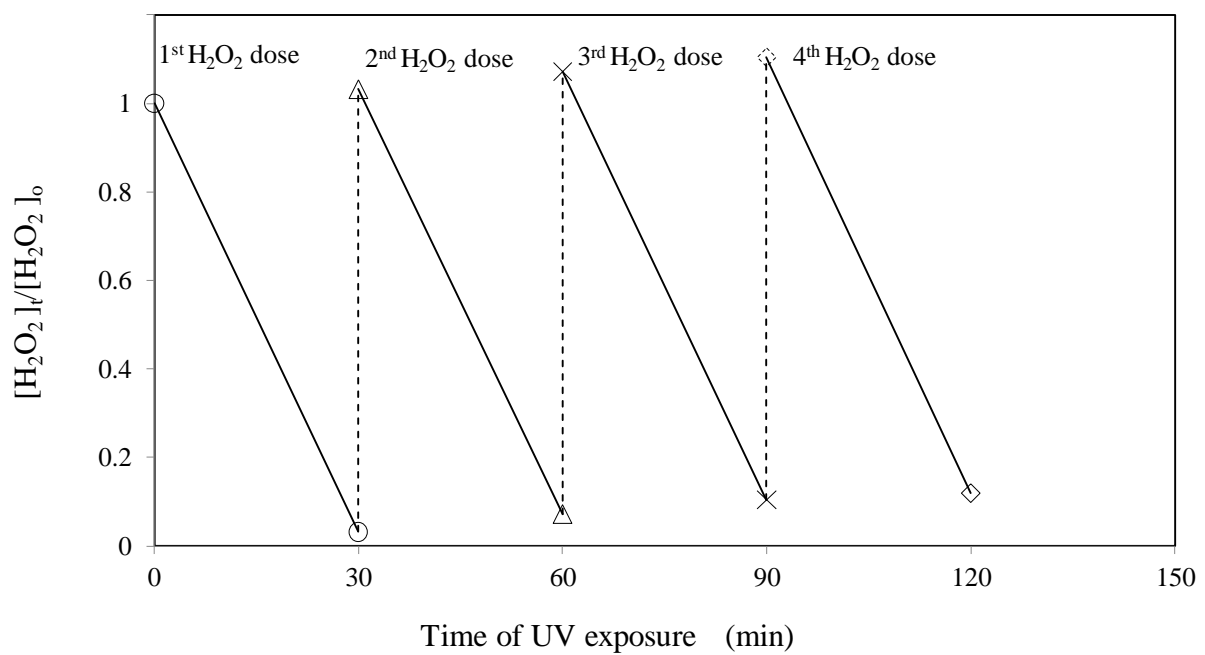


Figure 4.6. H₂O₂ variations versus reaction time in fed-batch photoreactor.
 $[PVA]_0 = 50 \text{ mg/L}$; [H₂O₂/PVA] mass ratio of 5, addition of H₂O₂ every 30 min.

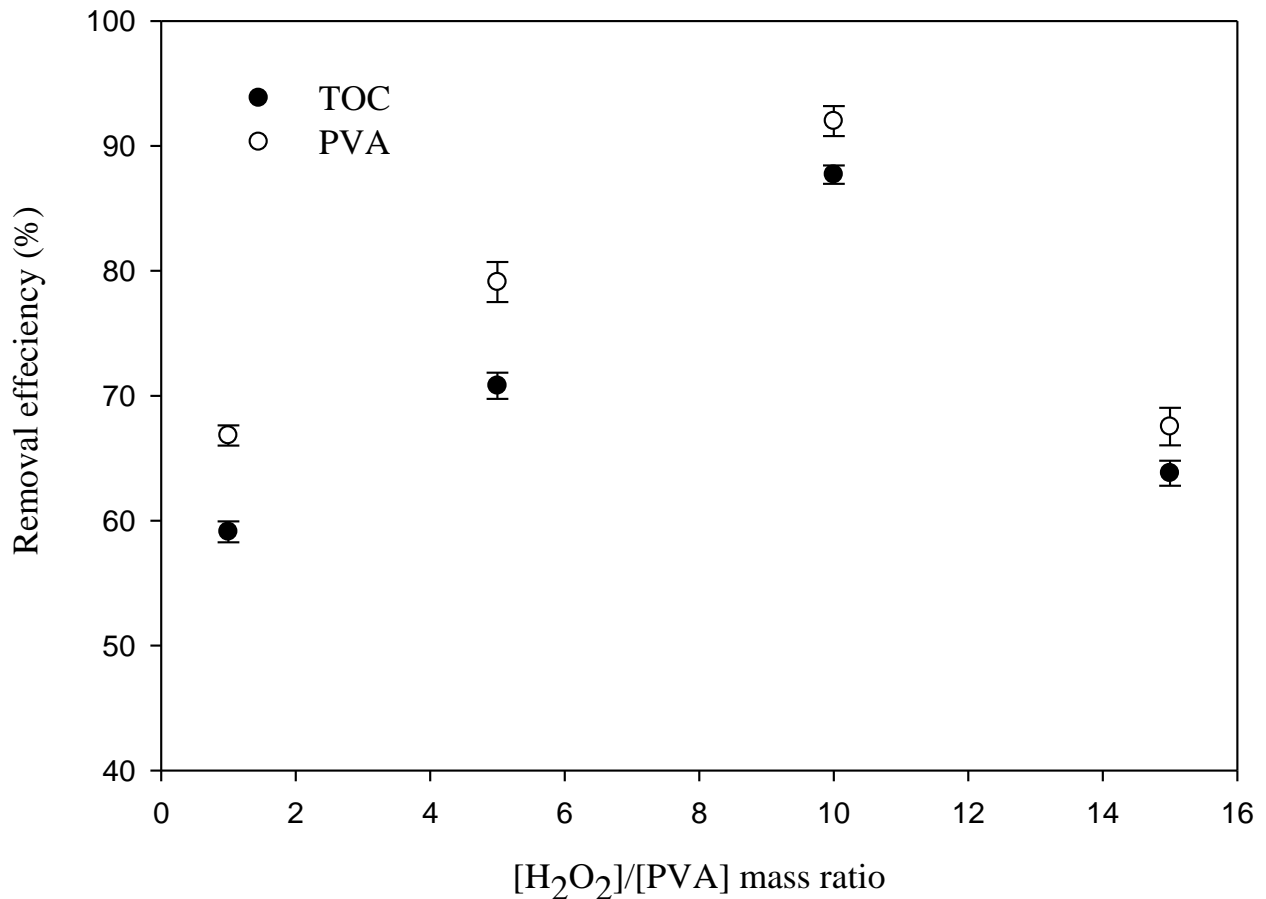


Figure 4.7. PVA degradation and TOC removal efficiencies versus $[H_2O_2]/[PVA]$ mass ratio.

$[PVA]_o = 500 \text{ mg/L}$, H_2O_2 dripped into the fed-batch photoreactor.

The difference between TOC and PVA removal efficiencies might be due to the presence of undesirable oxidation products such as acetic and formic acids produced towards the end of reaction and also to non-degraded polymer residuals which can slightly increase the TOC content of the treated solution. Even though the oxidant H_2O_2 should be applied in a certain amount in order to sustain the PVA polymer degradation under the effect of UV light, the trend of data in Figure 4.7 demonstrated that there are thresholds of $[\text{H}_2\text{O}_2]/[\text{PVA}]$ mass ratio at which both the TOC removal and PVA degradation efficiencies at maximum values. Actually, the purpose of this experimental investigation is to determine how much hydrogen peroxide must be provided so that the photochemical reaction performs at its best.

4.6. pH Variations during the PVA Degradation Process

Figure 4.8 shows the variation in pH versus reaction time when the UV/ H_2O_2 process is operated in stepwise and batch modes to treat PVA solutions using a $[\text{H}_2\text{O}_2]/[\text{PVA}]$ mass ratio of 10. A significant fall in pH was recorded in the first 60 min of the UV exposure for the experimental tests carried out in stepwise manner (drip procedure under fed-batch mode). After that, the data shows a regain in the pH of the solution. The pH decrease is related to the formation of intermediate oxidation products such as carboxylic acids (Zheng and Ling, 2007; Taghizadeh et al., 2015). However, the unexpected increase in pH of the solution can be explained by the degradation of organic acidic compounds that are oxidized to carbon dioxide that escape the system and water at the end of the reaction when the fed-batch process is operated in the stepwise manner. The high values of TOC removal obtained after 2 h exposure time supports this interpretation. Whereas in the third experiment, introducing hydrogen

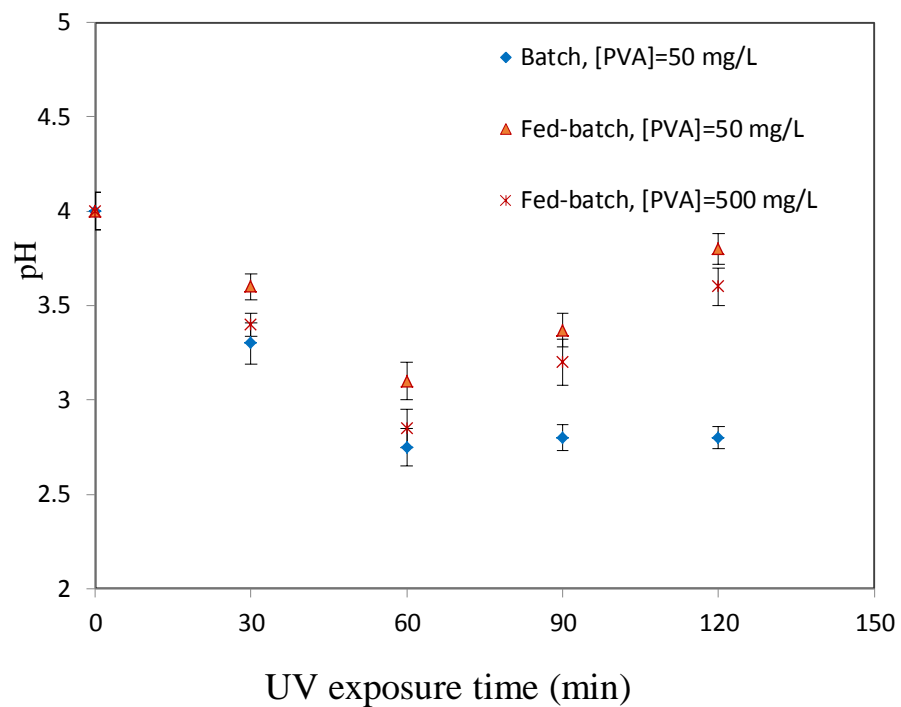


Figure 4.8. pH variations of PVA solutions versus reaction time.

Batch and fed-batch photoreactors, $[\text{H}_2\text{O}_2]/[\text{PVA}]$ mass ratio of 10.

peroxide in one single shot into the holding tank, the pH falls quickly in the first 60 min, then it remains steadily constant until the end of the photoreaction period. The decrease in the solution pH is related to the production of acids.

4.7. Polydispersity Variations and Molecular Weight Distribution

Starting with an aqueous solution of 500 mg/L polyvinyl alcohol of initial number average molecular weight (M_n) of 130 kg/mol and $[H_2O_2]/[PVA]$ mass ratio of 10, M_n was reduced to 10.9 kg/mol in fed-batch photoreactor after 90 min of reaction. Figure 4.9 shows the variation of number average molecular weight (M_n) of PVA molecular weight versus time. At the beginning of the reaction, a steep decrease in the polymer molecular weight averages is recorded in the first 30 min. The rapidly decaying profile of the polymer molecular weight averages during the PVA degradation reaction suggests that random chain scission of the C-C bonds in PVA is likely predominating the polymer degradation in the first 30 min. The reaction was repeated for three different $[H_2O_2]/[PVA]$ ratios. The samples were analyzed by means of GPC, as previously described in Section 3.6, to determine the average molecular weights of the polymer. The data shows that the higher H_2O_2 content (up to mass ratio of 10) in the solution, the faster the degradation of the PVA polymer. Accordingly, the polydispersity index (PDI) of the UV-irradiated polymer samples is reported in Table 4.3. The PDI that provides an insight about the polymer population dispersity, is calculated as follows:

$$PDI = \frac{M_w}{M_n} \quad (4.3)$$

The PDI increase implies a likely breakdown of the PVA chains into shorter-chain molecules such as oligomers, dimers, and monomers. The degraded polymer sample breaks

down into chemical species having different molecular weights. This fact is confirmed by a larger PDI value of 4.1. The experimental data presented in Figure 4.9 and Table 4.3 confirms clearly that the PVA polymer can be degraded under UV irradiation in presence of hydrogen peroxide. Simultaneous use of both experimental factors, UV-irradiation and H₂O₂, enhances the photochemical degradation of PVA leading to a broader molecular weight distribution of the PVA polymer. Two samples were taken after 30 and 90 min of reaction, were analyzed with GPC. Plots in Figures 4.10 and 4.11 demonstrate how the shape of the molecular weight distribution changes during the treatment periods of 30 and 90 min. Figure 4.10 shows that the untreated PVA (as purchased, Mn=130 kg/mol, Mw=148.2 kg/mol) has a uniform narrow distribution with a PDI of 1.14. After 30 min of reaction time, the sample contains a PVA polymer with shorter chain length and of course with lower molecular weights. The molecular weight averages Mn and Mw have dropped to 55.5 kg/mol and 85.88 kg/mol, respectively. For a further reaction time, the molecular weight averages, have significantly decreased to 10.9 kg/mol and 44.9 kg/mol, respectively. It is important to emphasize that polymeric elements with lower molecular weights are produced.

The breadth and shape of the MWD in Figure 4.11 reflect the dispersion of molecular weights of the polymer sample. Obviously, the distribution has shifted to the left during the degradation reaction since the polymer molecular weight has been considerably lowered. The broadness of the molecular weight distribution which is expressed by an increase in polydispersity is likely due to the fragmentation and chain-scission mechanism of the polymer degradation during the UV/H₂O₂ process.

The increase in PDI values presented in Table 4.3 is expected for a degraded polymer population, since irradiation promotes the breakage of the polymer chains. The chain scission

results in an increase in the number of polymer chains, reduction in the polymer molecular weight, and consequently increasing the polydispersity of the polymer sample, which represents the breadth of the distribution curve. Besides between reaction times 30 and 90 min, the molecular weight is almost halved whereas the average number of chains passed for 55.5 to 10.9 kg/mol.

Table 4.3. Variation of PDI of PVA in fed-batch photoreactor.

Irradiation time (min)	M _n (kg/mol)	M _w (kg/mol)	PDI
0	130.0	148.2	1.14
30	55.5	85.88	1.93
90	10.9	44.69	4.10

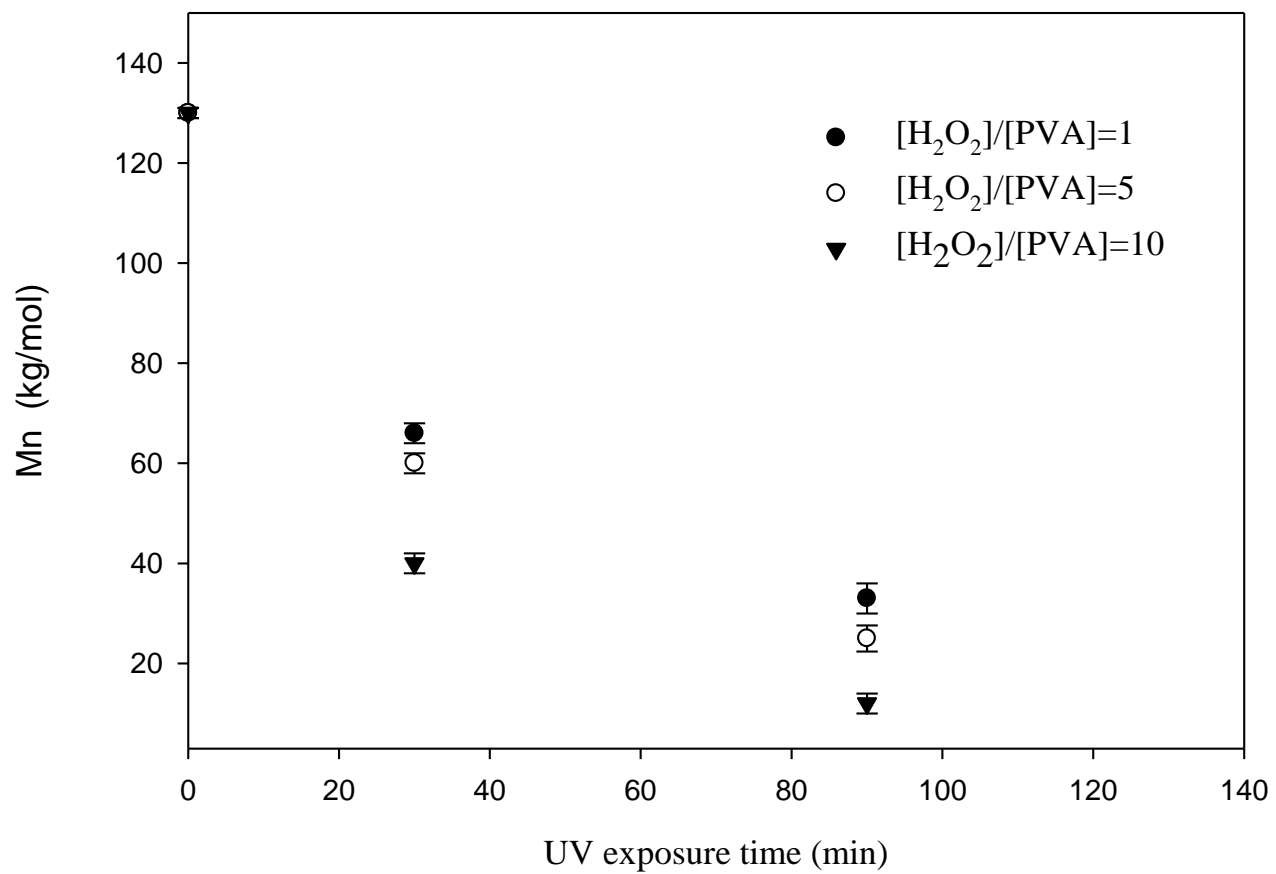


Figure 4.9. Number average molecular weights (Mn) versus UV exposure time.

[PVA]_o= 500 mg/L, H₂O₂ dripped into the fed-batch photoreactor,

[H₂O₂]/[PVA] mass ratio: 1, 5 and 10.

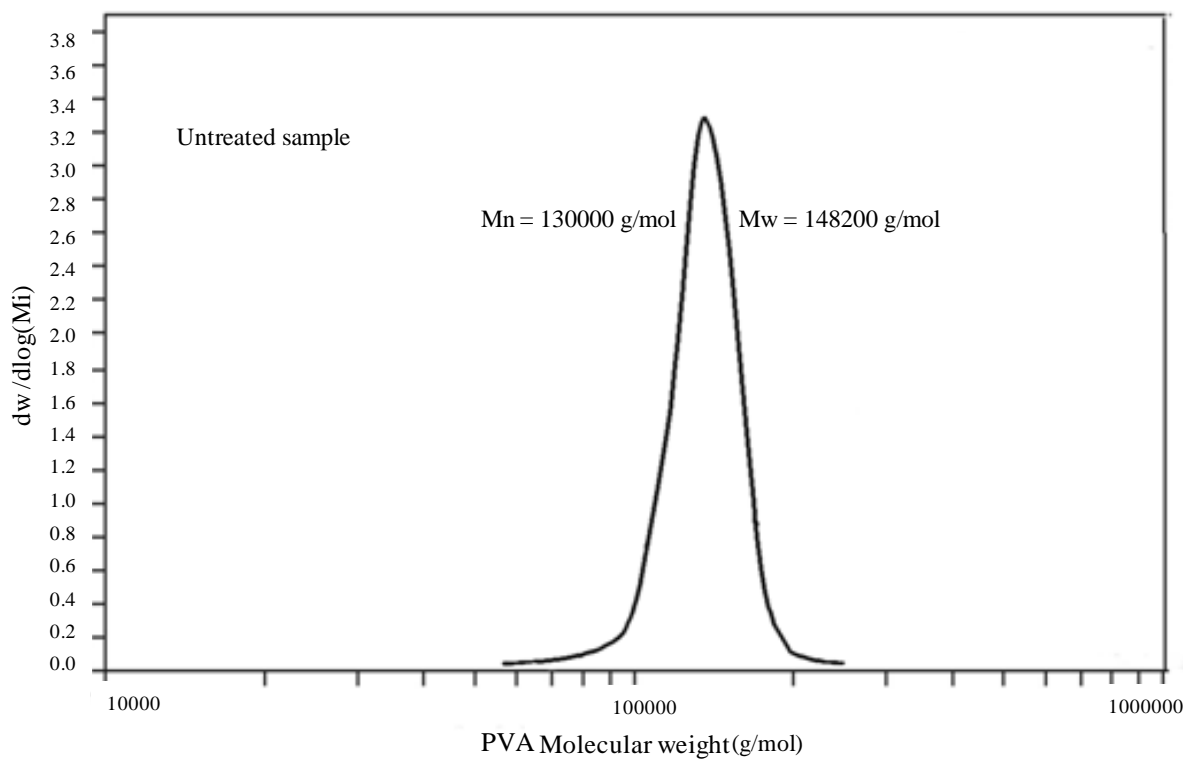


Figure 4.10. MWD of the untreated PVA.
[PVA]_o=500 mg/L.

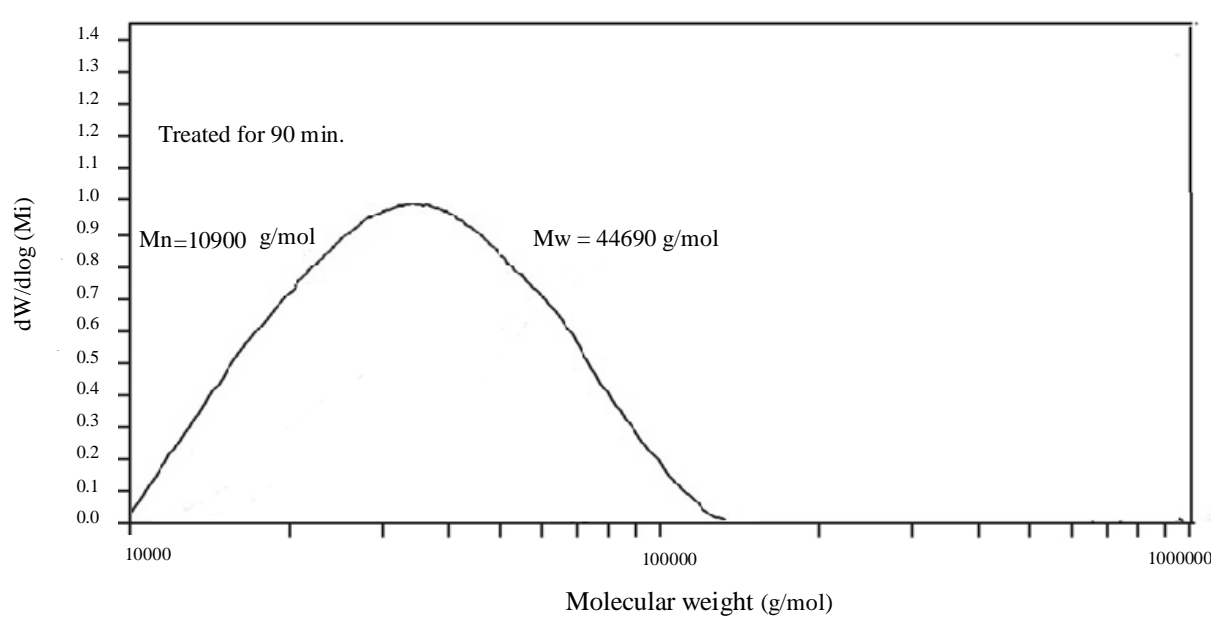
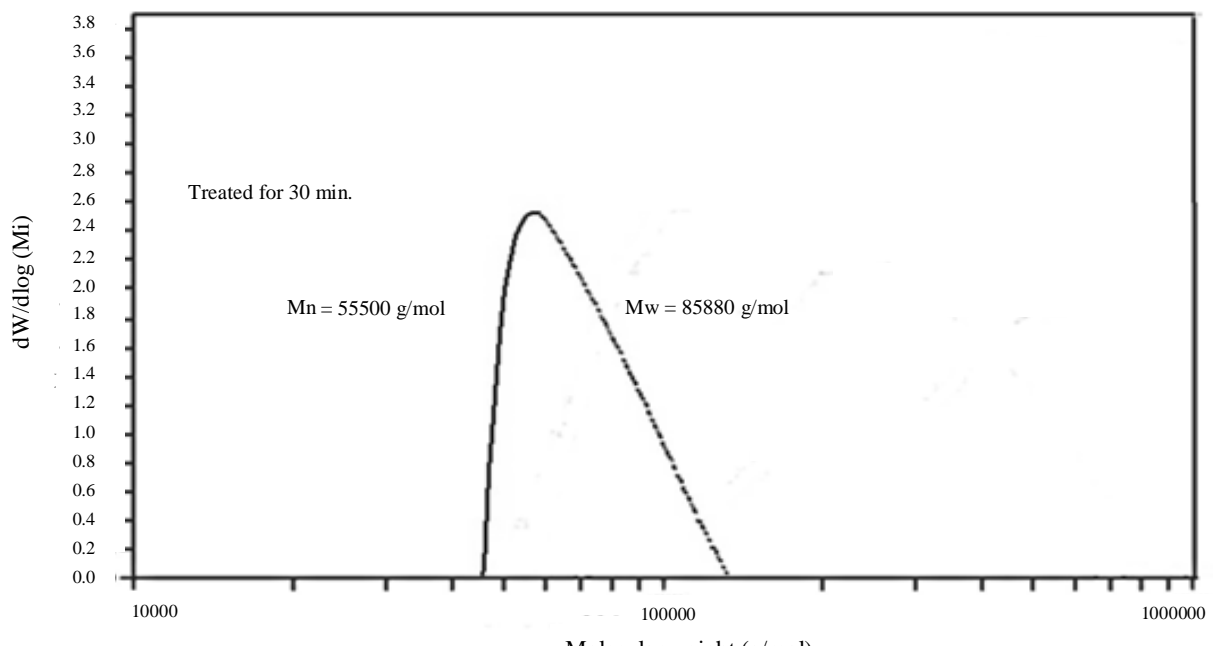


Figure 4.11. Variations of MWD of PVA.
 $[PVA]_0=500$ mg/L at $[H_2O_2]/[PVA]$ mass ratio of 10, H_2O_2 dripped into the fed-batch photoreactor.

4.8. Concluding Remarks

The performance of the UV/H₂O₂ advanced oxidation process was evaluated for the degradation of polyvinyl alcohol polymer (PVA) polluting wastewater in batch and fed-batch photoreactors. The photodegradation of 500 mg/L and 50 mg/L PVA samples was examined for two experimental sets in which hydrogen peroxide was introduced in one shot into the batch reactor and stepwise procedure into the fed-batch photoreactor. The results have shown that the way of introducing hydrogen peroxide into the UV photoreactor has a considerable impact on the PVA polymer degradation and TOC removal. Besides, the combination of UV light and hydrogen peroxide is required for this process. For instance, the results also show that nearly 87% of TOC removal and a polymer reduction to 10.9 kg/mol (91.6%) were achieved when an aqueous solution containing 500 mg/L of a 130 kg/mol PVA and H₂O₂/PVA mass ratio of 10 was treated in stepwise operation (fed-batch) for 2 h reaction time. Further, the study proves that the UV/H₂O₂ process can drastically modify the structure of the PVA polymer and be a potential practice for the degradation of water-soluble polymers in wastewater.

Chapter 5

PHOTOCHEMICAL KINETIC MODELING OF PVA DEGRADATION IN BATCH RECIRCULATING UV/H₂O₂ PHOTOREACTOR

5.1. Introduction

Recently, incentives in the degradation of water-soluble polymers emerged as a new branch of polymer science and engineering with industrial applications. Fortunately, polymer chains can undergo degradation or depolymerization in a UV/H₂O₂ process which is considered as an efficient treatment process leading to numerous full-scale applications (Alfano et al., 2009; Mohajerani et al., 2009; Santos et al., 2009; Poyatos et al., 2010). Henceforth, it is worthwhile to investigate the degradation of water-soluble synthetic polymer and the devolution of their molecular weight distribution.

Lately, several attempts have been made to comprehend the chemical kinetics generally dominating the degradation of water-soluble polymers without UV radiation (McCoy and Madras, 1997; Tayal and Khan, 2000; Sonntag, 2003). In the open literature, there is little information on the photochemical mechanism of the photo-oxidative degradation of PVA polymer solutions by the UV/H₂O₂ process. Recently, few studies have proposed kinetic models assuming constant pH (Audenaert et al., 2010; Ghafoori et al., 2014). Their model was validated

using total organic carbon (TOC) data only as a surrogate parameter instead of polymer concentrations or polymer molecular weights. In addition, the experimental data in Chapter 4 reveals that the solution pH variations during the PVA degradation process as mineral acids are formed. Several studies have demonstrated that solution pH has an important impact on the process efficiency (Vinu and Madras, 2008; Hamad et al., 2014).

Nevertheless, most models assumed a constant pH (Bielski and Cabelli, 1991), even though it is known that the pH of the solution treated is poised to decrease as organic compounds are oxidized into acidic intermediates. Besides, little is known about the molecular weight of the polymer being degraded. In addition, accurate prediction of the hydrogen peroxide residual present in UV/H₂O₂ applications is of high value for system design as well as cost reduction since it requires additional reagents for the quenching of hydrogen peroxide residual (Swaim et al., 2007).

This study presents a kinetic model to describe the photochemical degradation of water-soluble PVA polymer in a UV/H₂O₂ batch recirculation photoreactor. Under the effect of UV light, the photolysis of hydrogen peroxide into hydroxyl radicals can generate a series of polymer scission reactions. For better understanding and analysis of the UV/H₂O₂ process in the cracking of the PVA macromolecules, a chemical reaction mechanism depicting the degradation process is conceptualized as a typical free-radical depolymerization initiated by the photolysis of hydrogen peroxide into hydroxyl radicals under UV light. Polymer chain scission, hydrogen abstraction, and radical recombination are included. A relevant photochemical kinetic model is, therefore, proposed to describe the disintegration of the polymer chains. Taking into account the probabilistic nature of the polymer fragments, the statistical moment approach is considered to

model the molar population balance of live and dead polymer chains incorporating a wide range of free radical reactions, including reactions leading to low molecular weight intermediate-products; such as acids and monomer of PVA. The model considers the impact of hydrogen peroxide concentration on the PVA molecular weight reduction, acidity of the solution, and hydrogen peroxide residual. In addition to data presented in Chapter 4, a new set of experiments were conducted for model validation. The experimental data served also to determine the kinetic rate constants of the PVA photochemical degradation. Measurements of the average molecular weights of the polymer, hydrogen peroxide concentrations, and pH of the PVA solution were determinant factors in constructing a reliable photochemical model of the UV/H₂O₂ process.

5.2. Reaction Mechanism of Photodegradation

The principle in the AOP process is the formation of hydroxyl radicals which react immediately with organic contaminants in the wastewater media. Under the effect of UV light of specific wavelength and using an oxidant such as hydrogen peroxide, water-soluble polymer chains can break down into smaller chains. Under the effect of radiation energy, chemical bonds of polymer chains are destabilized and weakened. The chain scission reaction is, therefore, initiated and it is defined as a bond scission that takes place in the backbone of the polymer chain. As the reaction progresses, the large polymer molecules P_r eventually break down into live and dead polymer chains of lower molecular weights, and consequently new intermediate polymeric components are formed. A further molecular disintegration can ultimately lead to carbon dioxide and water as final products in case of a complete mineralization according to the following reaction:



Under the UV irradiation, the photolysis of hydrogen peroxide generates hydroxyl radicals as follows:



The highly reactive hydroxyl radical can undergo a series of promoted dissociation reactions. Several authors (Christensen et al., 1982; Buxton et al., 1988; Liao and Gurol, 1995; Stefan et al., 1996) have proposed a detailed chemical kinetic mechanism of hydrogen peroxide decomposition (Reactions (5.3) - (5.15)) as provided in Table 5.1.

Table 5.1. Photolysis reactions of hydrogen peroxide and the rate constants.

No.	Reaction Mechanism	Rate constant	References
(5.3)	$HO^\bullet + H_2O_2 \xrightarrow{k_1} HO_2^\bullet + H_2O$	2.7×10^7	L/mol. s
(5.4)	$H_2O_2 + HO_2^\bullet \xrightarrow{k_2} HO^\bullet + H_2O + O_2$	3.0	L/mol. s
(5.5)	$H_2O_2 + O_2^\bullet \xrightarrow{k_3} HO^\bullet + OH^- + O_2$	13×10^{-2}	L/mol. s
(5.6)	$HO^\bullet + HO_2^- \xrightarrow{k_4} HO_2^\bullet + OH^-$	7.5×10^9	L/mol. s
(5.7)	$O_2^\bullet + H^+ \xrightarrow{k_5} HO_2^\bullet$	1.0×10^{10}	L/mol. s
(5.8)	$HO^\bullet + HO^\bullet \xrightarrow{k_6} H_2O_2$	5.5×10^9	L/mol. s
(5.9)	$HO_2^\bullet + HO^\bullet \xrightarrow{k_7} H_2O + O_2$	6.6×10^9	L/mol. s
(5.10)	$HO_2^\bullet + HO_2^\bullet \xrightarrow{k_8} H_2O_2 + O_2$	8.3×10^5	L/mol. s
(5.11)	$HO_2^\bullet \xrightarrow{k_9} O_2^\bullet + H^+$	1.6×10^5	1/s
(5.12)	$HO_2^\bullet + O_2^\bullet \xrightarrow{k_{10}} O_2 + HO_2^-$	9.7×10^7	L/mol. s
(5.13)	$HO^\bullet + O_2^\bullet \xrightarrow{k_{11}} O_2 + OH^-$	7.0×10^9	L/mol. s
(5.14)	$H_2O_2 \xrightarrow{k_{12}} HO_2^- + H^+$	4.5×10^{-12}	1/s
(5.15)	$HO_2^- + H^+ \xrightarrow{k_{13}} H_2O_2$	2.0×10^{10}	L/mol. s

The experimental results obtained in Chapter 4 demonstrate the existence of chemical reactions between hydrogen peroxide and the PVA polymers. Considering this experimental evidence, a photochemical kinetic mechanism is proposed next. It can therefore be postulated that the degradation of the PVA polymer occurs mainly by means of free radical chain scission reactions, the hydroxyl radical HO^\bullet and hydroperoxyl radical HO_2^\bullet which react with polymer P_r of chain length r by a hydrogen abstraction scheme; thus, giving off live polymer radicals P_r^\bullet and the formation of H_2O and H_2O_2 products as follows:



Where P_r^\bullet and P_r are active polymer radical and dead polymer of chain length r , respectively.

The chemical structure of a PVA polymer molecule is made up of carbon-carbon and carbon-hydrogen bonds. The mechanism of the photo-oxidative degradation is primarily attributed to the HO^\bullet radicals attacking the α - or β -carbon atom of the polymer chain, thus, enabling the scission of the macroradicals and yielding to polymer of a shorter chain length s and mid-chain radical with an electron being eventually placed along its chain (Kodera and McCoy, 1997; Metha and Madras, 2001; Smagala and McCoy, 2003). For instance, during a binary kinetics fragmentation, a polymer of chain length r may eventually split into two new compounds of chain length s and $r - s$ such that $1 \leq s \leq r$



In cases = 1, the random scission is merely a chain-end scission reaction. Thus, the chain-end scission is a special case of the random scission, which is expressed as α -scission of the chain radical, yielding to a different polymer radical where the electron is placed at the chain end.



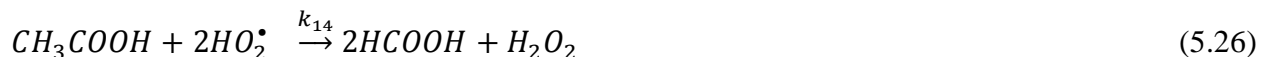
The sequence of the polymer fragmentation can be also terminated by a mutual annihilation of two live polymer radicals giving a dead polymer of chain length lower than r . Such termination reactions may occur by the combination of two polymer radicals of chain lengths s and $r - s$, thus forming a dead polymer of chain length r as follows:



The live polymer radicals may also be produced by direct photolysis of polymer according to the following reaction:



However, experimental evidence disapproved the occurrence of reaction (5.21). When polymer chain degradation goes to completion, it is postulated that a single monomer P_1 may be detached. In this case, the HO^\bullet radical and hydroperoxyl radical HO_2^\bullet can still attack one chain length polymer P_1 to form formic and acetic acids which would yield a pH change of the PVA solution. In fact, the experimental observations of Ogata et al. (1980), Zheng and Ling (2007), Taghizadeh et al. (2015) suggest the reactions below:





Besides, experimental tests performed in this study have proven an increase of the acidity of PVA aqueous solution during the course of the reaction.

5.3. Kinetic Modeling of PVA Degradation Using Batch Recirculating Photoreactor

A photochemical kinetic model was developed based on the mechanism presented in Reactions (5.2) to (5.28). For simplifications, the polymer degradation reactions are assumed irreversible and binary fragmentation is more likely to occur. For a batch reactor with recirculation, negligible degradation of the PVA polymer per pass and good mixing condition are assumed. The reaction rate constants are assumed independent of polymer chain length. Reaction (5.21) is neglected as it is experimentally proved that there is no direct photolysis of PVA polymer at the UV wavelength of 254 nm. Since the PVA degradation reaction is carried out at a constant temperature, close to ambient condition, therefore, there is no need to model the thermal energy dynamics. A theoretical description of the UV/H₂O₂ process incorporates a radiation balance of UV/H₂O₂ polymer system and a mole balance of all chemical species. Thus, the photochemical kinetic model describing the PVA polymer degradation by photo-oxidation comprises a radiation energy balance coupled with a molar balance of the chemical species participating in the degradation reactions of the polymer.

5.3.1. Photolysis rate and molar balance

The absorption of the ultraviolet energy activates the chemical species and generates

photo-oxidation reactions. Therefore, photo-oxidative chemical reactions are characterized by the generation of free radicals resulting from the interaction of photons of a proper energy level with molecules of the targeted chemical species. In fact, the absorption of the UV light by hydrogen peroxide is essential in the UV photolytic process to promote the formation of hydroxyl radicals (Jacob and Dranoff, 1970; Romero et al., 1997). As Johnson and Mehrvar (2008) suggested, the radiation balance for a single lamp annular photoreactor of nominal radius (r) is given by:

$$\frac{1}{r} \frac{d(rq)}{dr} = -q(2.303 \sum \epsilon_i C_i) \quad (5.29a)$$

Where q is the radiant energy flux (Einstein/ cm² s), ϵ_i is the molar absorptivity, C_i is the chemical species concentration. The integration of the irradiation governing Equation (5.29a) yields:

$$q = q_o \frac{R_i}{r} \left(e^{-2.303(r-R_i) \sum_{i=1}^N \epsilon_i C_i} \right) \quad (5.29b)$$

In which q_o and R_i are the energy flux on the sleeve wall before attenuation and the inner reactor radius (cm), respectively. Therefore and referring to the discussion in Section 2.3.2., the radiation-transfer equation of component i is expressed according to Beer–Lambert law as follows:

$$R_{UV,i} = \phi_i f_i q_o \frac{R_i}{r} \left(1 - \exp(-2.303 (r - R_i) \sum_{i=1}^N \epsilon_i C_i) \right) \quad (5.30)$$

Where the quantum yield ϕ_i is defined as ratio of number of moles of compound transformed to number of photon of wavelength (λ) absorbed by the compound. In which f_i is the fraction of the UV irradiation absorbed by i^{th} species:

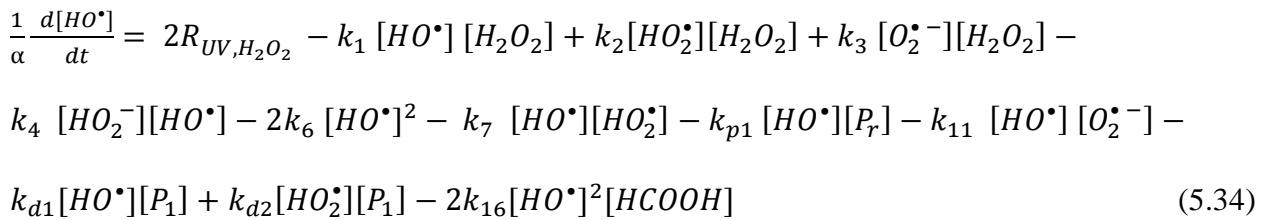
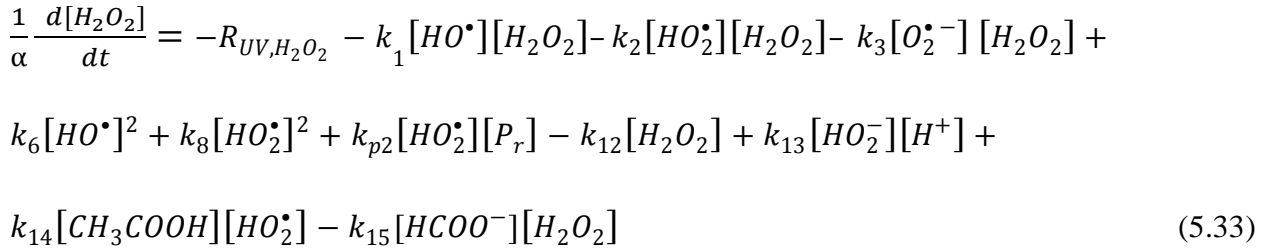
$$f_{H_2O_2} = \frac{\epsilon_{H_2O_2} C_{H_2O_2}}{\epsilon_{H_2O_2} C_{H_2O_2} + \epsilon_{PVA} C_{PVA}} \quad (5.31)$$

The quantum yield of PVA was negligible since there was no measurable change in PVA molecular weight under UV radiation alone (Hamad et al., 2014). The molar absorptivity of PVA was determined using spectrophotometer by measuring the absorbance of different concentrations of PVA aqueous solutions at wavelength of 254 nm. For the kinetics, the mole balance of a species i in a well-stirred batch recirculation reactor of a constant volume is given by (Romero et al., 1997; Alfano and Cassano, 2009):

$$\frac{1}{\alpha} \cdot \frac{dC_i}{dt} = \sum_{j=1}^m R_{ij}, \quad C_i(0) = C_{i0} \quad \text{where: } \alpha = \frac{V_{ph}}{V_T} \quad (5.32)$$

In which $C_i(t)$ is the i^{th} component concentration, V_{ph} is the volume of the photoreactor, V_T is the reservoir tank volume, $C_i(0)$ is the initial molar concentration of species i , and R_{ij} is the chemical reaction rate of component i in reaction j ($j = 1, 2, \dots, m$).

In addition to the basic photochemical mechanism given in Table 5.1, taking mole balance of small molecule species gives the following reaction rate equations:



$$\frac{1}{\alpha} \frac{d[H^+]}{dt} = -k_5[O_2^\bullet^-][H^+] + k_9[HO_2^\bullet] + k_{12}[H_2O_2] - k_{13}[H^+][HO_2^-] + k_{a1}[HCOOH]/[HCOO^-] + k_{a2}[CH_3COOH]/[CH_3COO^-] \quad (5.35)$$

$$\frac{1}{\alpha} \frac{d[HCOOH]}{dt} = k_{d1}[HO^\bullet][P_1] + k_{a1}^{-1}[H^+][HCOO^-] + k_{14}[HO_2^\bullet]^2[CH_3COOH] - k_{16}[HO^\bullet]^2[HCOOH] \quad (5.36)$$

$$\frac{1}{\alpha} \frac{d[CH_3COOH]}{dt} = k_{d2}[HO_2^\bullet][P_1] + k_{a2}^{-1}[H^+][CH_3COO^-] - k_{14}[HO^\bullet]^2[CH_3COOH] \quad (5.37)$$

$$\begin{aligned} \frac{1}{\alpha} \frac{d[HO_2^\bullet]}{dt} = & k_1 [HO^\bullet] [H_2O_2] - k_2 [HO_2^\bullet] [H_2O_2] + k_4 [HO_2^\bullet^-] [HO^\bullet] + k_5 [O_2^\bullet^-] [H^+] - \\ & k_7 [HO^\bullet] [HO_2^\bullet] - 2k_8 [HO_2^\bullet]^2 - k_9 [HO_2^\bullet] - k_{p2} [HO_2^\bullet] [P_r] - \\ & k_{10} [HO_2^\bullet] [O_2^\bullet^-] + k_{d1} [HO^\bullet] [P_1] - k_{d2} [HO_2^\bullet] [P_1] - 2k_{14} [HO_2^\bullet]^2 [CH_3COOH] \end{aligned} \quad (5.38)$$

$$\frac{1}{\alpha} \frac{d[HO_2^-]}{dt} = -k_4 [HO_2^-] [HO^\bullet] + k_{10} [HO_2^\bullet] [O_2^\bullet^-] + k_{12} [H_2O_2] - k_{13} [HO_2^-] [H^+] \quad (5.39)$$

$$\begin{aligned} \frac{1}{\alpha} \frac{d[O_2^\bullet^-]}{dt} = & -k_3 [O_2^\bullet^-] [H_2O_2] - k_5 [O_2^\bullet^-] [H^+] + k_9 [HO_2^\bullet] - k_{10} [HO_2^\bullet] [O_2^\bullet^-] - \\ & k_{11} [HO^\bullet] [O_2^\bullet^-] \end{aligned} \quad (5.40)$$

The molar balance of the macromolecules P_r and P_r^\bullet in Reactions (5.16) to (5.20) requires special modeling approach that is discussed in Section 5.3.2. As the PVA polymer is randomly broken down, polymer chains species of different sizes are subsequently generated and they are expected to degrade further. Therefore, the modeling of the polymer population is discussed next in Section 5.3.2.

5.3.2. Polymer breakage population balance

The concept of the population species is considered to express the variations of the photochemical degradation of PVA. The random degradation of polymer chains of length r can be described using breakage population balance of all polymer species. Macromolecular Reactions (5.16) – (5.20) show that the polymer consists of degrading active polymer radicals P_r^\bullet and dead polymer P_r . Polymer degradation is described by a discrete approach, so that a mass balance provides a difference-differential equation (summation). The discrete representations is therefore related by simple mathematical expressions



$$\frac{1}{\alpha} \frac{dp_r}{dt} = k_{tc} \sum_{s=1}^r [p_r^\bullet] [p_{r-s}^\bullet] \quad (5.41a)$$



This reaction requires the production of a specified scission product from any of a range of macromolecules, so a stoichiometric kernel $\Omega(r, s)$ is employed for a polymer chain of length r to represent the probability of getting shorter polymer chain lengths $r - s$ and s as presented in Equation (5.41b):

$$\frac{1}{\alpha} \frac{dp_r}{dt} = k_p \sum_{s=1}^r \Omega(r, s) [p_s^\bullet] \quad (5.41b)$$

The net accumulation rate of dead polymer chains of chain length r for Reactions (5.16), (5.17), (5.18) and (5.20) is given as follows:

$$\frac{1}{\alpha} \frac{dp_r}{dt} = -k_{p_1} [HO^\bullet] [p_r] - k_{p_2} [HO_2^\bullet] [p_r] + k_{tc} \sum_{s=1}^r [p_r^\bullet] [p_{r-s}^\bullet] + k_p \sum_{s=1}^r \Omega(r, s) [p_s^\bullet] \quad (5.41c)$$

Similarly, the net accumulation rate of live polymer radicals of chain length r is expressed as:

$$\frac{1}{\alpha} \frac{dp_r^\bullet}{dt} = k_{p_1} [HO^\bullet][p_r] + k_{p_2}[HO_2^\bullet] [p_r] - 2k_{tc} \sum_{s=1}^r [p_s^\bullet][p_{r-s}^\bullet] - k_p[p_r^\bullet] \\ + k_p \sum_{s=1}^r \Omega(r,s)[p_s^\bullet] \quad (5.42)$$

Where k_{p_1}, k_{p_2}, k_p and k_{tc} are the rate constants of Reactions (5.16) - (5.20). In general, polymer degradation occurs most likely by random chain scission. Therefore, in this study, it is postulated that there is a low probability of the occurrence of chain-end scission reactions. The stoichiometric kernel stands for the joint probability that considers the emerging polymer chains (Sonntag, 2003). For random chain scission, the distribution of shorter polymer chains is given as follows (Sterling and McCoy, 2001; Staggs, 2002):

$$\Omega(r,s) = 1/r \quad (5.43)$$

Using statistical mechanics, the concept of moments was applied to determine the molecular weight distribution of a polymer population which is given below for the dead polymer moments:

$$\mu_j = \sum_{r=1}^{\infty} r^j p_r \quad (5.44)$$

Where p_r is the polymer concentration with chain length r , μ_j is the j^{th} moment of the quantity p_r and j with values of 0, 1, or 2 stands for zeroth, first, and second moment, respectively. The application of the moment method allows converting the discrete differential population balance equations into ordinary differential ones. The moments of dead polymer P_r and live polymer radical P_r^\bullet are used to determine the average molecular weights of the polymer samples.

$$\frac{1}{\alpha} \frac{d[\mu_o]}{dt} = -k_{p1}[HO^\bullet]\mu_o - k_{p2}[HO_2^\bullet]\mu_o + k_{tc}\lambda_o^2 + k_p\lambda_o \quad (5.45)$$

$$\frac{1}{\alpha} \frac{d[\mu_1]}{dt} = -k_{p1}[HO^\bullet]\mu_1 - k_{p2}[HO_2^\bullet]\mu_1 + k_{tc}\lambda_1\lambda_1 + 0.5k_p\lambda_1 \quad (5.46)$$

$$\frac{1}{\alpha} \frac{d[\mu_2]}{dt} = -k_{p1}[HO^\bullet]\mu_2 - k_{p2}[HO_2^\bullet]\mu_2 + k_{tc}\lambda_2\lambda_2 + 0.33k_p\lambda_2 \quad (5.47)$$

The Live polymer moments is given below.

$$\lambda_j = \sum_{r=1}^{\infty} r^j p_r^\bullet \quad (5.48)$$

Where λ represents the total live polymer radical concentration. The rate of the change of the moments of live polymer radicals can be shown as follows:

$$\frac{1}{\alpha} \frac{d\lambda_o}{dt} = k_{p1}[HO^\bullet]\mu_o + k_{p2}[HO_2^\bullet]\mu_o - 2k_{tc}\lambda_o^2 \quad (5.49)$$

$$\frac{1}{\alpha} \frac{d\lambda_1}{dt} = k_{p1}[HO^\bullet]\mu_1 + k_{p2}[HO_2^\bullet]\mu_1 - 2k_{tc}\lambda_o\lambda_1 - 0.5k_p\lambda_1 \quad (5.50)$$

$$\frac{1}{\alpha} \frac{d\lambda_2}{dt} = k_{p1}[HO^\bullet]\mu_2 + k_{p2}[HO_2^\bullet]\mu_2 - 2k_{tc}\lambda_o\lambda_2 - 0.67k_p\lambda_2 \quad (5.51)$$

The number-average chain length (*NACL*) of the polymer is the ratio of the first moment to the zeroth moment of the summation of the dead polymer and the polymer radical (live polymer). It is given below:

$$NACL(t) = \frac{\mu_1(t) + \lambda_1(t)}{\mu_o(t) + \lambda_o(t)} \quad (5.52)$$

Taking the ratio of the second moments over first moments gives the weight-average chain length (*WACL*) as follows:

$$WACL(t) = \frac{\mu_2(t) + \lambda_2(t)}{\mu_1(t) + \lambda_1(t)} \quad (5.53)$$

Hence, the number average molecular weight M_n and the weight average molecular weight M_w are calculated according to:

$$M_n(t) = M_o \cdot NACL(t) \quad (5.54)$$

$$M_w(t) = M_o \cdot WACL(t) \quad (5.55)$$

Where M_o is the molecular weight of the monomer unit (i.e. Vinyl alcohol).

5.4. Experimental Approach for Model Verification

Once a mathematical model has been formulated for a process, a common approach is to compute the best estimates of the model parameters so that the model can give satisfactory predictions of the experimental data. The degradation of PVA polymer chains in aqueous solutions was carried out at constant temperature of $25\pm2^\circ\text{C}$ by means of a heat exchanger shown in Figure 3.1. A new set of experiments was performed beside the experimental data obtained in Chapter 4 to get enough data points for the validation of the model. Experimental data of 50 mg/L PVA aqueous solution and initial hydrogen peroxide concentrations of 0, 50, 250, 500 mg/L (corresponding $[\text{H}_2\text{O}_2]/[\text{PVA}]$ mass ratios of 0, 1, 5, 10 for batch system was used for estimating the unknown reaction rate constants. Also, new set of batch experiments was conducted in the present study on aqueous PVA solution of 500 mg/L and different $[\text{H}_2\text{O}_2]/[\text{PVA}]$ mass ratio for model validation. As previously mentioned PVA samples have an initial number average molecular weight of 130,000 g/mole and weight average molecular weight of 148,000 g/mole.

5.5. Selection of Parameter Estimation

The rate constants of the hydrogen peroxide photolysis reactions are listed in Table 5.1 in Reactions (5.3) to (5.15). However the rate constants in the PVA degradation reactions are not

available in the open literature. For instance, a parameter estimation scheme of $k_{p_1}, k_{p_2}, k_p, k_{d_1}, k_{d_2}$, and k_{tc} was performed in this study for the PVA photodegradation model Equations (5.33)-(5.40), (5.45)-(5.47), and (5.49)-(5.51). The variables selected to formulate the objective function were the effluent hydrogen peroxide concentration, average molecular weights, and the pH of the solution. The objective function $J(k)$ is the summation of squared errors between the model predictions and experimental data defined as follows:

$$\begin{aligned} \min J(k) = \sum_{i=1}^4 & \left[\left(1 - \frac{[H_2O_2](k)}{[H_2O_2]_{exp}} \right)_i^2 + \left(1 - \frac{M_w(k)}{M_w exp} \right)_i^2 + \left(1 - \frac{M_n(k)}{M_n exp} \right)_i^2 \right. \\ & \left. + \left(1 - \frac{pH(k)}{pH_{exp}} \right)_i^2 \right] \end{aligned} \quad (5.56)$$

Where $k = [k_{p_1} \ k_{p_2} \ k_p \ k_{d_1} \ k_{d_2} \ k_{tc}]^T$ is the vector of the rate constants to be adjusted. The parameter estimation scheme is formulated to determine the estimates of $k_{p_1}, k_{p_2}, k_p, k_{d_1}, k_{d_2}$, and k_{tc} by minimizing $J(k)$ which is subjected to the kinetic model equations (5.23)-(5.40), (5.45)-(5.47), and (5.49)-(5.55). Standard MATLAB routines of the optimization toolbox were used along with the integration routine (Version 8.1, R2013a). The process variables: H₂O₂, Mn, Mw, and pH are function of both the time t and kinetic rate constants k . Process parameters and kinetic model parameters used in this study are given in Tables 5.2 and 5.3, respectively.

Table 5.2. Physical parameters of the UV/H₂O₂ process.

UV Model Parameter		Value		References
Quantum yield of H ₂ O ₂	\emptyset_1	5.00×10^{-1}	Mol /Einstein ^b	Buxton et al., 1988
Quantum yield of PVA ^a	\emptyset_2	0.00×10^1	Mol /Einstein ^b	this study
Molar absorptivity of H ₂ O ₂	ε_1	1.87×10^1	L/mol.cm	Buxton et al., 1988
Molar absorptivity of PVA ^a	ε_2	1.75×10^2	L/mol.cm	this study
UV light intensity ^a	q_o	1.97×10^{-8}	Einstein ^b /L.s	this study

^a Parameters that are measured/calculated in this study^b Einstein= energy in one mole of photons**Table 5.3.** New estimates of reaction rate constants for PVA degradation in the UV/H₂O₂ photoreactor.

Kinetic Model Parameters		Values
k_{p1}		8.06×10^6 L/mol.s
k_{p2}		4.69×10^{-1} L/mol.s
k_p		3.66×10^2 1/s
k_{d1}		1.89×10^6 L/mol.s
k_{d2}		1.35×10^2 L/mol.s
k_{tc}		4.44×10^2 L/mol.s

5.6. Model Validation

This study discusses the development of a photochemical kinetic model to improve the current understanding of the photodegradation of a water-soluble polymer in a UV/H₂O₂ recirculating batch photochemical reactor. The numerical values of kinetic rate constants are

given in Table 5.1 and 5.3 for the hydrogen peroxide photolysis and the PVA photodegradation, respectively.

The reactor model stems for a mole balance of all the chemical species and UV radiation energy balance. Unlike most existing kinetic models on UV/H₂O₂ oxidation process, the model developed in this study does not assume a steady state hypothesis and it describes the UV/H₂O₂ dynamics in a batch photoreactor and it takes into account the variation of pH in the reacting solution. The hydrogen peroxide, pH, Mn, and Mw profiles were obtained by solving numerically the model equations (Equations (5.33)-(5.40), (5.45)-(5.47), and (5.49)-(5.55) using the MATLAB (version 8.1, R2013a) function “ode15s” since the kinetic model is composed of nonlinear and stiff ordinary differential equations. The MATLAB integration algorithm (ode15s) is a variable-order solver based on the Gear’s method using both Runge–Kutta method and backward differentiation formulas.

The experimental results showed a substantial degradation of the PVA solution in the UV/H₂O₂ process. Considering the unknown dynamical behavior of the PVA degradation process, the development of a theoretical model deemed necessary to help interpret the results of the experimental data. The experiments were repeated in replicate. The error made in the determining of the polymer molecular weights was less than 3%, whereas the error in the hydrogen peroxide concentration and pH were around 1%, as a result, error bars for experimental data are not provided. Once the parameter estimation was accomplished, a model validation was performed to test the validity of the parameter estimates. Taking into account the variation of pH, the model is able to give very good predictions for most experimental data, which confirm the adequacy of the photochemical mechanism that is proposed as well as the adequacy of the photochemical kinetic model. To further support this argument, the goodness-of-fit between

experimental y_{exp} and predicted \bar{y}_m data for each variable was then determined by calculating root mean square error (RMSE) for n' data points which is calculated as:

$$RMSE = \left(\frac{1}{n'} \sum_{i=1}^{n'} (\bar{y}_{im} - y_{iexp})^2 \right)^{1/2} \quad (5.57)$$

The results based on the polymer number and weight averages molecular weights, hydrogen peroxide residual, and pH for model prediction and the experimental data are presented in Figures 5.1 and 5.2, respectively. It is evident in this figures, there is a good agreement between the model predictions and the experimental results confirming the adequacy of the developed photochemical kinetic model.

5.7. Prediction of PVA Molecular Weights Reduction

The previous investigation (Hamad et al., 2014) demonstrated how the PVA polymer could be effectively degraded in a UV/H₂O₂ photochemical reactor. The study concluded that the rate of polymer degradation and the rate of TOC removal did not match with each other. In fact, the TOC accounts for the carbon content of all chemical species, including PVA polymers. Usually, the mineralization starts directly with pollutant degradation, however, for PVA it occurs at a later stage of the reaction. In this case, it is desired to model a specific polymer degradation as the TOC is not the right parameter to choose for the development of an adequate model for polymer disintegration in a photo-oxidation process. It is plausible to develop a model that takes into account the polymer molecular weights. Therefore, the validity of the proposed kinetic model has been examined via a direct comparison of model predictions with experimental data of the number-average molecular weights M_n and weight-average molecular weights M_w of PVA.

The polymer molecular weight averages decrease with an increase of hydrogen peroxide concentration up to a certain limit. Therefore, a higher level of hydrogen peroxide has an adverse effect on the molecular weight decrease. The molecular weight reduction threshold can be interpreted by the scavenging effect of H_2O_2 over hydroxyl radicals which hinders the radical degradation since the amount of H_2O_2 added to the system is proportionally high. Figures 5.3 and 5.4 show the model predictions of the decay of both M_n and M_w as a function of irradiation time. The R^2 and RMSE values of 0.9915 and 0.036 for M_n and 0.9938 and 0.032 for M_w , respectively reveal that an excellent agreement was obtained between theoretical and experimental data. Evidently, the PVA molecular weights continue to fall with irradiation time which supports the success of the degradation process. The reduction in molecular weights is quite rapid in the first 60 min of the irradiation and it slows down in subsequent radiation time periods. Therefore, the rapid decrease in the polymer molecular weights asserts that random chain scission mechanism dominates initially in the photo-oxidative degradation of polyvinyl alcohol. In random chain scission, all bonds may have an equal probability of being cleaved along the polymer chain. Obviously, the degradation process leads to a steep decrease in molecular weights. In other words, the chain cleavage occurs and effectively shortens the polymer chains. After the first 60 min of reaction, the chain scission reactions occurring most likely at the polymer chain end giving off a single monomer molecule when the polymer PVA has been considerably degraded whereas at the beginning of the reaction, the PVA degradation occurs mostly by random chain scission which explains the drastic decrease in the polymer concentration.

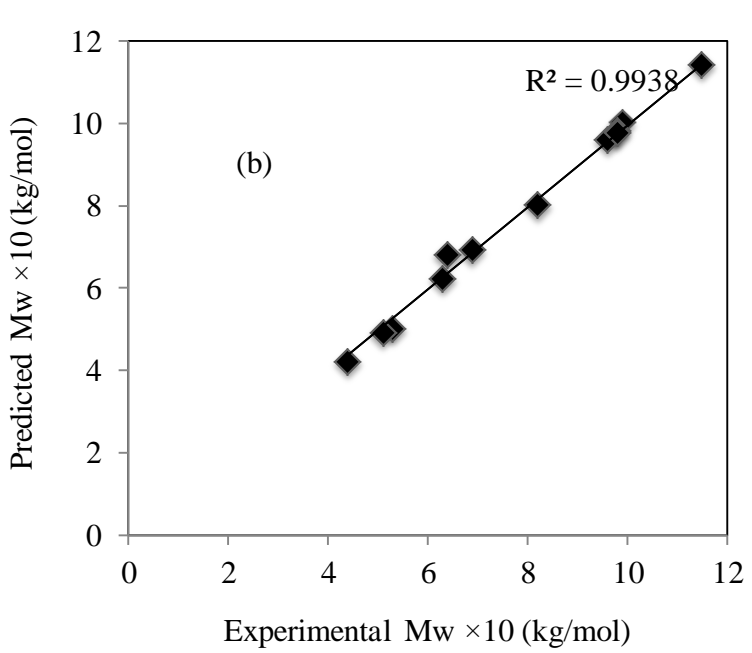
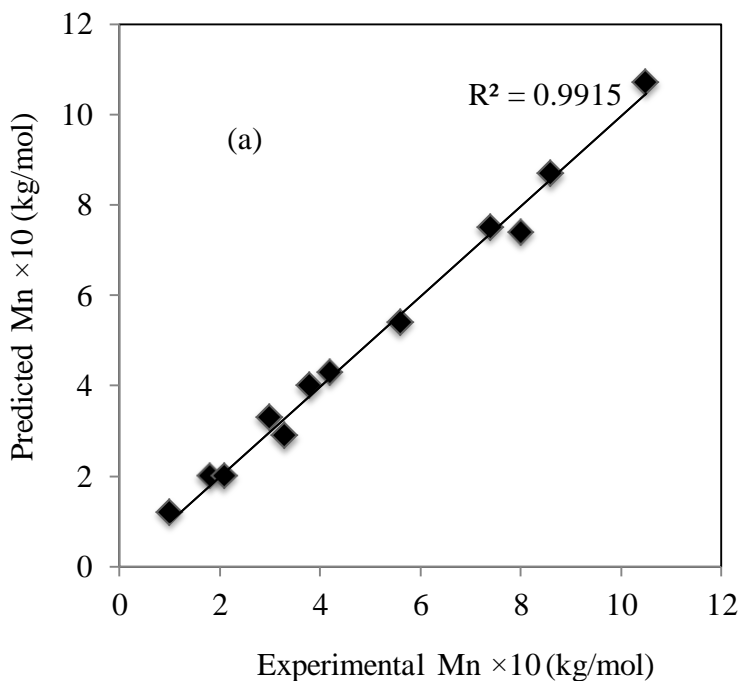


Figure 5.1. Model verification plots for PVA (a) number and (b) weight averages molecular weights in a batch UV/H₂O₂ photoreactor, [PVA]₀=500 mg/L at H₂O₂/PVA mass ratios of 0.2, 1, and 5.

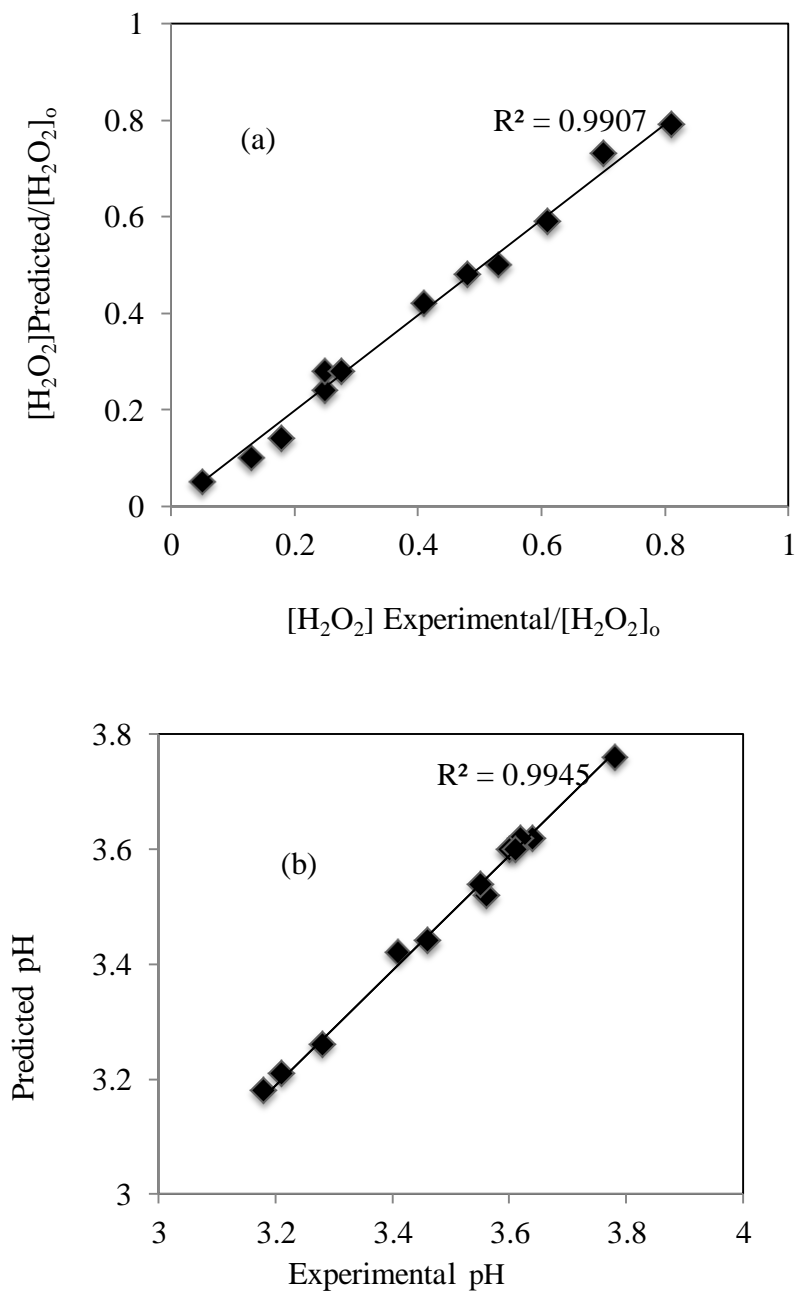


Figure 5.2. Model verification plots for (a) hydrogen peroxide residual and (b) solution pH in a batch UV/ H_2O_2 photoreactor, $[\text{PVA}]_0=500 \text{ mg/L}$ at $\text{H}_2\text{O}_2/\text{PVA}$ mass ratios of 0.2, 1, and 5.

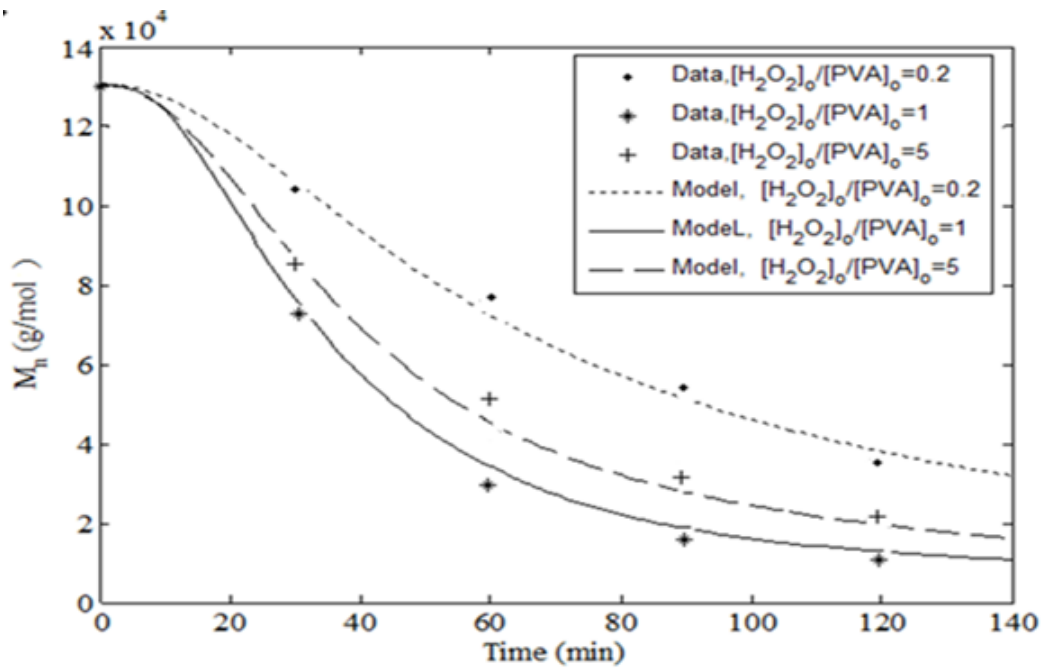


Figure 5.3. Variation of the number average molecular weight M_n of PVA in a batch UV/ H_2O_2 photoreactor, $[PVA]_0=500\text{ mg/L}$ at $[H_2O_2]/[PVA]$ mass ratios of 0.2, 1, and 5.

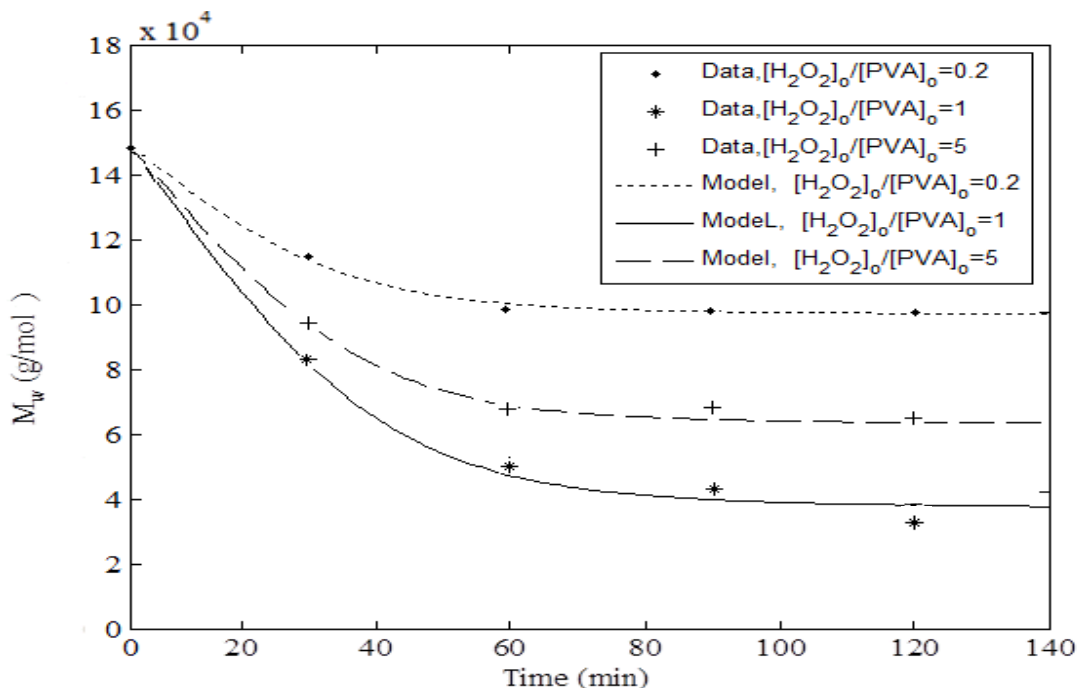


Figure 5.4. Variation of the weight average molecular weight M_w of PVA in a batch UV/ H_2O_2 photoreactor, $[PVA]_0=500\text{ mg/L}$ at $[H_2O_2]/[PVA]$ mass ratios of 0.2, 1, and 5.

5.8. Predictions of Hydrogen Peroxide Consumption

In fact, the initial amount of H_2O_2 poured into PVA solution affects considerably the performance of the reaction. The magnitude of the hydrogen peroxide impacting on the PVA degradation has been experimentally discussed in Section 4.3. For better representation of the experimental and theoretical data profile, it is convenient to plot hydrogen peroxide residual ratio versus time.

For instant, Figure 5.5 shows the variation of the hydrogen peroxide concentration versus time for both experimental data and model predictions as it indicates a successful model validation. The high coefficient of determination R^2 value of 0.9907 as shown in Figure 5.2a, and low RMSE value of 0.022 confirmed a good agreement between experimental data and model predictions.

Under the effect of UV light, hydrogen peroxide is readily decomposed into hydroxyl radicals of high reactivity which become oxidizing agents and can immediately attack the chains resulting in polymer disintegration. In addition, increasing the initial hydrogen peroxide concentration lowers the rate of hydrogen peroxide consumption. This characteristic is better represented by Beer-Lambert law and the definition of overall quantum yield. Under UV irradiation, the overall photolysis rate of a pure hydrogen peroxide solution is expressed as:

$$R_{UV,H_2O_2} = \phi_{H_2O_2} I_o (1 - e^{-A'}) \quad (5.58)$$

$$\text{Where } A' = 2.303 b \cdot \varepsilon \cdot [H_2O_2] \quad (5.59)$$

In which $\phi_{H_2O_2}$ is the overall quantum yield of hydrogen peroxide with concentration $[H_2O_2]$ and A' is the optical density of the system, which is primarily a function of hydrogen peroxide concentration.

The photolysis rate expression $R_{UV,i}$ can, therefore, be simplified. For a very small value of A' , the photolysis of hydrogen peroxide is reduced to a first order reaction rate as:

$$R_{UV,i} \approx \phi_{H_2O_2} I_o A' \approx \phi_{H_2O_2} I_o 2.303 b. \varepsilon. [H_2O_2] \quad (5.60)$$

Therefore, the H_2O_2 photolysis rate is directly proportional to the initial concentration of hydrogen peroxide.

However, when the optical density A' becomes important, the exponential term e^{-A} vanishes and the H_2O_2 photolysis rate becomes independent of the initial concentration as follows:

$$R_{UV,i} \approx \phi_{H_2O_2} I_o \quad (5.61)$$

This result implies that using excess hydrogen peroxide in the treatment process not only impedes the removal rate of the organic pollutants, but also high hydrogen peroxide residual remains in the treated solution which can negatively affect the operating cost of the photoreactor system.

5.9. Predictions of the Acidity of the Treated Polymer Solution

Knowing the important amount of acids in wastewater treatment, the solution pH was measured during the experimental testing. It has been proven experimentally (Vinu and Madras, 2008; Hamad et al., 2014) that the acidity of the polymer solution did not remain constant, rather it became more acidic. The experimental finding indicates that there is evidence of the formation of carboxylic acids associated with the degradation of the monomer produced at complete degradation of PVA polymer. Therefore, the photochemical kinetic mechanism incorporates the acidity aspect of the solution as the polymer degradation progresses.

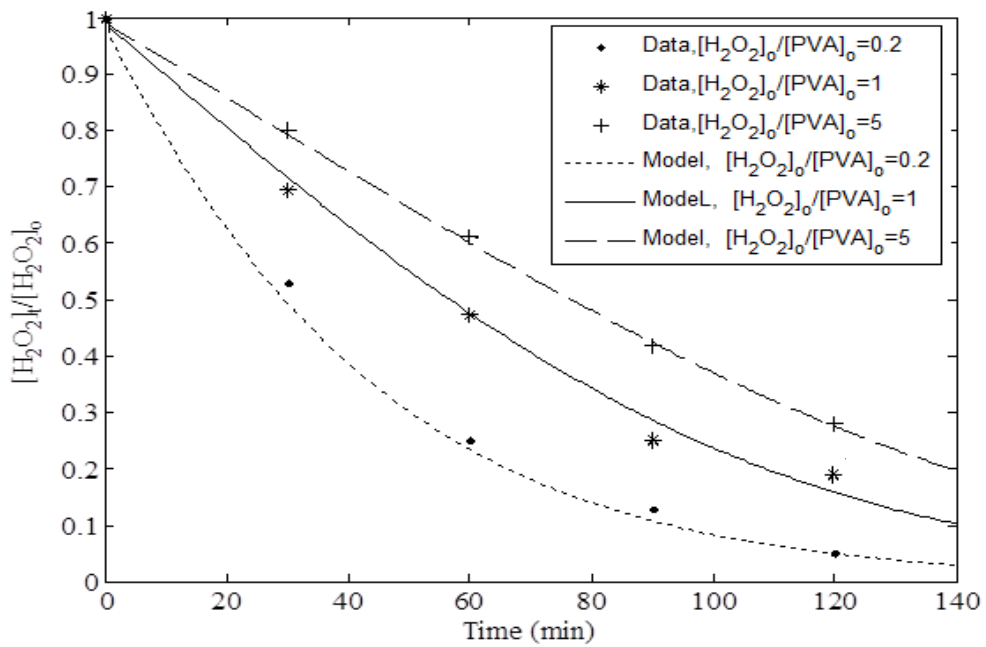


Figure 5.5. Model prediction versus experimental data for hydrogen peroxide consumption during the degradation of PVA in a batch UV/ H_2O_2 photoreactor. $[PVA]_0=500$ mg/L at $[H_2O_2]/[PVA]$ mass ratios of 0.2, 1, and 5.

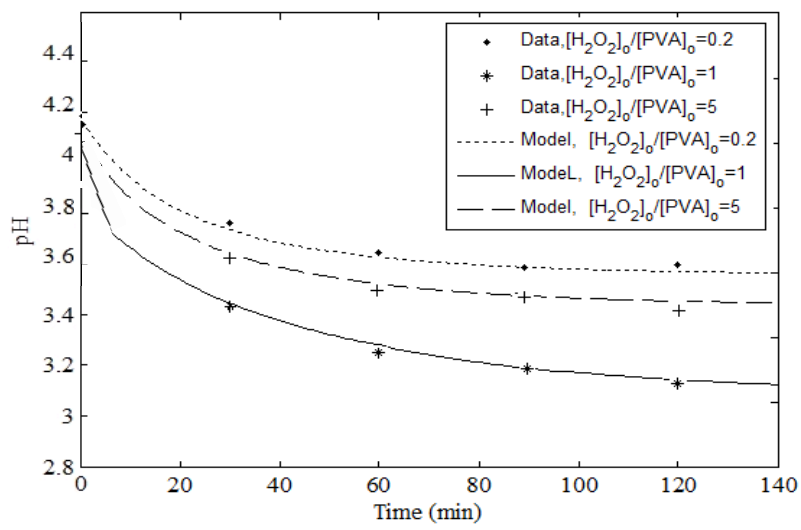


Figure 5.6. Variation of pH during the degradation of PVA in a batch UV/H₂O₂ photoreactor.

[PVA]₀=500 mg/L at [H₂O₂]/[PVA] mass ratios of 0.2, 1, and 5.

The photochemical kinetic model provides the concentration of H^+ from which the pH of the polymer solution was calculated:

$$pH = -\log[H^+] \quad (5.62)$$

Figure 5.6 shows the variation of the solution pH versus time. The model predicts the pH experimental data with R^2 value of 0.9945 and RMSE value of 0.017.

The observed decrease of the polymer solution pH is evidently associated with the formation of acidic organic intermediates remaining in the treatment process. The removal of total organic carbon (TOC) was found to be relatively lower than the PVA removal which could be interpreted by the presence of intermediate oxidation products, proving a growing acidity of the solution as the PVA degradation proceeds. Although the PVA molecular weight averages decreased considerably, the mineralization did not occur during the 2 h photochemical reaction. Yet, the pH tends to stabilize after 60 min. The stability of the pH may be due to the resistance of some intermediate products to photo-oxidation such as acetic acid. The acids could be oxidized further to produce carbon dioxide and water if the necessary oxidative conditions were provided. Formic acid is a carboxyl acid with a small molecular weight and it is more biodegradable than PVA polymer while acetic acid in particular is known to be refractory to photo-oxidation which is considered as a major limitation of the advanced oxidation technology.

5.10. Concluding Remarks

Using molar balance of all chemical species and radiation energy balance, a photochemical kinetic model was developed based on a postulated photochemical mechanism. The model describes the hydrogen peroxide consumption, PVA molecular weights variation, production of acids, and hence, the reduction of the solution pH. Using experimental data collected in a half-liter photochemical batch reactor, parameter estimation was performed to

determine the optimal estimates of the reaction rate constants. The proposed model is an adequate representation of the degradation of PVA in a UV/H₂O₂ batch recirculating process. Considering the importance of hydrogen peroxide in the AOP performance, the model can be used to determine optimum H₂O₂ concentrations for a better photochemical degradation of PVA in wastewater.

In comparison to previous studies, this model incorporates novel features by accounting for the scavenging effect of hydrogen peroxide as well as the variation of pH, therefore it provides a good understanding of the real characterization of UV/H₂O₂ process. Experimental data showed an increase of the solution acidity as the long polymer chains are broken down. The kinetic rate constants were determined by parameter estimation scheme. The estimated values of the kinetic parameters k_{p1} , k_{p2} , k_p , k_{d1} , k_{d2} , and k_{tc} were found to be 8.06×10^6 L/mol.s, 4.69×10^{-1} L/mol.s, 3.66×10^2 1/s, 1.89×10^6 L/mol.s, 1.35×10^2 L/mol.s, and 4.44×10^2 L/mol.s. The model predictions are in good agreement with experimental data of hydrogen peroxide, polymer average molecular weights, and pH of the solution with maximum RMSE of less than 4% for all the estimations. The proposed model represents a new approach to investigate the variations in polymer molecular weights. This study can contribute in enhancing the design of industrial UV/H₂O₂ processes for the treatment of wastewaters contaminated with water-soluble polymers.

Chapter 6

A NOVEL CONTINUOUS PHOTOREACTOR

In this chapter, a novel continuous UV/H₂O₂ photochemical reactor system was designed and experimentally tested to demonstrate its performance to disintegrate PVA polymer in aqueous solutions. A high caliber performance of a photoreactor using hydrogen peroxide as an oxidant to degrade unwanted organic components can only be achieved if there is a continuous supply of the oxidant.

6.1. Introduction

The introduction of hydrogen peroxide into the UV/H₂O₂ process is very important since its lower amount leads to lower efficiency while its higher amount causes to reverse the photoreaction due to its scavenging effect on hydroxyl radicals (Mehrvar et al., 2001; Hamad et al., 2014; 2015b). In addition, any residual of hydrogen peroxide beyond threshold amount in the effluent is toxic to microorganisms. Therefore, an innovative treatment technique with hydrogen peroxide feeding strategies was designed and applied in order to minimize the UV dosage and hydrogen peroxide consumption and residual, while to enhance the process performance. This study investigates the reduction of the polymer molecular weights and TOC concentration in aqueous PVA solutions in a continuous UV/H₂O₂ photoreactor, which performance was examined for different inlet PVA and hydrogen peroxide concentrations and different various

flow rates. Response surface methodology involving the Box-Behnken method is adopted to design a set of experiments for a better understanding of the operating variables impact on the process performance.

In the first part of this section, an experimental design is used to investigate the advanced oxidation of aqueous PVA, a non-biodegradable synthetic water-soluble polymer. Also, the effects of the inlet PVA concentration, the inlet H₂O₂ dosage, and the feed flow rate on the photodegradation of PVA by UV/H₂O₂ process are investigated. The optimal values of parameters are determined by means of three-factor, three-level Box-Behnken design (BBD) combined with response surface methodology (RSM) and quadratic programming. In the second part of this study, a mathematical model is developed to predict the percent TOC removal, PVA molecular weight, and percent hydrogen peroxide residual as the output variable in the UV/H₂O₂ process.

6.2. Photoreactor Design and Operation

Most of the experimental studies were carried out in a conventional batch operation for wastewater treatment (Ranby, 1989; Kaczmarek et al., 1998; Zhang et al., 2004; 2011; Santos et al., 2009). The limitation of this process has been somehow overlooked in open literature. Exploiting the advantages of studying the effect of hydrogen peroxide feeding strategy is quite scarce. All previously published data employed systems where hydrogen peroxide was injected into the feed tank containing wastewater prior to the UV radiation. Therefore, the purpose of this new investigation is to establish a qualitative study on a continuous UV/H₂O₂ process for the degradation of water-soluble polymers.

A schematic diagram of the entire system consisting of the photoreactors, pumps, and storage tanks, is shown in Figure 3.2 The experimental setup has been explained in Section 3.4 Referring to the UV/H₂O₂ process diagram in Figure 3.2, the present study describes a new experimental procedure with two photoreactors connected in series where the PVA solution is fed into the first photoreactor and hydrogen peroxide can be continuously fed into the inlet of each photoreactor. The photoreactor is provided with a horizontal tube as an outlet extending into the zone of UV radiation for directing hydrogen peroxide into the waste stream exactly at the UV radiation zone. The tubing for injection is disposed to prevent H₂O₂ from being affected by the UV irradiation prior to mixing with waste stream. The inserted tube for the hydrogen peroxide is extended toward the middle and vertically to the direction of flow. This design arrangement ensured that the hydrogen peroxide load does not exposed to the UV light or mixed with the polymer solution until all three components (polymer solution, hydrogen peroxide, and UV light) are present simultaneously.

This aim of this process is to determine the desirable dosage level of the oxidant to obtain higher rates of TOC removal and polymer degradation with the minimum hydrogen peroxide residual. Furthermore, hydrogen peroxide is directly injected into the UV radiation zone. The UV lamp is switched on and operated on the mixture for a period of five minute before the first sample is collected and before any hydrogen peroxide has been introduced. In these experiments, various volumes of hydrogen peroxide were supplied and delivered to the inlet of photoreactor by employing a peristaltic pump. The pump rate can be adjusted so that the entire charge of hydrogen peroxide is delivered equivalently to the UV photoreactor over the reaction time. Polymer solution is delivered to the system by a peristaltic pump from the holding tank.

The experimental procedure includes preparing a stock solution using solid PVA for the purpose of the runs as described in Section 3.3, then delivering the solution with a known PVA concentration into the photoreactor by a peristaltic pump (model A-100N FLEXFLO, Blue-White) with a flow capacity of 600 mL/min and simultaneously introducing the required amount of hydrogen peroxide into the inlet of each photoreactor. Basically, hydrogen peroxide stream was merged into the untreated polymer solution immediately before the exposure to UV irradiation zone. After a specified residence time, samples of the treated solution were withdrawn from the effluent tank, and then analyzed for TOC content, remaining hydrogen peroxide residual, and the PVA molecular weight distributions.

6.3. Experimental Design Using Box-Behnken Design (BBD)

The Box-Behnken design method incorporating quadratic programming (QP) was employed to determine process conditions that lead to maximize the TOC removal as well as to minimize the PVA polymer molecular weight (M_w) and hydrogen peroxide residuals. The quadratic programming is a multivariable optimization problem which has a quadratic objective function constrained by a set of linear equations.

Referring to Table 6.1., the variables x_1 , x_2 , and x_3 denote the inlet concentrations of PVA, H_2O_2 , and flow rate of the feed, respectively. These variables are selected as the key factors or independent variables of the UV/ H_2O_2 process operating in continuous mode. The percent TOC removal, the polymer molecular weight, and the hydrogen peroxide residual are considered as the dependent factors or process responses.

Due to the expected interaction between the variables considered, linear relations are not suitable to estimate process response data. Therefore, the experimental data were fitted to the following second-order equation:

$$y = b_o + \sum_{i=1}^n b_i x_i + \sum_{i=1}^n b_{ii} x_i^2 + \sum_{i=1}^{n-1} \sum_{j=2}^n b_{ij} x_i x_j \quad (6.1)$$

Where y represents the process outputs, n is the number of key independent factors or variables, b_o is the regression coefficient at the intercept, and b_i , b_{ii} , and b_{ij} are the regression coefficients for the linear, quadratic, and interaction of each factor x_i , respectively. According to the design of experiments, the mathematical model is used for theoretical prediction of process responses and determination of the optimum operating conditions. The multiple response approach enables the optimization of all factors simultaneously. Therefore, the inlet concentration of hydrogen peroxide can be adjusted to the required target level. As previously mentioned, PVA aqueous solutions with concentrations of 500, 1000, and 1500 mg/L were considered for the experimental tests. In fact, PVA samples with concentrations of 500 to 1500 mg/L are fairly a good paradigm of polymer concentration existing in actual effluents in the textile industrial plants (Kang et al., 2000; Ciner et al. 2003). Nonetheless, experiments with dilute solution (10-50 mg/L) of PVA remain merely academic exercise and the outcome of which would not reflect the conditions of actual plants.

The variables were coded at three levels -1 , 0 , and $+1$; to represent the lowest, average and highest numerical values of each inlet variable (i.e. key variable) as shown in Table 6.1. Experimental values were compared with the predicted ones to validate the adequacy of the developed RSM model. An experiment at the proposed optimum operating conditions was also conducted to verify the optimum response values predicted by the model.

The continuous operation of the photoreactors shown in Figure 3.2 consists of varying the PVA solution flow rates, the polymer inlet concentration, and the concentration of hydrogen peroxides fed into the photoreactors. First, the tank was filled with a PVA aqueous solution of a given concentration which was continuously pumped into the photoreactor for a period equal to the residence time depending on a selected flow rate. The extent of the PVA degradation in the UV/H₂O₂ process was analyzed for the continuous mode of operation.

6.4. Response Surface Methodology for Model Development

Response surface methodology (RSM) based on the Box-Behnken design (BBD) was employed to develop a set of experiments to determine a relationship between independent and response variables. Based on the data in Table 6.1, a set of fifteen experiments generated by Box-Behnken experimental design (Table 6.2) with three variables were conducted to determine the response pattern and then to establish an input-output model.

Table 6.1. Experimental ranges and coded levels of the independent variables employed in Box-Behnken design.

Independent Variable	Level and Range of independent variable			
		-1	0	1
Actual variable	Coded variable			
PVA inlet concentration (mg/L)	x_1	500	1000	1500
H ₂ O ₂ inlet concentration (mg/L)	x_2	390	585	780
Feed flow rate (mL/min)	x_3	50	100	150

Table 6.2. Three-factor three-level experimental design generated by Box-Behnken design.

Run	Independent Coded Variable		
	PVA inlet concentration (mg/L)	H ₂ O ₂ inlet concentration (mg/L)	Feed flow rate (mL/min)
1	1000 (0)	585 (0)	100 (0)
2	500 (-1)	390 (-1)	100 (0)
3	500 (-1)	585 (0)	150 (1)
4	1000 (0)	390 (-1)	150 (1)
5	1500 (1)	585 (0)	150 (1)
6	1500 (1)	585 (0)	50 (-1)
7	1000 (0)	780 (1)	150 (1)
8	500 (-1)	780 (1)	100 (0)
9	1000 (0)	585 (0)	100 (0)
10	1500 (1)	780 (1)	50 (-1)
11	1500 (1)	780 (1)	100 (0)
12	1000 (0)	390 (-1)	50 (-1)
13	1500 (1)	390 (-1)	100 (0)
14	500 (-1)	585 (0)	50 (-1)
15	1000 (0)	585 (0)	100 (0)

All experimental runs were conducted in the two photoreactor processes (Figure 3.2) operating in a continuous mode. The samples were collected at the outlet of the second photoreactor and were subsequently analyzed to determine the amount of TOC removed, the extent of degradation of the PVA polymer chains and the amount of hydrogen peroxide remaining in the outlet stream. The experimental results in Table 6.3 demonstrate that a TOC removal varying from 16.11 % (run #13) to 42.70% (run #14) along with a reduction of the PVA molecular weight ranging between 56.29 kg/mol (run #13) and 5.46 kg/mol (run #3) (corresponding to 56.7 % and 95.30% reduction) were achieved. This is a considerable reduction of the PVA polymer number average molecular weight from its initial value of 130 kg/mol.

The TOC removal was significantly lower than the molecular weight reduction due to the generation of the intermediate oxidation products which contribute to the TOC content of the treated PVA solution. The results also show that the maximum value of hydrogen peroxide residual was 4.25% (run #3). Therefore, the continuous UV/H₂O₂ process evidently facilitated the degradation of highly concentrated polymer solutions using a relatively low hydrogen peroxide inlet concentration in a short residence time ranging from 6.13 to 18.4 min. Having performed all fifteen experimental tests as indicated in Table 6.2 with their results in Table 6.3, it is worth to develop an input-output experimental model by means of the BBD procedure. Hence, a response surface quadratic model was established as follows:

$$y_1 = 27.2375 - 0.04895 x_1 + 0.13897 x_2 - 0.01408 x_3 - 0.00001 x_1^2 + 0.00011 x_1 x_2 - 0.00002 x_1 x_3 - 0.00020 x_2^2 - 0.00004 x_2 x_3 - 0.00034 x_3^2 \quad (6.2)$$

Table 6.3. Experimental results of the measured responses of PVA degradation in continuous UV/H₂O₂ process.

Run	Process Responses		
	TOC removal%	PVA M _n (kg/mol)	H ₂ O ₂ residual%*
1	33.38	15.34	2.02
2	41.71	06.11	1.16
3	34.08	05.46	4.25
4	22.23	44.46	1.39
5	29.40	43.29	2.50
6	35.68	18.47	1.52
7	30.24	24.83	1.71
8	19.43	29.12	3.84
9	33.42	15.86	1.93
10	40.06	17.17	0.82
11	37.37	20.41	1.07
12	30.45	26.50	1.12
13	16.11	56.29	1.67
14	42.70	06.50	3.33
15	33.04	16.38	1.94

$$* H_2O_2 \text{ residual \%} = \frac{[H_2O_2]_{outlet}}{[H_2O_2]_{inlet}} \times 100$$

$$y_2 = 27.4334 + 0.07604 x_1 - 0.18683 x_2 + 0.09372 x_3 + 0.00005 x_1^2 - 0.00015 x_1 x_2 + 0.00026 x_1 x_3 + 0.00029 x_2^2 + 0.00026 x_2 x_3 + 0.00057 x_3^2 \quad (6.3)$$

$$y_3 = -4.02513 - 0.00552 x_1 + 0.03199 x_2 + 0.01242 x_3 - 0.00001 x_1^2 - 0.00001 x_1 x_2 + 0.00002 x_2^2 + 0.00002 x_2 x_3 + 0.00005 x_3^2 \quad (6.4)$$

Where y_1 , y_2 , and y_3 are the TOC percent removal, the PVA molecular weight (g/mol), and the hydrogen peroxide percent residual, respectively; whereas x_1 , x_2 , and x_3 are input variables defined in Table 6.1. The model can be used to predict the process responses at other experimental conditions within the ranges specified in Table 6.2. The predictive quality and reliability of the model are discussed in Section 6.5. The predicted values were compared with experimental data to validate the adequacy of the developed RSM model. An experimental test at the proposed optimum operating conditions was also conducted to verify the optimum response values predicted by the model. In addition, seven random experimental runs were also performed to validate the model.

6.5. Statistical Data Analysis

On the basis of the analysis of variance (ANOVA) and the multi-regression method, the quadratic model (Equations (6.2) - (6.3)) was found to accurately represent the experimental data. As shown in Figures 6.1 to 6.3, there is a good agreement between the experimental data and the model with the coefficients of determination (R^2) of 95.34, 96.22, and 92.42%, respectively. Table 6.4 shows the coefficients of each process response (TOC removal %, MW kg/mol, H₂O₂ residual %) and the p-value of each coefficient in the model. The *p*-value indicates the probability value used to set the confidence level at 95% as well as to ascertain the importance of each coefficient. The low probability value (*p*-value < 0.05) indicates that the

corresponding key variable is highly significant. In addition, the high values of coefficient of determination R^2 and adjusted R_{adj}^2 indicate that the developed RSM model (Equations (6.2)-(6.4)) predicts accurately the experimental data within the experimental conditions for the collected data. Besides the high R_{adj}^2 values (in Table 6.4) reflect the model capability to predict the experimental points that are not used for model development.

6.6. Model Predictions for the Individual Effect of Process Parameters

The performance of the UV/H₂O₂ process for the treatment of aqueous PVA during a continuous flow operation was assessed by three-factor, three-level Box-Behnken experimental design which employs three dependent process responses that are the TOC removal, the PVA polymer molecular weight, and the hydrogen peroxide residual. Table 6.5 shows the seven experimental runs conducted to verify the model validity. The single effects of the independent variables (inlet PVA concentration, inlet hydrogen peroxide concentration, and feed flow rate) are quite significant. Therefore, each key factor can affect the efficiency of the PVA degradation process. Figures 6.4-6.6 show the variation of the process responses with the independent variables.

Compiling the data of all fifteen experimental runs (Table 6.3) and using RSM analysis, the plots shown in Figures 6.4-6.6 were generated to study the individual effects of process parameters. Each plot depicts the variation of one response with respect to one key factor while the other two factors were kept invariant at their respective central points. According to Table 6.5, the *p*-values of the independent variables (inlet PVA concentration, inlet hydrogen peroxide concentration, and feed flow rate) are less than 0.05. Therefore, each key factor can

significantly affect the efficiency of the PVA degradation in a continuous process. Figures 6.4 to 6.6 show the variations of the process responses with the key variables. For instance, to study the single effect of PVA inlet concentration, plots (a) in Figures 6.4 to 6.5 were obtained as both the hydrogen peroxide inlet concentration and the flow rate were kept constant and equal to their central values of 585 mg/L and 100 mL/min, respectively. As shown in plots (a) in Figures 6.4 and 6.5, TOC removals of 28 and 33% were achieved with PVA average molecular weight reductions of almost 30 and 16 kg/mol for inlet PVA concentrations of 1500 to 500 mg/L, respectively. In fact, the inlet PVA concentration inversely affected the TOC removal. The reduction in the degradation rate can be interpreted by the decrease in the production of hydroxyl radicals. Since increasing the polymer concentration in the solution reduces the absorbance of UV radiation by hydrogen peroxide, it results in a reduction of hydroxyl radicals (Hamad et al., 2015a).



As previously mentioned, hydroxyl radicals are mainly responsible for the polymer chain degradation. Hydroxyl radicals react with the PVA polymer P_r by a hydrogen abstraction, thus giving off active polymer radicals P_r^\bullet of chain length r which may eventually split into two smaller molecules of chain length s and $r - s$ such that $1 \leq s \leq r$ according to the following reactions:



Table 6.4. Regression coefficients and probability values of statistical analysis for the prediction of the process responses of the continuous UV/H₂O₂ photoreactor.

Regression Coefficient	Coefficient for TOC model	p-value	Coefficient for polymer Mw	p-value	Coefficient for H ₂ O ₂ residual	p-value
b_1	-0.04895	0.0244*	0.07604	0.0100*	-0.00552	0.0032*
b_2	0.13897	0.0321*	-0.18683	0.0380*	0.03199	0.0046*
b_3	-0.01408	0.0423*	0.09372	0.0430*	0.01242	0.0224*
b_{11}	-0.00001	0.1236	0.00005	0.1211	-0.00111	0.0199*
b_{12}	0.00011	0.0008*	-0.00015	0.0002*	-0.00001	0.0309*
b_{13}	-0.00002	0.0225*	0.00026	0.0066*	0.00000	0.9092
b_{22}	-0.00020	0.0048*	0.00029	0.0480*	0.00002	0.0401*
b_{23}	-0.00004	0.8042	0.00026	0.3908	0.00002	0.3452
b_{33}	-0.00034	0.6180	0.00057	0.5820	0.00005	0.5202
R^2	95.34		96.22		92.42	
R^2_{adj}	90.90		93.65		90.38	

*Significant value at the level of p-value ≤ 0.05

Table 6.5. Randomized experimental runs for the RSM model verification of the continuous UV/H₂O₂ process.

Run	Independent Variable		
	PVA inlet concentration (mg/L)	H ₂ O ₂ inlet concentration (mg/L)	Feed flow rate (mL/min)
1	500	585	100
2	1000	585	100
3	1500	585	100
4	1000	390	100
5	1000	780	100
6	1000	585	50
7	1000	585	150

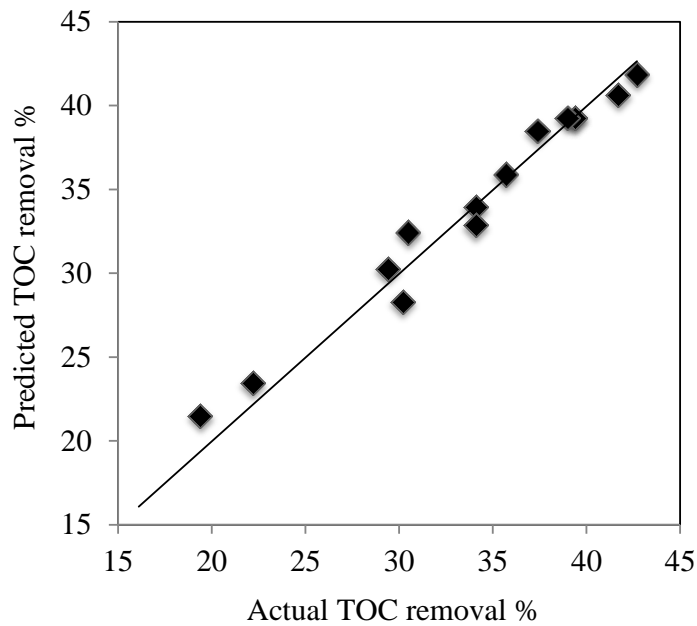


Figure 6.1. RSM model verification plots for percent TOC removal response in the continuous UV/H₂O₂ process.

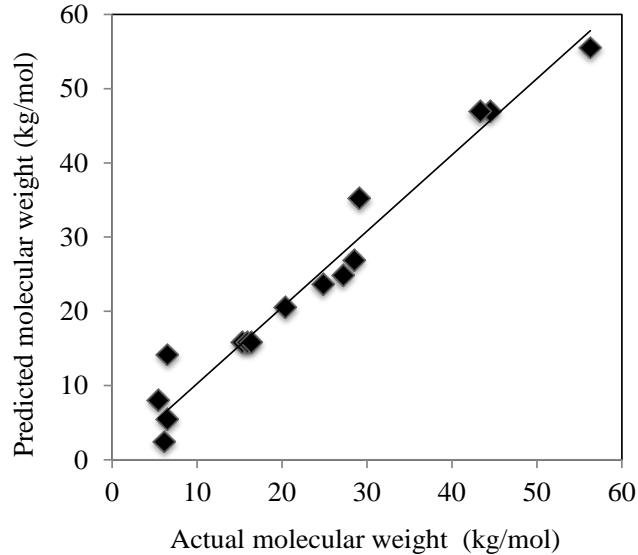


Figure 6.2. RSM model verification plots for PVA molecular weight (kg/mol) response in the continuous UV/H₂O₂ process.

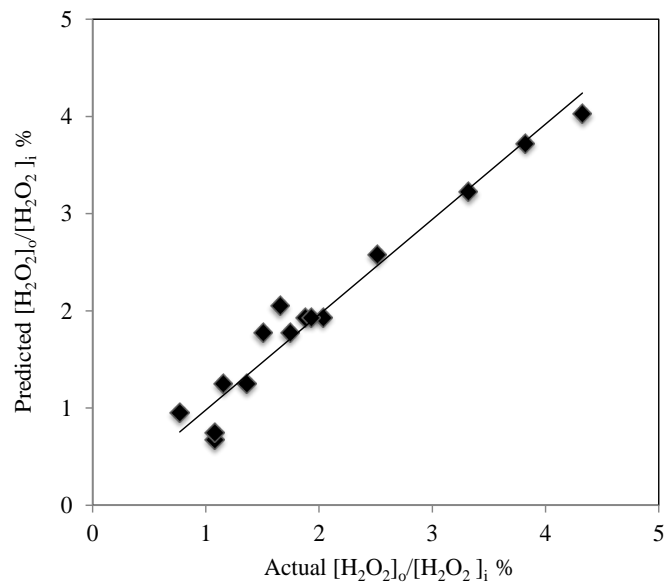


Figure 6.3. RSM model verification plot for percent H₂O₂ residual as an output response in the continuous UV/H₂O₂ process.

On the other hand, maintaining the inlet PVA concentration invariant at central value of 1000 mg/L and the inlet hydrogen peroxide concentrations at 585 mg/L (plots c in Figures 6.4 and 6.5), the continuous operation of the photoreactor increased the TOC removal from 29 to 36% and reduced the molecular weight of the PVA polymer to about 20.8 and 6.5 kg/mol, when the flow rate changed from 150 to 50 mL/min, respectively. However, by keeping both the inlet PVA concentration and the flow rate constant (plots b in Figures 6.4 and 6.5) and varying the inlet hydrogen peroxide concentration from 390 to 780 mg/L, the TOC removal of 25% with PVA molecular weight of 32 kg/mol augmented to 34% TOC removal with PVA molecular weight of 15 kg/mol and then the TOC was decreased to about 29% with PVA molecular weight of 22 kg/mol. Plots b in Figures 6.4 and 6.5 depict the dual effects of hydrogen peroxide for the degradation of PVA. The effect of hydrogen peroxide on the PVA degradation can be interpreted in terms of two aspects. First, increasing hydrogen peroxide enhances the PVA chain degradation due to the increase in the production of the hydroxyl radicals according to Reaction (6.5). Second, further increase in hydrogen peroxide beyond the optimum concentration results in a decrease in the degradation rate due to the consumption of hydroxyl radicals by hydrogen peroxide which acts as free radical scavenger according to the following reaction (Mehrvar et al., 2001):



Increasing the exposure time by lowering the feed flow rate resulted in higher degradation efficiency as confirmed by the linear and quadratic regression coefficients of the feed flow rate (x_3) presented in Table 6.4.

Moreover, the signs of the regression coefficient terms in Equations (6.2)–(6.4) provide physical significance of the obtained results. For instance, the positive value of the linear

regression coefficient (b_2) indicates that larger hydrogen peroxide inlet concentration (x_2) value will result in a higher TOC removal (y_1).

On the other hand, the influence of the quadratic term (b_{22}) is negative due to the fact that an excess of hydrogen peroxide has a scavenging effect that consumes the hydroxyl radicals (Hamad et al., 2015a). Thus, a proper amount of hydrogen peroxide can improve the photodegradation rate of PVA. However, further increase in hydrogen peroxide concentration may not only inhibit the system efficiency but also increase the hydrogen peroxide residual which is clearly shown in plot b in Figure 6.6. Plots a-c in Figure 6.6 show the effects of each variable on hydrogen peroxide residual. The percentage of hydrogen peroxide residual is a ratio of the outlet hydrogen peroxide to its inlet concentration. It is obvious that increasing the polymer concentration requires more hydrogen peroxide which results in a decrease in hydrogen peroxide residual as shown in plot (a) in Figure 6.6, however, increasing the feed flow rate results in higher hydrogen peroxide residual due to smaller residence time (plot c in Figure 6.6). Increasing hydrogen peroxide inlet concentration beyond the optimum level significantly increases the hydrogen peroxide residual as shown in plot (b) in Figure 6.6. Therefore, there is an optimum concentration of H_2O_2 for the degradation of PVA polymer, but the optimum value depends mainly on the inlet polymer concentration. Increasing the inlet concentration of the polymer requires a higher optimal concentration of H_2O_2 . As mentioned before, RSM model in Equations (6.2)-(6.4) was validated by performing seven additional experiments as in Table 6.5. All experimental results, presented in Figures 6.3-6.5 showed no significant difference between the actual and the predicted values; thus indicating high adequacy and fitness of the models.

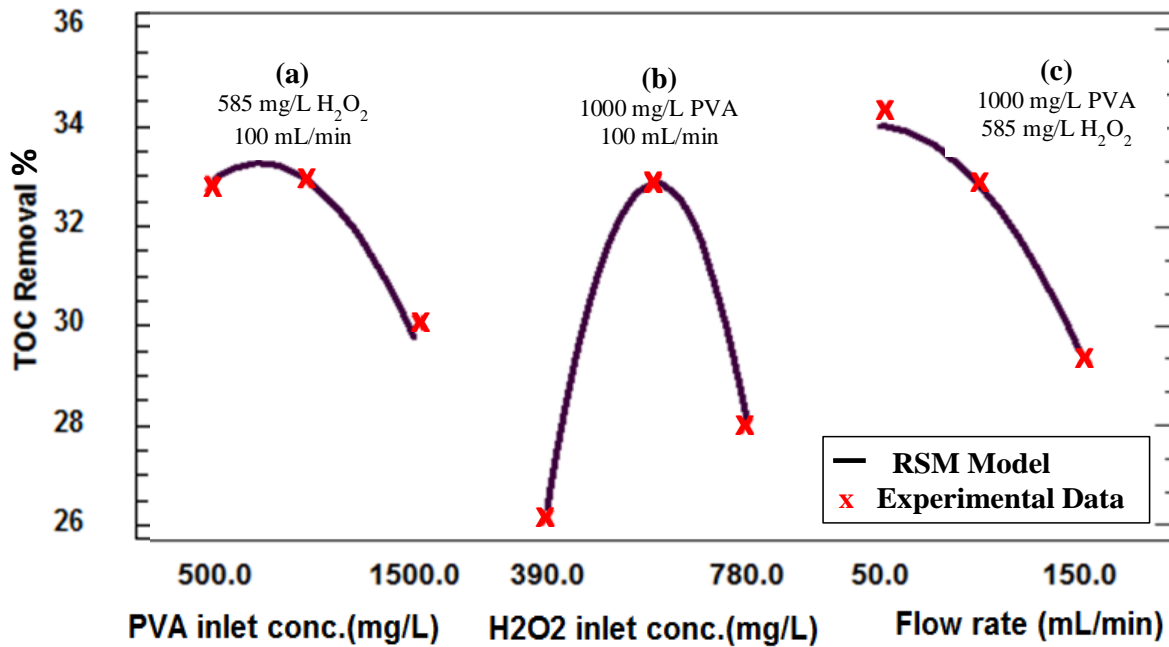


Figure 6.4. Individual effects of operating parameters on the percent of TOC removal in the continuous system.

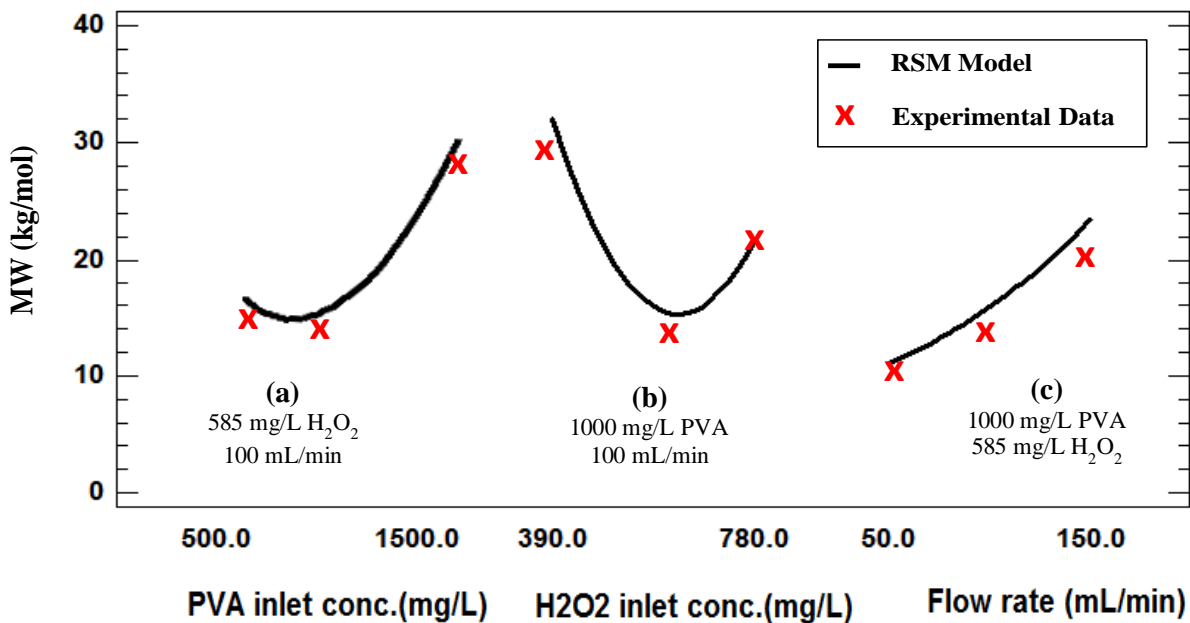


Figure 6.5. Individual effects of operating parameters of the continuous system on PVA molecular weight (kg/mol).

6.7. Interactions of Process Parameters

According to the ANOVA results, the interaction between inlet concentrations of H₂O₂ and PVA has the most significant effect on the PVA degradation and the TOC removal efficiencies. As indicated in Table 6.4, *p*-values of 0.008 and 0.002 for the interactive term (b_{12}) have demonstrated that the PVA and hydrogen peroxide concentrations are highly correlated and contribute significantly to the PVA degradation process. Interaction effect is considered significant when the effect of one factor depends on the level of the other factor. The possible interactions can be visualized by interactions plots in Figures 6.7-6.9 that illustrate the correlations of the operating parameters and their effects on the process responses. As shown in plot (a) in Figures 6.7 and 6.9, the interaction effect of the inlet concentrations of PVA and hydrogen peroxide is more significant than their individual effect which is confirmed by their *p*-values.

This strong interaction is due to the fact that the effect of the inlet hydrogen peroxide concentration varies for different inlet PVA concentrations. For instance, the process performance at low PVA concentrations is higher with low concentration of hydrogen peroxide. The reverse trend was found at high PVA concentrations. Plot (a) in Figures 6.7 and 6.9 show that the individual linear effect of inlet concentration of PVA on TOC removal and PVA degradation (*p*-values of 0.0244 and 0.0100) is slightly more significant than the linear effect of inlet hydrogen peroxide concentration (*p*-values of 0.0321 and 0.0380) as confirmed by their *p*-values in Table 6.5.

There is no significant interaction between the feed flow rate and the hydrogen peroxide concentration (*p*-values > 0.05) as illustrated in plot (c) in Figures 6.7-6.9. However, their linear effects are significant on the process responses.

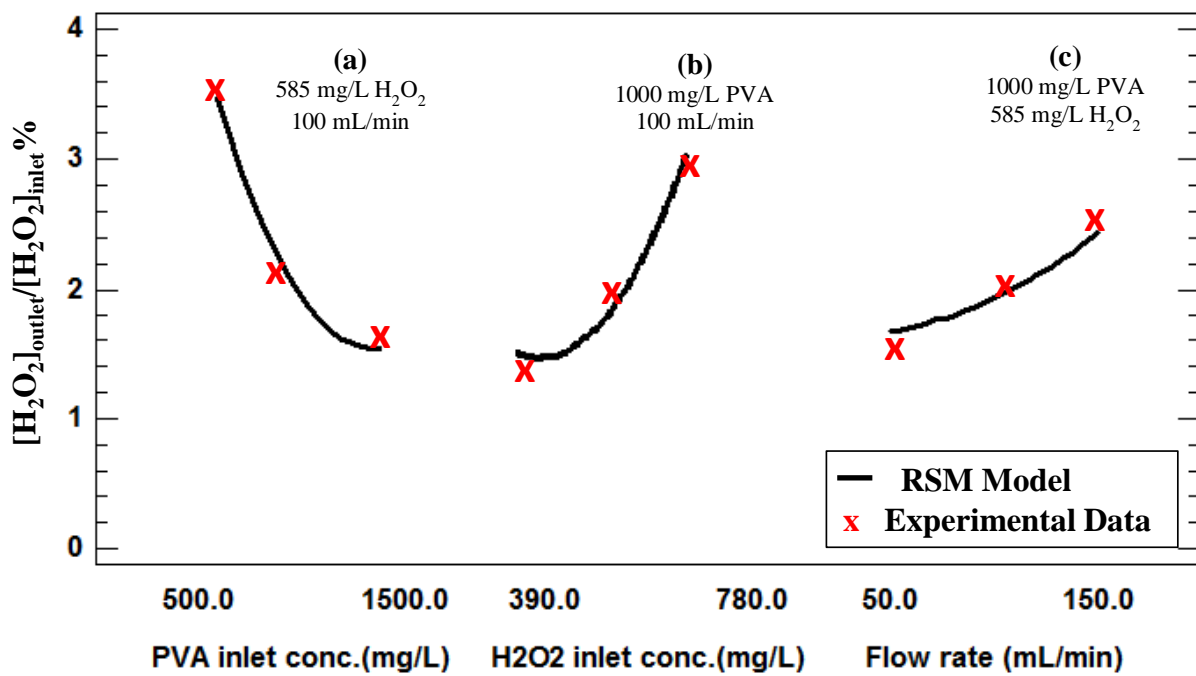


Figure 6.6. Individual effects of operating parameters of the continuous system on percent of hydrogen peroxide residual.

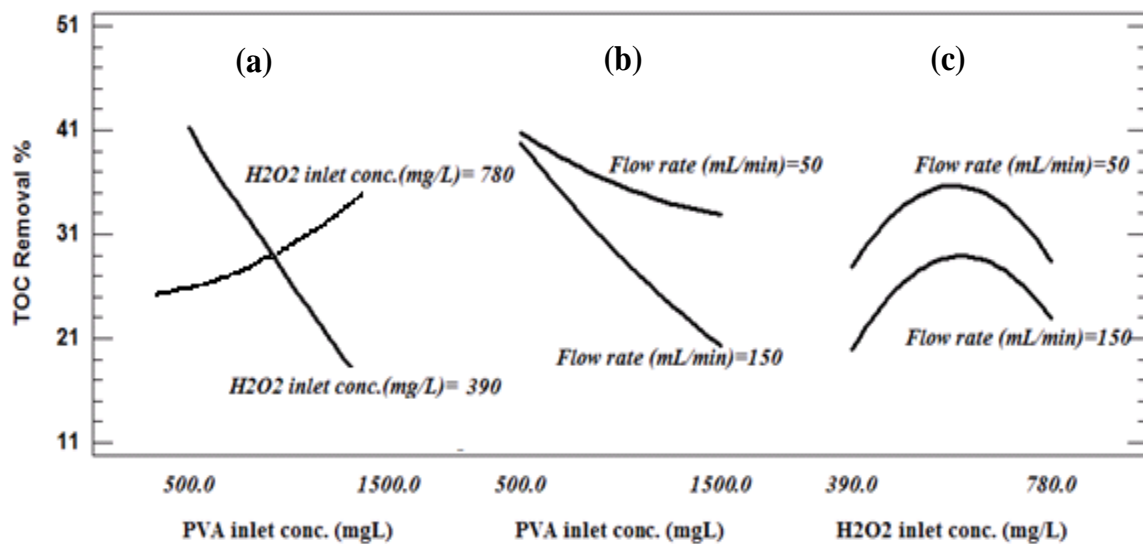


Figure 6.7. Interaction of operating parameters for PVA degradation by continuous UV/H₂O₂ process and their effects on the TOC removal % .

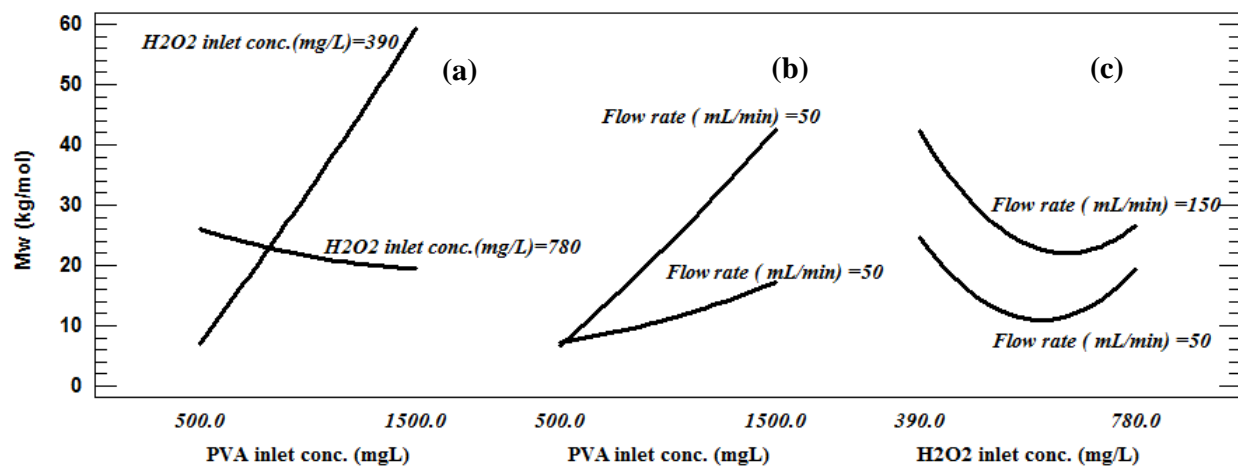


Figure 6.8. Interaction of operating parameters for PVA degradation by continuous UV/H₂O₂ process and their effects on the polymer molecular weight (kg/mol).

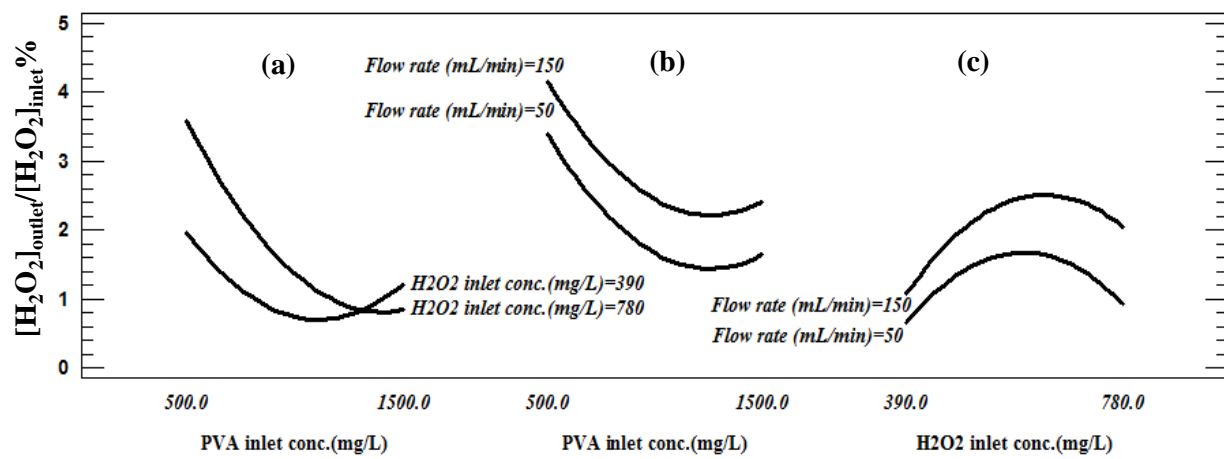


Figure 6.9. Interaction of operating parameters for PVA degradation by continuous UV/H₂O₂ process and their effects on the hydrogen peroxide residual %.

The low feed flow rate has higher PVA degradation than the high flow rate at all levels of hydrogen peroxide concentrations. Plot (b) in Figure 6.7 shows slight interaction between the feed flow rate and the inlet PVA concentration confirming that the effect of the flow rate is only significant at high PVA concentration. However, each of them negatively affects the PVA degradation and the TOC removal efficiencies. At high levels of feed flow rate and inlet PVA concentration, lower TOC removal and lower PVA degradation (high polymer molecular weight) were observed. It can be concluded from the *p*-values presented in Table 6.4, which are clearly illustrated in Figures 6.4-6.9, that the most significant effect on decreasing PVA degradation rate is due to the quadratic term of hydrogen peroxide (b_{22}) followed by PVA inlet concentrations (b_1) and feed flow rate (b_3). However, the interaction between PVA and hydrogen peroxide inlet concentrations (b_{12}) results in the most significant impact on increasing the PVA degradation rate. The response surfaces of the TOC removal, the PVA molecular weight, and the hydrogen peroxide residual are graphically represented in Figures 6.10- 6.12 demonstrating the importance of hydrogen peroxide role in the UV/H₂O₂ process and confirming that increasing the inlet hydrogen peroxide concentration does not necessarily improve the removal efficiency. Therefore, in order to enhance the PVA degradation process, the amount of hydrogen peroxide should be optimized.

6.8. Optimal Operating Conditions and Experimental Validation

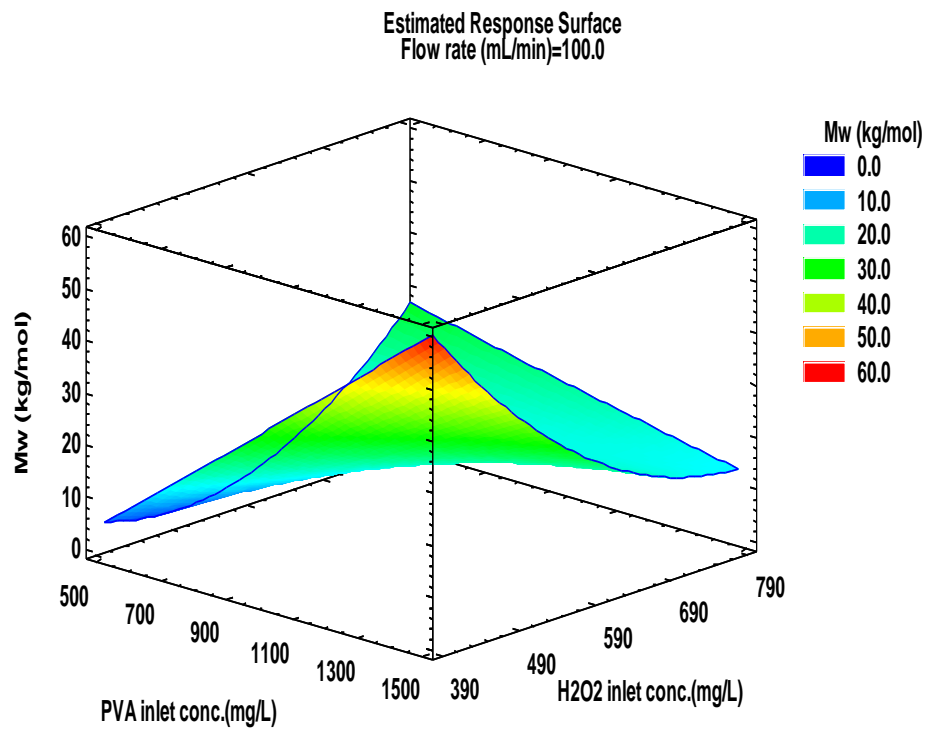
A crucial feature in the design of a continuous UV/ H₂O₂ process is the optimization of operating conditions such as the hydrogen peroxide dosage and the flow rate. The RSM was employed to obtain the best combination of the operating factors in order to achieve the

maximum reduction of TOC and molecular weight with minimum hydrogen peroxide residual at the outlet of the photoreactor. When several responses suggest different optimal operating conditions, a balance between the responses is achieved using desirability method by finding operating conditions that provide simultaneously the most desirable response variables (Costa and Lourenço, 2014). The sensitivity of all responses is set to “medium”, which means that the desirability of each response increases in a linear fashion throughout the specified range with an optimized desirability of 0.89. The optimal operating conditions of the inlet PVA concentration, the inlet H₂O₂ concentration, and the feed flow rate were 665 mg/L, 560 mg/L, and 50 mL/min, respectively. At the optimum conditions, 37.92% of TOC reduction was achieved after 18.4 min with 3.84 mg/L of hydrogen peroxide residual. The PVA molecular weight was reduced from 130 to 3.9 kg/mol under the optimal operating conditions. Finally, the validity and productivity of the mathematical model were evaluated by performing experiments under optimal operating conditions. The optimum responses obtained by the mathematical model were then compared to the experimental results and the error obtained was less than 5% for all responses confirming a good agreement with RSM results.

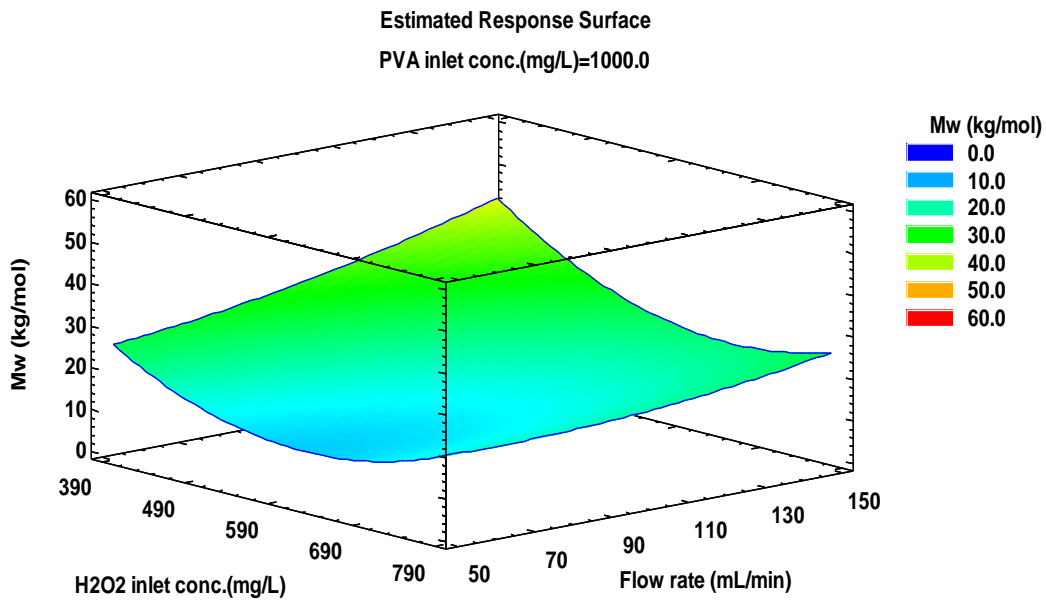
6.9. Concluding Remarks

The degradation of PVA (130 kg/mol) was performed in a continuous UV/H₂O₂ system made up of two photochemical reactors in series. Response surface methodology using Box-Behnken experiment design was implemented for the experimental design. An experimental model incorporating three quadratic equations was developed to predict the TOC removal, the PVA molecular weight, and the hydrogen peroxide residuals at the effluent of the photoreactors.

a)



b)



c)

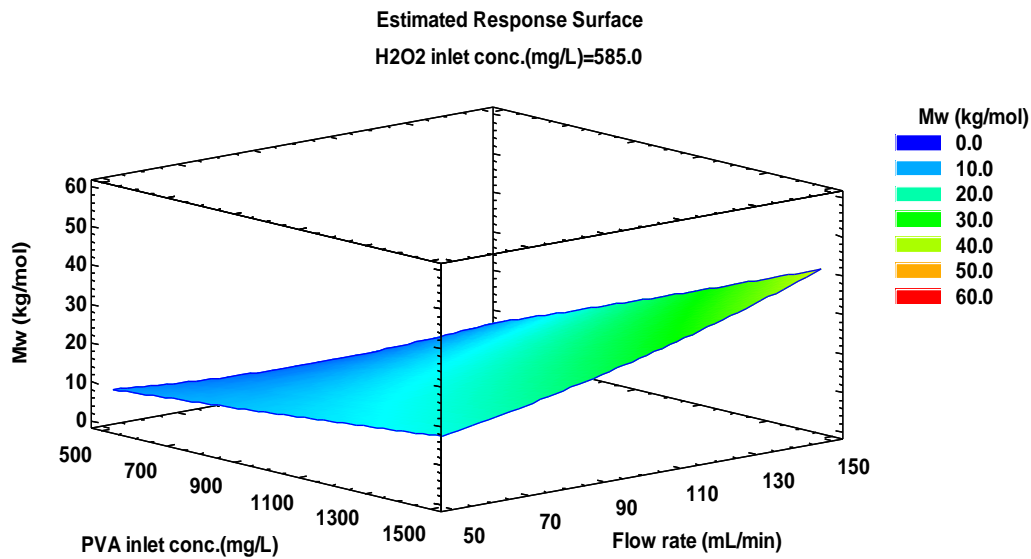
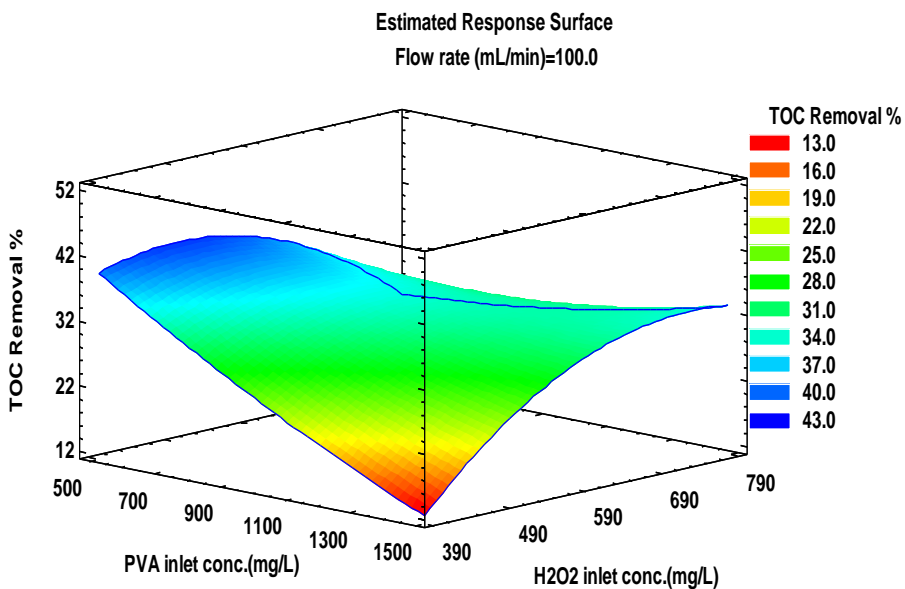
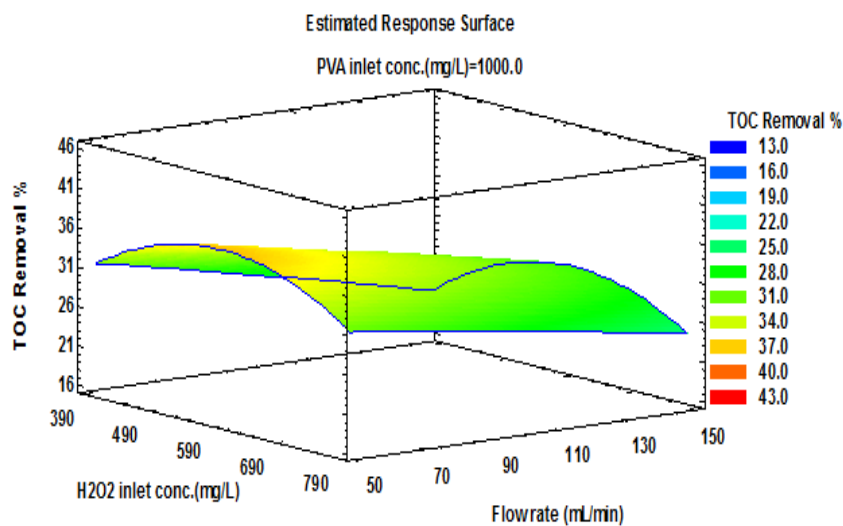


Figure 6.10. Response surface plots of operating parameters for continuous UV/H₂O₂ process, interaction effects of a) PVA and H₂O₂ inlet concentrations (mg/L), b) H₂O₂ inlet concentrations (mg/L) and feed flow rate mL/min, c) PVA inlet concentrations (mg/L) and feed flow rate mL/min, on PVA molecular weight (kg/mol).

a)



b)



c)

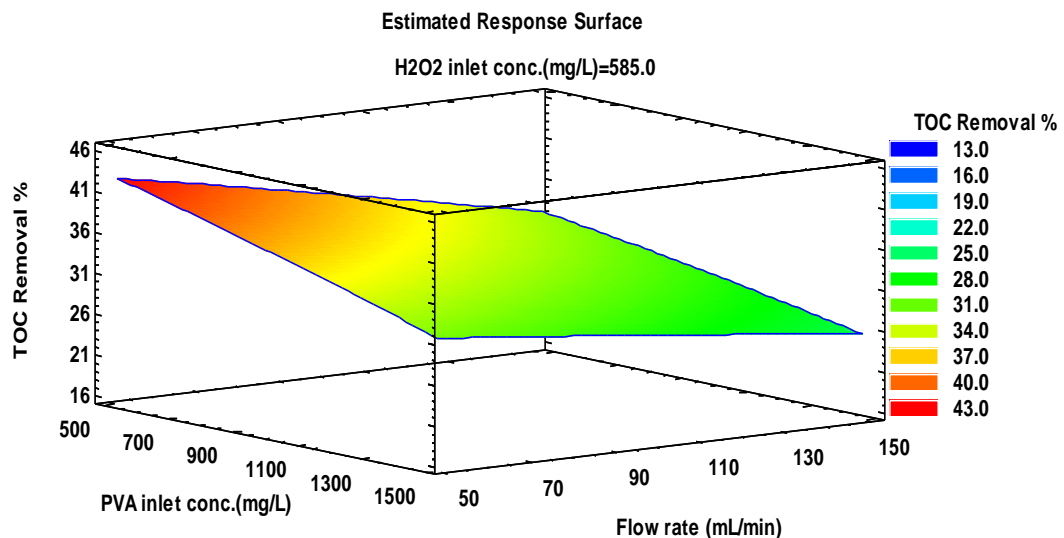
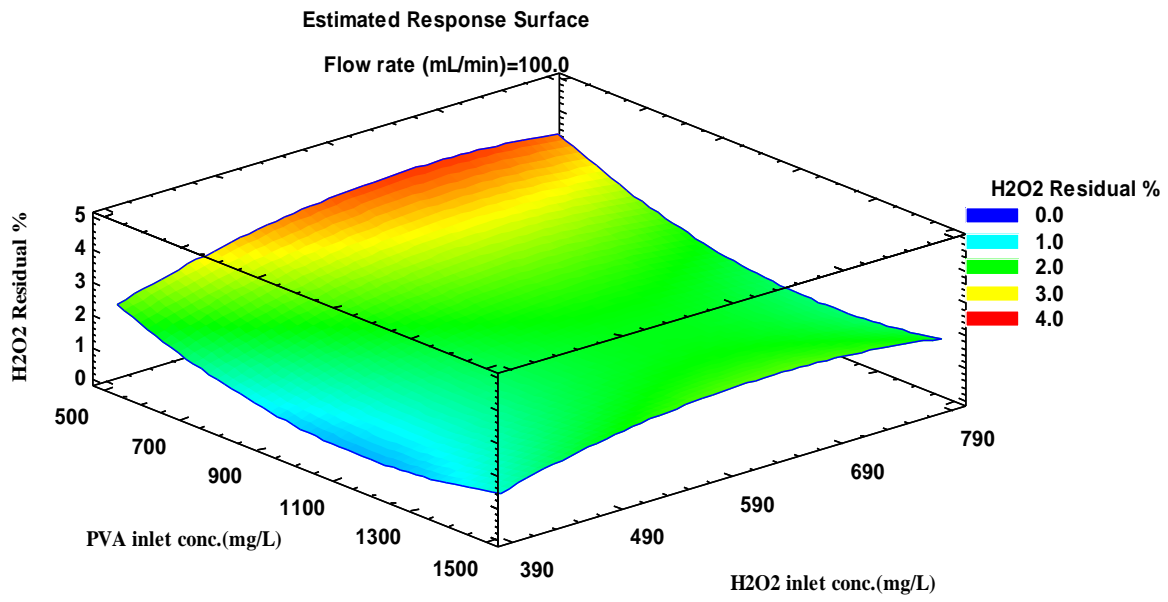
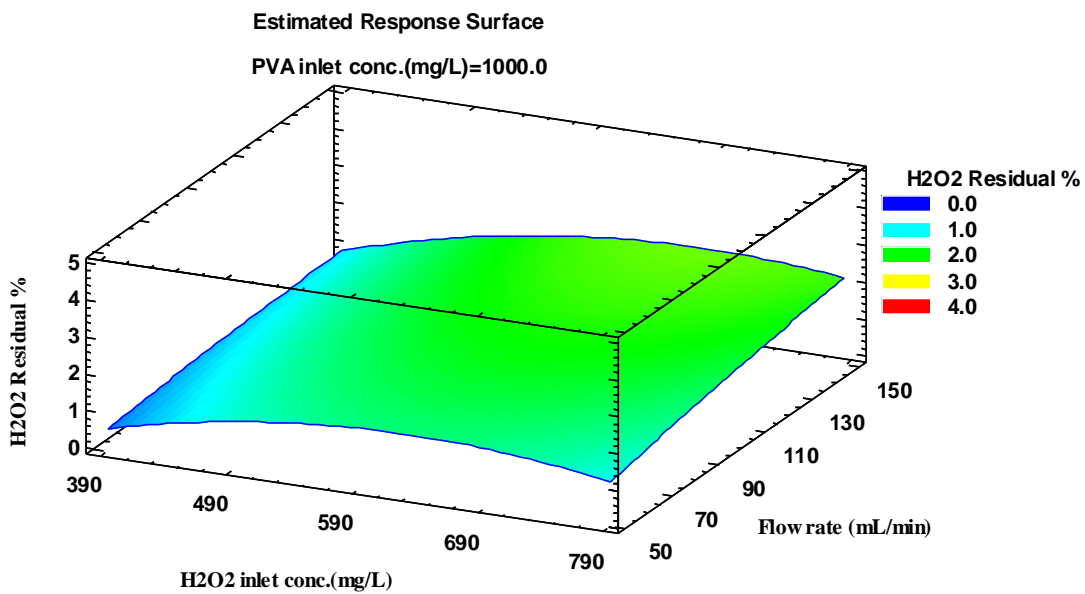


Figure 6.11. Response surface plots of operating parameters for continuous UV/ H_2O_2 process, interaction effects of a) PVA and H_2O_2 inlet concentrations, b) H_2O_2 inlet concentration and feed flow rate, c) PVA inlet concentration and feed flow rate on the TOC Removal %.

a)



b)



c)

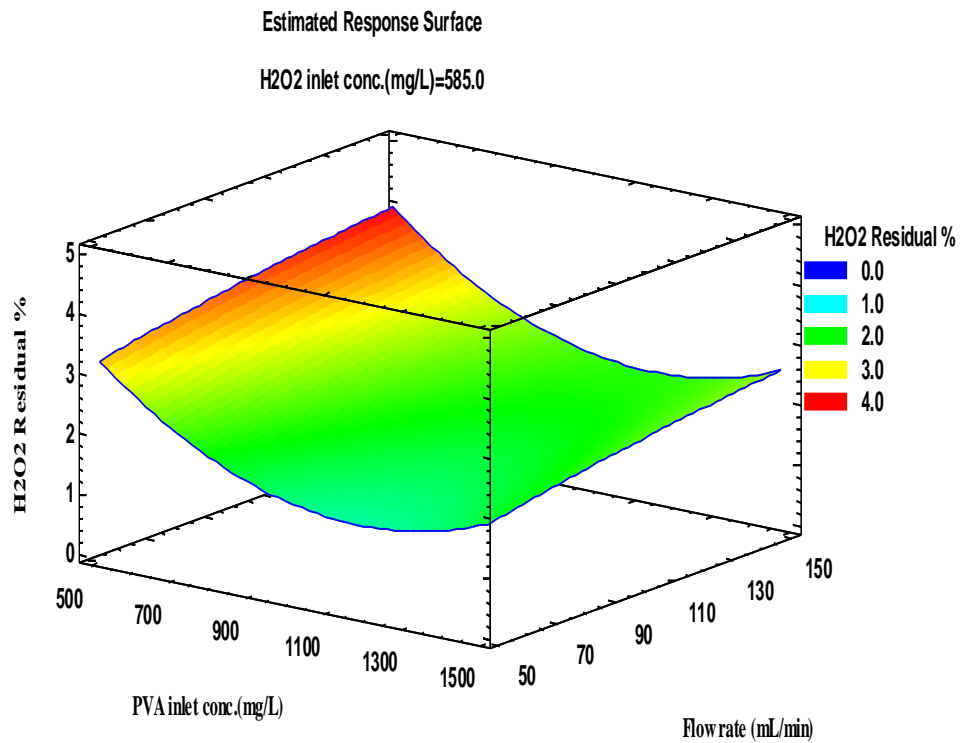


Figure 6.12. Response surface plots of operating parameters for continuous UV/H₂O₂ process. interaction effects of a) PVA and H₂O₂ inlet concentrations (mg/L), b) H₂O₂ inlet concentrations (mg/L) and feed flow rate mL/min, c) PVA inlet concentrations (mg/L) and feed flow rate mL/min, on the percent H₂O₂ residual.

The simultaneous exposure of the feed stream to continuous flow of H₂O₂ and UV irradiation resulted in a significant reduction in polymer molecular weight and TOC along with the reduction in hydrogen peroxide consumption and residual.

The interaction between the hydrogen peroxide and PVA inlet concentrations was the most significant factor influencing the PVA degradation within the range of the operating condition. Experimental analysis showed that the TOC removal varied from 16.11 to 42.70% along with a reduction of the PVA molecular weights ranging between 56.7 and 95.30%. Besides, the results demonstrated that a continuous feeding of hydrogen peroxide favors the PVA degradation once the hydrogen peroxide concentration was kept below a given threshold [H₂O₂]/[PVA] mass ratio of 0.7.

Chapter 7

COMPARATIVE STUDY OF POLYVINYL ALCOHOL PHOTODEGRADATION IN BATCH, FED-BATCH, AND CONTINUOUS PHOTOREACTORS

7.1. Introduction

Most experimental studied has been carried out in a conventional batch operation for wastewater treatment (Ranby, 1989; Kaczmarek et al., 1998; Zhang et al., 2004; 2011; Santos et al., 2009); Ghafoori et al., 2014). The purpose of this section is to conduct a comparative study for the degradation water-soluble polymer (PVA) in the UV/H₂O₂ processes operated under batch, fed-batch, and continuous modes. Experimental results in Section 4.1 and 4.3 confirmed the importance of the feeding strategies of hydrogen peroxide for the degradation of PVA in batch and fed-batch photoreactors. Even though the rate of PVA degradation (TOC removal and PVA reduction) was adequate and the results showed an improvement in comparison to published data in open literature, the UV exposure time is around 6 h (Aarthi et al., 2007; Santos et al., 2009). Therefore, it was concluded that the feeding strategies of hydrogen peroxide must be considered again for further process enhancement. The operational variables; hydrogen peroxide feeding strategies, photoreactor residence time, and mass ratio of hydrogen peroxide to polymer were examined for their impacts on the molecular weight distribution of PVA and total organic carbon (TOC) removal.

Furthermore, the power consumption required for PVA degradation in the UV/H₂O₂ process has also been assessed for different UV dosage and hydrogen peroxide concentration in all the three reactor types to ensure the possibility of scaling-up the UV/H₂O₂ process.

7.2. Experimental Setups and Procedures

This study employs batch recirculation, fed-batch recirculation, and continuous modes to degrade synthetic aqueous PVA wastewater. The experimental setup of the photochemical reactor system is presented in Figure 3.2. The experimental set up consists of two reservoir tanks, two peristaltic pumps and two stainless steel photoreactors model SL-LAB 2 (Siemens Inc.). Each photoreactor is equipped with an internal quartz glass containing a low pressure mercury 14-watt UV lamp of 254 nm. Reactants were fed into the system either at once, intermittently dripped, or continuously at a flow rate controlled by means of peristaltic pumps. The experimental procedures for both systems are explained in Section 3.3. For the continuous mode, the experimental procedures are discussed in Sections 3.4 and 3.5. The specifications of the photoreactors are listed in Table 3.1. For comparison purpose, all experiments were carried out at the same initial conditions for all three reactor operations. The photoreactor was operated at room temperature and experiments were carried out in triplicate. Aqueous solutions with initial PVA concentration of 500 mg/L were treated in the photoreactor system, according to the experimental design in Table 7.1. The volumetric flow rate was varied from 30 to 100 mL/min provided the system with a hydraulic residence time of 9.2-30.6 min/pass in continuous mode.

The MWD of PVA and the TOC removal in the continuous flow operation were assessed and compared with those obtained in a batch and fed-batch circulation photoreactors.

7.3. Preliminary Experimental Testing

In order to test the stability of the reaction components in the continuous system, two blind experiments were carried out for PVA initial concentration of 500 mg/L. First, the reaction system was irradiated for 18.4 min in the absence of hydrogen peroxide to study the photostability of PVA. No significance decrease in PVA molecular weight was observed indicating that there was no direct photolysis of PVA macromolecular compound. However, more energy would be required to break the polymer chains. In the second experiment, the complete reaction system ($[PVA]_0=500$ mg/L), $[H_2O_2]/[PVA]$ mass ratio of 1) was tested without irradiation for 18.4 min. PVA was stable and there was no observable reduction in TOC and PVA molecular weights. Consequently, it was concluded that the UV light can only be effective in the presence of hydrogen peroxide in the reaction medium. Similar observations for batch system are reported (Santos et al., 2009; Hamad et al., 2014).

Table 7.1. Operating condition of the PVA in UV/ H_2O_2 photoreactors.

Operation modes	$[PVA]_0$ (mg/L)	$[H_2O_2]/[PVA]$	Flow rate (mL/min)
Batch recirculation	500	0.20, 0.78, 1.00, 5.00, 10.0, 15.0	100
Fed-batch recirculation	500	0.20, 0.78, 1.00, 5.00, 10.0, 15.0	100
Continuous	500	0.20, 0.78, 1.00, 1.56	30, 50, 100

7.4. H₂O₂ Feeding Strategies for TOC Removal

Different concentrations of H₂O₂ were used at a constant PVA concentration of 500 mg/L. In the batch operation, hydrogen peroxide was poured once at the start of the experiment. As a result, it was not possible to keep the hydrogen peroxide concentration at the required level inside the photoreactor during the exposure time. Thus, the TOC removal rates observed in a continuous photoreactor was superior to that in other reactors as shown in Figure 7.1. This means that the concentration of H₂O₂ can be easily controlled in a continuous photoreactor. Classically, a batch photoreactor provides the highest conversion, which means that highest TOC removal is expected in batch reactor. However, the performance of UV/H₂O₂ batch photoreactor does not comply with the performance of a regular chemical batch reactor. Further, as shown in Figure 7.1, it is evident that a fed-batch operation is more effective to degrade the aqueous PVA polymer than a batch photoreactor, but the H₂O₂/PVA ratio is also a very important factor that affects the polymer degradation reactions. The continuous mode prevails and produces the highest TOC removal.

In batch and fed-batch modes, at [H₂O₂]/[PVA] mass ratio of 1, the maximum TOC removal of 41% and 64% were achieved in 2 h, respectively. Through the continuous addition of hydrogen peroxide, it was possible to reach a per pass TOC removal of 94.4% at a [H₂O₂]/[PVA] mass ratio of 1 in 30.6 min only. These unexpected results in a batch process are mainly due to the dominant scavenging effect (Reaction 7.1) of hydrogen peroxide which can be significant in this type of wastewater treatment when the process is operated in batch mode.



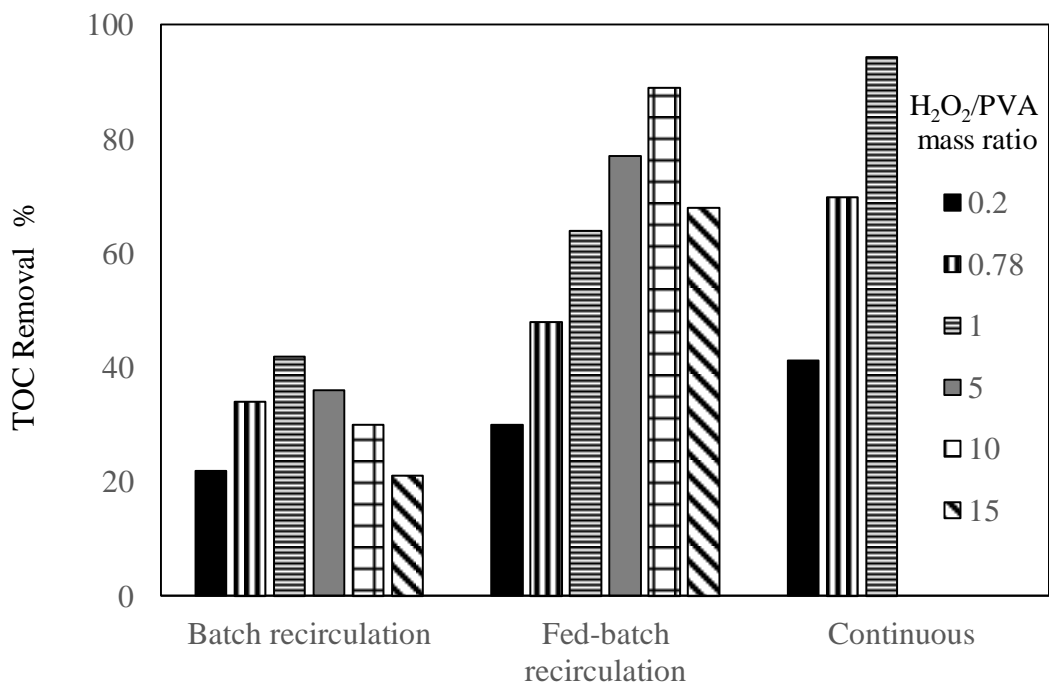


Figure 7.1. Comparison of TOC removal in batch and fed-batch (2 h) and continuous (30.6 min. residence time) UV/ H_2O_2 photoreactors; $[\text{PVA}]_0 = 500 \text{ mg/L}$, different $[\text{H}_2\text{O}_2]/[\text{PVA}]$ mass ratios.

Introducing a very high concentration of hydrogen peroxide can lead to a photochemical reaction between the hydrogen peroxide and hydroxyl radicals producing less active hydroperoxyl radical (HO_2^\bullet). Therefore, the probability of hydroxyl radicals attacking organic species can be significantly reduced:



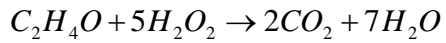
According to the principles of competitive reaction kinetics (Reactions (7.1) and (7.2)), the reaction rate depends on the values of the rate constants and the concentrations of competitive components. Reported reaction rate constants of Reactions (7.1) and (7.2) are $2.7 \times 10^7 \text{ L/mol.s}$ (Buxton et al., 1988) and $8.06 \times 10^6 \text{ L/mol.s}$ (Hamad et al., 2015b), respectively. According to this study, the values of the concentration ranges of hydrogen peroxide and PVA are $(3-220) \times 10^{-3}$ and $3.8 \times 10^{-6} \text{ mol/L}$, respectively. The hydroxyl radical concentration is around $1 \times 10^{-11} \text{ mol/L}$ (Christensen et al., 1982; Hamad et al., 2015b). In fact, the rate constant for the reaction of hydroxyl radical HO^\bullet with PVA polymer (Reactions 7.2) is found to be one order of magnitude smaller than the rate constant of the reaction of HO^\bullet with H_2O_2 (Reactions 7.1).

As a result, a continuous feeding of H_2O_2 (at an appropriate concentration) into the photoreactor enables Reaction (7.2) to overcome Reaction (7.1) (i.e. the production of HO_2^\bullet radical is reduced). The consumption of hydrogen peroxide during the degradation reaction of the PVA polymer is illustrated in Figures 7.2 and 7.3. The declining trend of hydrogen peroxide content in Figure 7.2 exhibits the rate at which the hydrogen peroxide molecules break down into hydroxyl radicals under UV light effect.

Referring to Figure 7.3, It is clear that the batch photoreactor (single shot) resulted in hydrogen peroxide residual as high as 17% compared to 3% residual in the fed-batch photoreactor (four small dosages).

However, a residual of less than 1% (4 mg/L) has been achieved in the continuous feeding strategy. This indicates that the feeding strategy is an operation factor as important as hydrogen peroxide dosage and residence times for the formation of hydroxyl radicals.

Moreover, for making the UV/H₂O₂ process competitive with other AOPs process, it is crucial to ensure a low operation cost, which necessarily requiring a lower consumption of H₂O₂. In fact, meticulously controlled concentration of H₂O₂ can cause a higher TOC reduction in short time, limiting the scavenging effect of H₂O₂ (Hamad et al., 2014), highlighted the need to perform the reaction with an adjusted concentration of H₂O₂ during the PVA photodegradation reaction.



The specific hydrogen peroxide consumption per g TOC removed was evaluated in UV/H₂O₂ process operated under three modes at PVA of 500 mg/L and [H₂O₂]/[PVA] mass ratio of 1 (presented in Figure 7.1). The ratio of mol H₂O₂ consumed/mol C removed was found to be 1.5 (i.e. 4.4 g H₂O₂/g C) in the batch system with 1.0 mol H₂O₂/mol C (i.e. 2.8 g H₂O₂/g C) in the fed-batch mode, and 0.6 mol H₂O₂/mol C (i.e. 1.7 g H₂O₂/g C) in the continuous mode.

Operation of continuous photoreactor required the lowest concentration of H₂O₂ to get optimal level compared to that of fed-batch system. In fact, with the continuous supply of hydrogen peroxide, the reaction medium was well balanced resulting in a considerable decrease in hydrogen peroxide residual.

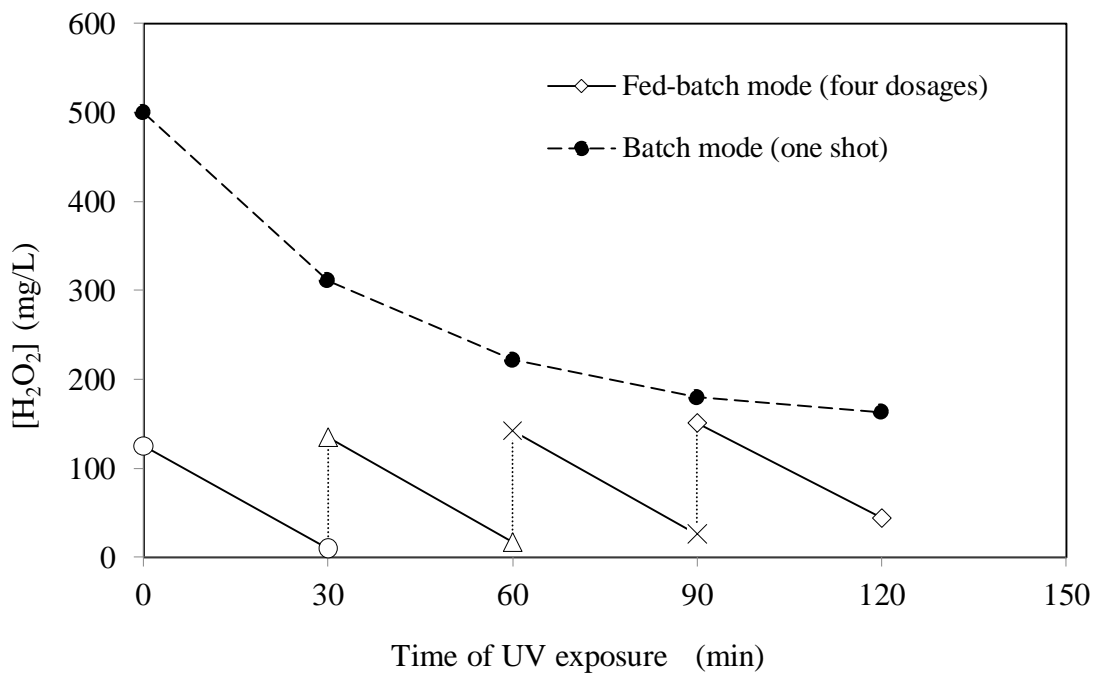


Figure 7.2. Hydrogen peroxide residual versus reaction time PVA degradation in UV/ H₂O₂ batch and fed-batch photoreactors, [PVA]_o= 500 mg/L, [H₂O₂]/[PVA]=1(mass ratio).

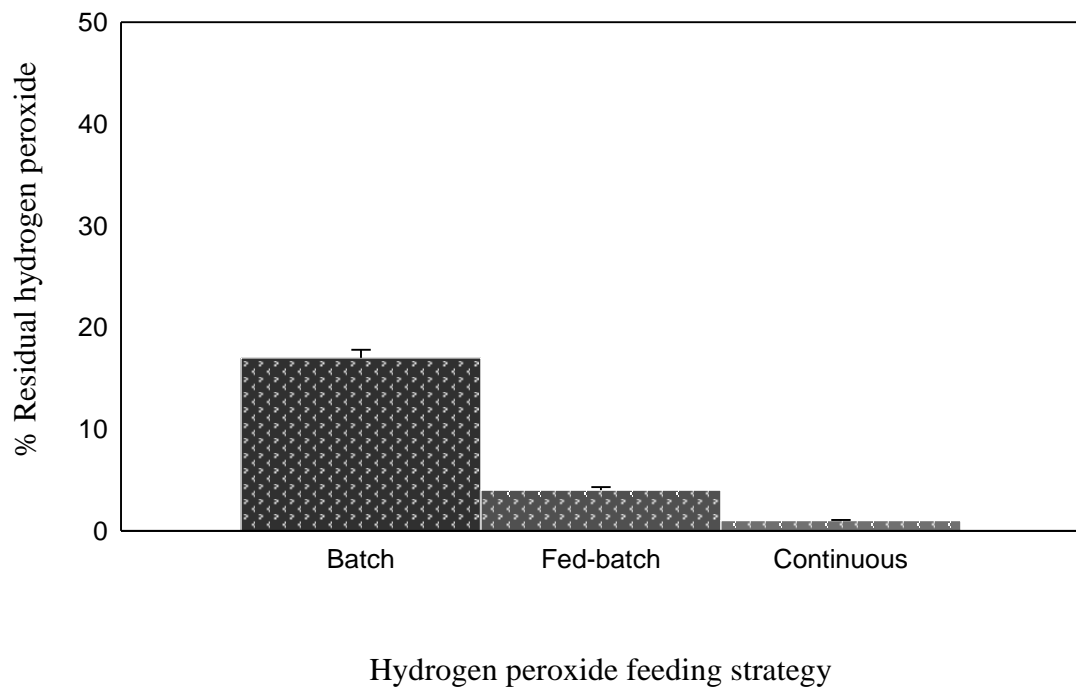


Figure 7.3. Hydrogen peroxide residual in each UV/H₂O₂ photoreactor; batch , fed-batch (2 h), continuous (residence time of 30.6 min). [PVA]_o=500 mg/L; [H₂O₂]/[PVA]=1(mass ratio).

In other words, addition of H₂O₂ in continuous mode provided the most suitable utilization of the produced hydroxyl radicals for the PVA photo-oxidation reaction.

7.5. Variation of PVA molecular weight distribution with hydrogen peroxide feeding strategies

Starting with a polymer sample with number average molecular weight (M_n) of 130 kg/mol and an initial (or inlet) concentration of aqueous PVA solution of 500 mg/L, the polymer solution was treated with hydrogen peroxide under UV light for 2 h in batch or fed-batch photoreactor and for 30.6 min in a continuous photoreactor. Figure 7.4 shows clearly the impact of the feeding strategies on the reduction of the polymer molecular weight. The MWD of the polymer samples were measured using a GPC (Gel Permeation Chromatograph). The initial polymer molecular weights were reduced to 24.9, 20.3, and 2.2 kg/mol in the batch, fed-batch, and continuous photoreactors, respectively. Again, introducing the oxidant in a continuous manner enriches the reaction mixture with enough hydroxyl radicals. The experimental results support the option of the continuous procedure to improve the efficiency of the UV/H₂O₂ process.

The reduction in molecular weights of PVA in UV/H₂O₂ process is well explained by monitoring the MWD of the treated polymer. First, the molecular weight distribution of the untreated PVA polymer (M_n=130 kg/mol, M_w=148 kg/mol, PDI=1.14) shown in Figure 7.5 is unimodal narrow distribution with a single sharp peak. Plots in Figures 7.6 -7.8 present very important new results. They show the effects of the operation modes with UV exposure time on polymer chain scission mechanism and consequently the MWDs.

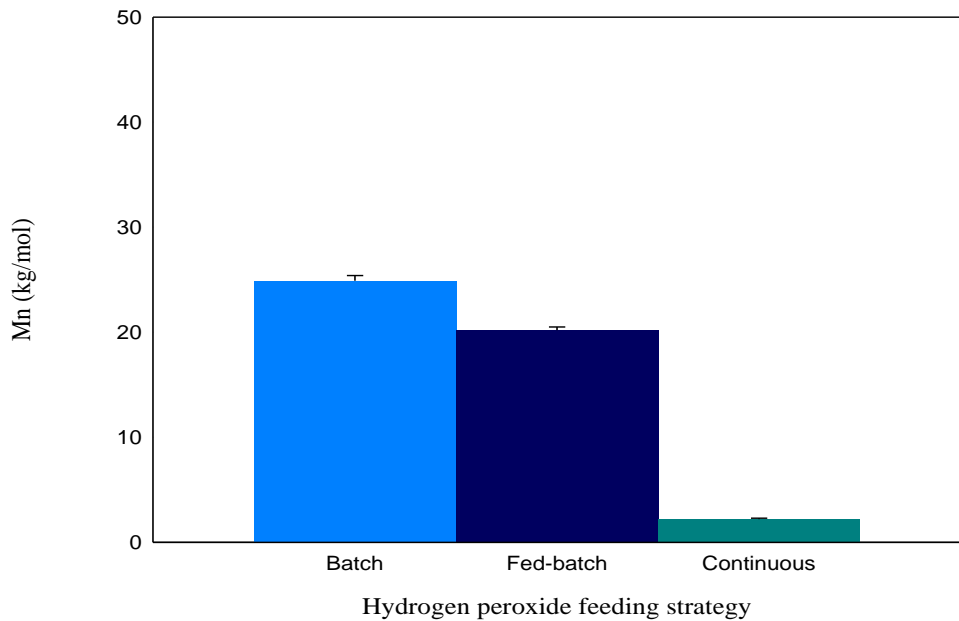


Figure 7.4. Variation of number average molecular weights (Mn) of PVA degradation by UV/ H_2O_2 operated at different hydrogen peroxide feeding strategies.

[PVA]_o=500 mg/L, Mn_o=130 kg/mol, [H₂O₂]/[PVA]=1 (mass ratio), 2 h reaction for batch and fed-batch, 30.6 min residence time for continuous.

The polymer MWD decreases with time. Monitoring the time evolution of MWDs of PVA, the degradation of the polymer has obvious advantages. The polydispersity index represents the breadth of the distribution curve. Figures 7.6-7.8 show profiles of the differential and cumulative MWD of PVA in batch, fed-batch and continuous UV/H₂O₂ photoreactors, respectively. First, Figure 7.6 shows the MWD of PVA samples taken at 30, 60, 90, and 120 min batch reaction time, respectively indicated by plots a, b, c, and d. The appearance of a tail is observed in the MWD at high molecular weights and a marked broadening of the distribution after 60 to 120 min exposure time (plots b-d). Pouring the whole dosage of hydrogen peroxide as one single shot at the beginning of the reaction resulted in variation of the relative amounts of the high and low molecular weight fractions in the obtained polymer sample which lead to a broad MWD. Under fed-batch mode, Figure 7.7 depicts the decrease in the polymer molecular weights for 30 to 120 min UV exposure time confirming that the degradation of PVA chains results in broad molecular weight distribution.

The molecular weight distribution demonstrates a progressive disappearance of the higher molecular weight fractions, in accordance with the proposed mechanism suggesting that polymer photodegradation occurs by random scission of PVA chains in solution followed by chain-end scission (Hamad et al., 2015b). In fact, by increasing the exposure time, the molecular weight distribution tends to shift to low molecular weight population as illustrated by all plots in Figures 7.6-7.8. Besides, small molecules are produced as the photodegradation reaction proceeds, which contribute to a broadening distribution and a decreasing peak with residence time.

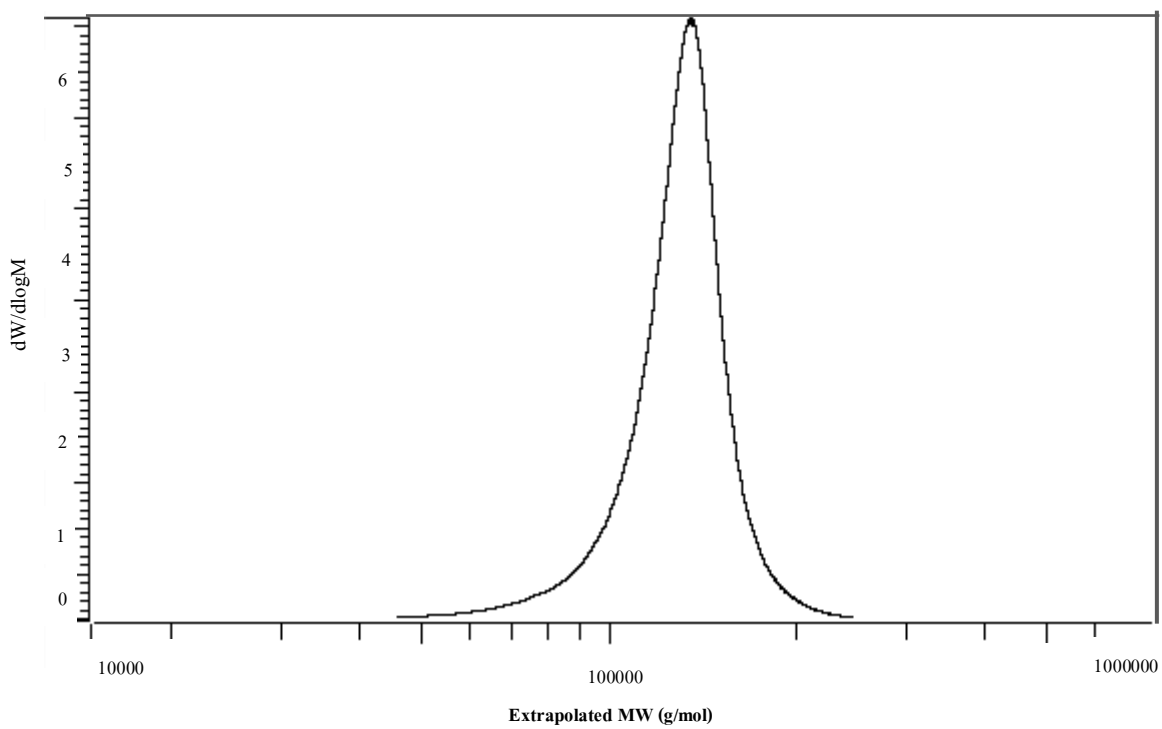


Figure 7.5. The molecular weight distribution of initial untreated PVA polymer sample.

$M_{n_0}=130 \text{ kg/mol}$, $M_{w_0}=148 \text{ kg/mol}$, PDI=1.14.

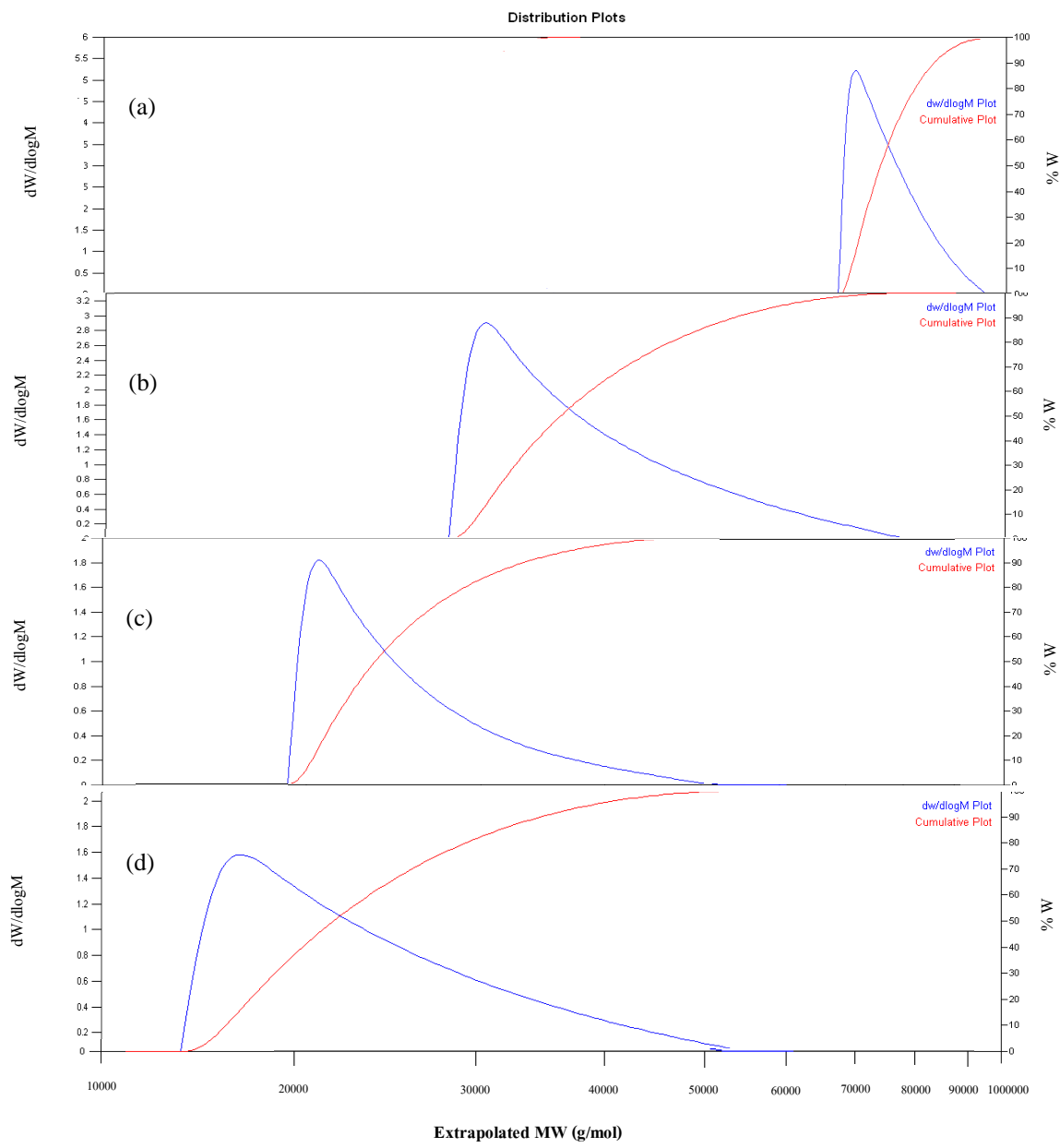


Figure 7.6. Time evolution of MWD of PVA degradation in a batch reactor, $[PVA]_0=500 \text{ mg/L}$.
Exposure time: a) 30 min, b) 60 min, c) 90 min, and d) 120 min.

The operation of the continuous photoreactor depends mainly on the variations of the PVA solution flow rates and the concentration of hydrogen peroxides continuously fed into the photoreactor. The most interesting results of continuous mode of the UV/H₂O₂ process for PVA degradation, which also accounts for the effect on polydispersity, is the non-random nature of the degradation process. This is clearly illustrated in Figure 7.8, where the concentration of the initial polymer sample falls during irradiation.

At a feed flow rate of 100 mL/min (Figure 7.8 plot a), the MWD of PVA has a molecular weight around 10 times less than its original value. Further increase in the residence time, meaning lower the feed flow rate resulted in a sharp decrease in PVA molecular weights (plots a-d of Figure 7.8). In a 30.6-min residence time, the number average molecular weights reduced to 2.2 kg/mol using a [H₂O₂]/[PVA] mass ratio of 1. A relatively narrow distribution of PVA degradation was obtained in a continuous mode of operation which can be interpreted by the consistency of the hydrogen peroxide dosage throughout the degradation process.

In addition, the MWD of PVA is bimodal and has shifted towards lower molecular weights with a small shoulder peak as shown in Figure 7.8. The experimental results confirm previous argument reported in literature (Price and Smith, 1991; Florea, 1993; McCoy and Madras, 1997) which suggested that during degradation process, the MWD can have a bimodal shape. The bimodal distribution characteristic of PVA is exhibited by two peaks. The lower molecular weight peak of PVA is likely due to the reactions of intermediate oxidation products with hydroxyl radicals, where the high shoulder represents the high molecular weight of PVA.

At the highest level of degradation under fed-batch mode (plot c in Figure 7.7), the presence of two peaks was also detected denoting that the distribution becomes slightly bimodal towards the end of the reaction. This indicates the presence of low molecular weight species, as

well as polymer with low molecular weights. The bimodal behavior can be also due to differences in the degradation rate resulting from two different mechanisms, i.e., random and chain end scission, which are involved in the degradation process (Hamad et al. 2014; 2015b, c), as the chain scission can be more extensive at the final stage of the degradation reaction. Another feature to note is the decreasing heights of the curves. These height changes may be due to a decrease in the refractive index increment difference for the polymer in the solvent due to changes in the polymer chemical composition. Although, the molecular weights have not changed much in plots c and d of Figure 7.8, the TOC removal efficiency has notably increased (from 88 to 94.4%) as the hydrogen peroxide to polymer mass ratio increased from 0.78 to 1. This is clearly attributed to the sufficient concentration of hydroxyl radicals in the medium which drives the reaction towards a complete mineralization (i.e. reaction between the hydroxyl radicals and the intermediates). In fact, the operation of the continuous photoreactor depends mainly on the variations of the PVA solution flow rates and the amount of hydrogen peroxides continuously fed into the reactor.

Modifying the way hydrogen peroxide was introduced to the system favored a higher PVA degradation rate, and resulted in a remarkable decrease of its molecular weights. In summary, the continuous addition of H_2O_2 during the degradation reaction sustained a high utilization of the produced hydroxyl radicals for the PVA photo-oxidation reaction.

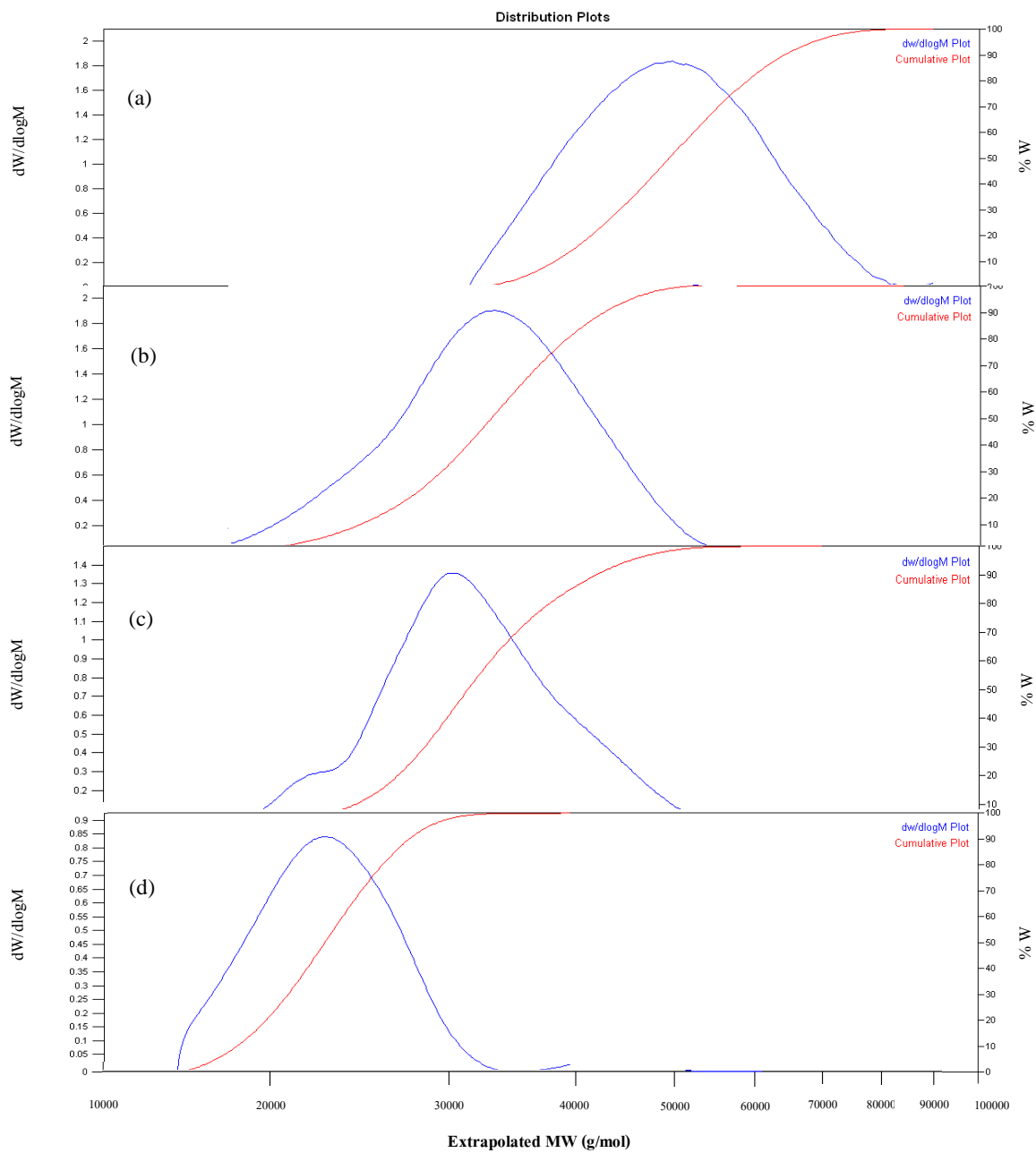


Figure 7.7. Time evolution of MWD of PVA degradation in a fed-batch reactor.
 $[PVA]_o = 500 \text{ mg/L}$, $[H_2O_2]/[PVA]$ mass ratio of 1, a) 30 min, b) 60 min, c) 90 min, and d) 120 min.

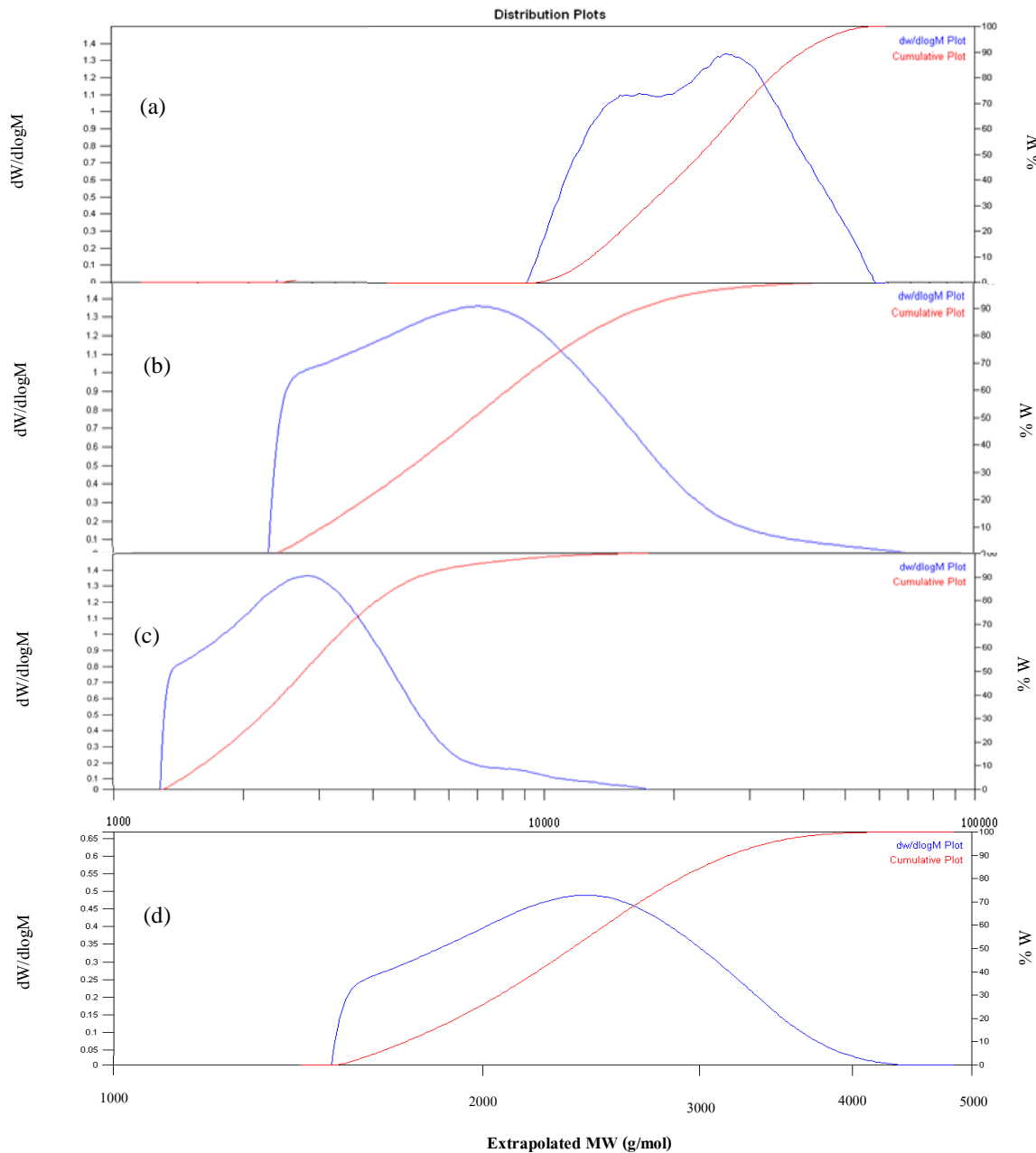


Figure 7.8. Time evolution of MWD of PVA degradation in a continuous reactor.
 $[PVA]_o = 500 \text{ mg/L}$, $[H_2O_2]/[PVA]$ mass ratio of 0.78 and 1 for plots a-c, and d, respectively at residence time a) 9.2 min, b) 18.4 min, c) 30.6 min., and d) 30.6 min.

In this case, the hydrogen peroxide was mainly directed towards the hydroxyl radicals' production resulting in very high PVA degradation indicating that the feeding strategy is a factor as important hydrogen peroxide dosages and residence time in the formation of hydroxyl radicals. Still, this apparent advantage must be confirmed in terms of power usage to establish an economic output of the PVA degradation in UV/ H₂O₂ photoreactors.

7.6. Power Consumption of PVA Degradation by UV/H₂O₂ Process

Cost-effectiveness analysis of the removal of the total organic carbon from synthetic wastewater contaminated with PVA polymers using UV/H₂O₂ process has been developed to compare the performance and the treatment capability of three modes of operation. The total cost of each system was calculated by adding the operating and maintenance costs as well as the power consumption. All three systems have nearly the same installation cost. The operating maintenance costs consisted of the lamp replacement, consumable chemical (hydrogen peroxide (\$2.5/L), sodium hypochlorite (NaOCl) (\$8/L), and electrical consumptions of the pumps and the lamp (shown in Tables 7.2 and 7.3). Reagents such as sodium hypochlorite have to be added to the solution for quenching the hydrogen peroxide residual. The stoichiometric amount required for quenching process is determined according to the following reaction (Liua et al., 2003):



The power consumption was calculated for each UV/H₂O₂ photoreactors based on the values of the TOC removal (presented in Figure 7.1). The cost of electricity per mass of TOC

removed was estimated by Equation (7.5) for batch and fed batch systems (Bustillo-LeCompte et al. 2014) and by Equation (7.6) for continuous system as follows (Bolton et al. 2001)

$$J_E = E_r \left(\frac{10^6 p t}{V(C_i - C_f)} \right) \quad (7.5)$$

$$J_E = E_r \left(\frac{10^6 p}{F(C_i - C_f)} \right) \quad (7.6)$$

where, J_E is electricity cost (\$/kg of TOC removed), E_r is energy rate (\$0.115/kWh), p is power rating of system (kW), C_i is TOC concentration in the influent (mg/L), C_f is TOC concentration in the effluent (mg/L), t is hydraulic residence time (h), V' is the volume of treated wastewater (L), and F is the volumetric flow rate (L/h). Referring to Tables 7.2 and 7.3, the operation cost has been estimated for each system using different concentrations of hydrogen peroxide. Figure 7.9 shows that the total operational costs for PVA (500 mg/L) degradation in batch, fed-batch, and continuous photoreactors at $[H_2O_2]/[PVA]$ mass ratio of 1 are \$89.5, \$64.3, and \$29.3 per kg TOC removed, respectively. The electricity consumption in the batch UV/ H_2O_2 process is about 3 times higher than that of the continuous processes. This result confirms furthermore that the feeding strategy has a considerable impact on the efficiency and operational costs of the UV/ H_2O_2 process.

7.7. Concluding Remarks

The UV/ H_2O_2 process is proved to be powerful method for reducing PVA polymer content in wastewater. The performance of the continuous photochemical reactor system was compared with that of a batch and fed-batch reactors.

The experimental testing was done for PVA inlet concentration of 500 mg/L, a PVA solution flow rate from 30 to 100 mL/min using different hydrogen peroxide to polymer mass ratios. The results showed that the PVA number average molecular weight was progressively reduced from an initial value of 130 kg/mol to 24.9, 20.3, and 2.2 kg/mol corresponding to percent TOC removal of 41.0, 58.6, and 94.4 by UV/H₂O₂ process in batch, fed-batch (120-min exposure time), and continuous (30.6 min residence time) photoreactors, respectively.

The high efficiency of the UV/H₂O₂ reactor in continuous mode is mainly due to a slow and continuous injection of H₂O₂ into the reactor that balances the concentration of H₂O₂ along the reactor and promotes the efficient usage of hydrogen peroxide-derived radicals by overcoming the competing or scavenging effect of hydrogen peroxide. From an industrial viewpoint, the electricity consumption in the batch UV/H₂O₂ process is about three times higher than the continuous processes confirming that the feeding strategy has a significant effect on the efficiency and operational costs of the UV/H₂O₂ process. The experimental results are encouraging and support the potential of using the continuous operation to improve the efficiency of the UV/H₂O₂ process for the PVA degradation.

Table 7.2. Operating conditions for the UV/H₂O₂ processes; [PVA]_o= 500 mg/L.

Photoreactors System	[H₂O₂]/[PVA] mass ratio	H₂O₂ Residual %	TOC Removal %
Batch with circulation; [PVA]=500 mg/L, one shot of hydrogen peroxide into the holding tank, V=2 L, n _p =2, t=2 h.	0.20	5.26	22.15
	0.78	8.01	34.32
	1.00	17.12	41.54
	5.00	21.04	36.01
	10.00	25.33	30.33
	15.00	30.41	21.95
Fed-batch with circulation; [PVA]=500 mg/L, dripping 4 shots of hydrogen peroxide into the holding tank in stepwise manner, V=2 L, n _p =2, t=2 h.	0.20	0.00	30.28
	0.78	0.88	48.84
	1.00	3.01	64.21
	5.00	5.56	77.07
	10.00	9.24	89.31
	15.00	14.14	68.00
Continuous; [PVA]=500 mg/L, continuous separate streams of polymer feed solution and hydrogen peroxide, F=1.8 L/h, n _p =2.	0.20	0.00	41.39
	0.78	1.16	69.90
	1.00	0.81	94.40

*n_p is number of pumps

Table 7.3. Electric power consumption for the UV/H₂O₂ process.

Item	Electric power (kW)
UV Lamp	0.014
Varistaltic pump for feed introduction	0.075
Peristaltic-pump for H ₂ O ₂ dosage*	0.007

*The peristaltic pump was used for fed-batch (stepwise manner) and continuous systems.

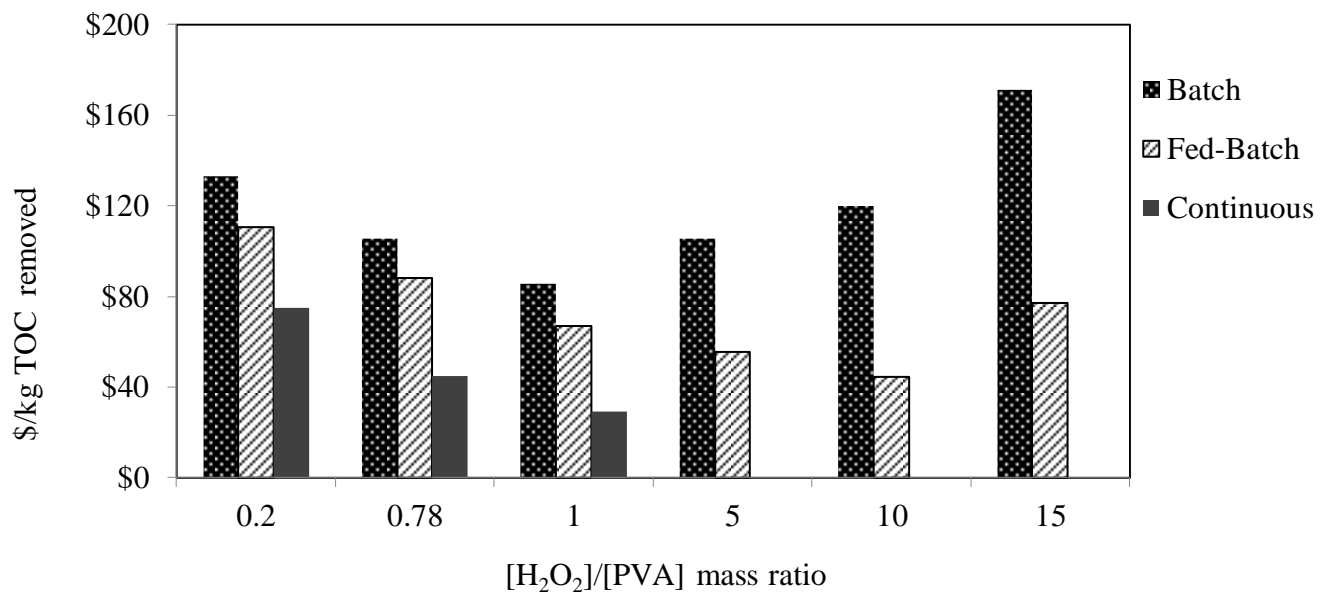


Figure 7.9. Operation costs per kilogram of TOC removed in batch and fed-batch (2 h) and continuous (30.6 min. residence time) UV/ H_2O_2 photoreactors.
 $[PVA]_o = 500 \text{ mg/L}$, $[H_2O_2]/[PVA]$ mass ratio: 0.2, 0.78, 1, 5, 10, and 15.

Chapter 8

CONCLUSIONS AND RECOMMENDATIONS

In this chapter, the main conclusions obtained throughout this study are presented. In addition, recommendations for future work are suggested.

8.1. CONCLUSIONS

A methodical and instrumental investigation has been devised and accomplished throughout this research project. First, a set of experiments were performed using an existing batch UV/H₂O₂ photoreactor system that has been previously used to treat wastewater systems. Using the UV light as the energy source and hydrogen peroxide as the oxidant, the photoreactor process was operated and experimentally tested to degrade a well-known water-soluble polymer (Polyvinyl alcohol) for different hydrogen peroxide concentrations and initial polymer contents in aqueous solutions. These experimental tests were primarily done to determine the feasibility and limitations of the existing UV/H₂O₂ photoreactor when operated in batch and fed-batch modes. The outcome of the first part of this study was very encouraging and led to carry out further experimental and theoretical work for an in-depth understanding of the UV/H₂O₂ process.

As a result, one of the main contributions of the research carried out in this study is the design and implementation of a two UV/H₂O₂ photoreactors that were operated in continuous mode and extensively compared with the performance of a batch and fed-batch reactors.

Therefore, most of the study focused on the innovative technique of feeding strategy to overcome the limitation associated with conventional batch UV/H₂O₂ process.

The main results achieved in this research project are summarized as follows:

1. Achieving a considerable reduction in TOC (up to 94%).
2. Significant decrease in polymer molecular weight (98%).
3. Decreasing hydrogen peroxide consumption (the hydrogen peroxide/polymer mass ratio) by a factor of ten.
4. Achieving a minimal hydrogen peroxide concentration less than 5 mg/L in effluents.
5. Eliminating the additional treatment required for quenching of H₂O₂ residual.
6. Decreasing the UV dosage and energy consumption (up to 70%)

On the basis of economic and environmental considerations, the commercialization of water-soluble polymers will continue to be important in the market. Since commodity products have a relatively short-use lifetime and they end up in the aqueous environment plants; thus creating obvious pollution concerns as they are non-biodegradable to any extent. Therefore, the current need for efficient methods of polymeric wastewater treatment, that can overcome the limitations of the conventional methods, is directing the present project for the development of a new setup, in parallel with some modification on the experimental procedure, to enhance the performance of UV/H₂O₂ process for degrading water-soluble polymers.

The following conclusions can be drawn from this thesis research project:

1. The study has shown that the way of introducing hydrogen peroxide into the UV photoreactor has a considerable impact on the PVA polymer degradation and TOC removal.

2. On treating an aqueous solution containing 500 mg/L PVA of 130 kg/mol for 2 h, TOC removal of 87% was achieved in fed-batch (a stepwise manner) photoreactor at $[H_2O_2]/[PVA]$ mass ratio of 10 but maximum TOC removal of 38 % only was obtained in batch (single shot) photoreactor at $[H_2O_2]/[PVA]$ mass ratio of 1. An increase in the polydispersity index from 1.14 to 4 of the UV-irradiated polymer samples was observed implying an expected breakdown of the polymer chains into shorter-chain molecules. The study proves that the feeding strategy is an important key design of UV/ H_2O_2 process which can drastically modify the structure of the PVA polymer and be a potential practice for the degradation of water-soluble polymers.
3. The experimental results obtained with the batch photoreactor confirmed that the PVA polymer was effectively disintegrated by the oxidant hydrogen peroxide under UV light. A photochemical kinetics mechanism and a chemical kinetic model were developed. Population balance provided an adequate representation of the degradation of PVA polymer in a UV/ H_2O_2 batch process that describes the devolution of number and weight averages molecular weights, the hydrogen peroxide consumption, and the variation of the solution pH. In comparison with previous studies, this model incorporated novel features by accounting for the scavenging effect of hydrogen peroxide as well as the variation of pH, thereby provide a good understanding of the real characterization of UV/ H_2O_2 process and contribute in enhancing the design of industrial processes for the treatment of wastewaters contaminated with water-soluble polymers.
4. An innovative treatment technique with a continuous hydrogen peroxide feeding strategy was designed and applied in order to minimize UV dosage and hydrogen peroxide consumption and residual, while to enhance the process performance. The simultaneous exposure of the

feed stream to continuous flow of H₂O₂ and UV irradiation resulted in a significant reduction in polymer molecular weights and TOC along with the reduction in hydrogen peroxide consumption and residual. Response surface methodology (RSM) involving the Box-Behnken method that was adopted for the experimental design, provided an understanding of the impact of operating variables on the continuous process performance. RSM model consisting of three quadratic equations revealed a good prediction of the TOC removal, the PVA molecular weight, and the hydrogen peroxide residual in the aqueous solution exiting the continuous photoreactor. Experimental analysis showed that the TOC removal varies from 16.11 to 42.70% along with a reduction of the PVA molecular weights ranges between 56.7 and 95.30% at residence time 6.3–18.4 min, inlet PVA solution of 500 – 1500 mg/L.

The interaction between PVA and hydrogen peroxide inlet concentrations was the most significant factor influencing on increasing the PVA degradation in a continuous UV/H₂O₂ process within the range of the operating condition. The optimal operating conditions of the inlet PVA concentration (665 mg/L), the inlet H₂O₂ concentration (560 mg/L), and the feed flow rate (50 mL/min) were found to achieve 37.92% TOC reduction efficiency and a final polymer molecular weight of 3.98 kg/mol after 18.4 min with 3.84 mg/L of hydrogen peroxide residual.

5. The results of the comparative study for the degradation water-soluble polymers in the UV/H₂O₂ processes operated under batch, fed-batch (120-min exposure time), and continuous (30-min residence time) modes showed that the PVA number average molecular weight was reduced from an initial value of 130 kg/mol to 24.9, 20.3, and 2.2 kg/mol corresponding to percent TOC removal of 41.5, 64.2, and 94.4 %, respectively.

The molecular weight distribution (MWD) shows a progressive reduction of the higher molecular weight fractions that was in accordance with the proposed random chains scission mechanism that followed by polymer chain-end scission. Such data shows clearly how hydrogen peroxide feeding strategy and the mode of operation can affect the mechanism of the degradation reactions providing an insight into the photodegradation process.

Finally, the electricity consumption in the continuous UV/H₂O₂ process is about three times less than that in a batch process. Again the results confirm that the feeding strategy has a significant effect on the efficiency and operational cost of the UV/H₂O₂ process.

The continuous UV/H₂O₂ process is a simple, practical, and economical technique that meets stringent environmental standards. Measurements of the MWDs present a framework for interpreting the macromolecular degradation processes and show that bimodal MWDs can evolve during PVA degradation. These results can be used as a guide for the design of industrial continuous UV/H₂O₂ photochemical processes for the removal of water-soluble polymers from industrial wastewater effluents at large scale.

8.2. RECOMMENDATIONS FOR FUTURE WORK

Based on the results achieved in this study, the following topics are suggested for future work. Although this study provides an innovative technique for improvement of UV/H₂O₂ process highlighting the effect of feeding strategy on the polymer degradation by advanced oxidation technologies, there are still some areas for future consideration as follows:

1. To investigate the integration of the UV/H₂O₂ process and biological processes for the complete removal of polymeric wastewater at reduced cost. The UV/H₂O₂ process having no hydrogen peroxide residual in the effluent can safely be employed as a pretreatment method to biological degradation of polymeric wastewater.
2. To investigate the effect of the actual polymeric wastewater, especially from the effluent of textile industry that usually contains a blend of polymers, on the UV/H₂O₂ process performance. In addition, the interaction between polymers in polymer blend has also to be investigated.
3. To extend the dynamic model for different hydrogen peroxide feeding strategies in a continuous photo reactor. Currently the model has the ability to simulate the degradation of PVA polymer in batch recirculating UV/H₂O₂ photoreactor.
4. To design a control system based on instantaneous, on-line, and in-process viscosity measurement instrumentation to provide a continuous monitoring of the degradation process. Manipulating hydrogen peroxide feed according to the viscosity of polymer solution that is directly related to the viscosity average molecular weight of the polymer; also online measurement of hydrogen peroxide in the effluent.

References

- Aarthi T., Shaama M., Madras G. Degradation of water-soluble polymers under combined ultrasonic and ultraviolet radiation. *J. Ind. Eng. Chem. Res.* 46(19): 6204-6210, 2007.
- Alfano O., Cassano A. Scaling-up of photoreactors: applications to advanced oxidation processes. INTRC Publishers. Chapter 7: 229-286, 2009.
- Audenaert W., Callewaert M., Nopens I., Cromphout J., Vanhoucke R., Dumoulin A., Dejans P., Van Hulle S. Full-scale modelling of an ozone reactor for drinking water treatment. *Chem. Eng. J.* 157: 551-557, 2010.
- Beñard A., Darcos V. Fluorescence Versus radioactivity labeling for lab-scale investigation of the fate of water-soluble polymers in wastewater treatment plants. *J. Polym. Environ.* 18(4): 1-9, 2010.
- Bielski B., Cabelli D. Highlights of current research involving superoxide and perhydroxyl radicals in aqueous solutions. *Int. J. Radiat. Biol.* 59(2): 291-319, 1991.
- Bielski B., Cabelli D., Arudi R., Ross A. Reactivity of HO₂/O²⁻ radicals in aqueous solution. *J. Phys. Chem. Ref. Data.* 14: 1041-1051, 1985.
- Bolton J.R., Bircher K.G., Tumas W., Tolman C.A. Figures-of-merit for the technical development and application of advanced oxidation technologies for both electric- and solar-driven systems. *Pure App. Chem.* 73(4): 627-637, 2001.
- Bolton J. Calculation of ultraviolet rate distributions in an annular reactor: significance of refraction and reflection. *Water Res. J.* 34: 3315-3324, 2000.
- Brandrup J., Immergut E., Edmund H., Grulke A., Abe A., Bloch R. *Polymer Handbook*, 4th Edition, Wiley And Sons, 2005.

Bustillo-Lecompte C., Knight M., Mehrvar M. Assessing The Performance Of UV/H₂O₂ As A Pretreatment Process In TOC Removal Of An Actual Petroleum Refinery Wastewater And Its Inhibitory Effects On Activated sludge. Can. J. Chem. Eng. 93(5): 798-807, 2015.

Bustillo-Lecompte C.F., Mehrvar M., Quiñones-Bolaños E. Cost-effectiveness analysis of TOC removal from slaughterhouse wastewater using combined anaerobic aerobic and UV/H₂O₂ processes. J. Environ. Manag. 134: 145-152, 2014.

Buxton G., Greenstock C., Helman W., Ross A. Critical review of rate constants for reactions of hydrated electrons, hydrogen atoms and hydroxyl radicals ('OH/'O) in aqueous solution. Phys. Chem. Ref. Data.17: 513-886, 1988.

Chen Y., Sun Z., Yang Y., Ke Q. Heterogeneous photocatalytic oxidation of polyvinyl alcohol in water. Photochem. Photobiol. 142(1): 85-89, 2001.

Christensen H., Sehested K., Corfitzen H. Reactions of hydroxyl radicals with hydrogen peroxide at ambient and elevated temperatures. J. Phys. Chem. 86:1588-1590, 1982.

Ciner F., Akal Solmaz, S.K., Yonar, T., Ustun, G.E. Treatability studies on wastewater from textile dyeing factories in Bursa, Turkey. Int. J. Environ. Pollut. 19, 403-407, 2003.

Costa N., Lourenço, J. A comparative study of multi-response optimization criteria working ability. Chemometr. Intell. Lab.138, 171–177, 2014.

Crittenden J.C., Hu S., Hand D.W., Green S. A kinetic model for UV/H₂O₂ process in a completely mixed batch reactor. Water Res. J. 33: 2315-2328, 1999.

De Sena R., Moreira R., José H. Assessment of polyacrylamide degradation using advanced oxidation processes and ferrate oxidation. Chem. Eng. Commun. 200(2): 235-252, 2013.

Edalatmanesh M., Dhib R., Mehrvar M. Kinetic modeling of aqueous phenol degradation by UV/H₂O₂ process. *Int. J. Chem. Kinet.* 40(1): 34-43, 2008a.

Edalatmanesh M., Mehrvar M., Dhib R. Optimization of phenol degradation in a combined photochemical-biological wastewater treatment system. *Chem. Eng. Res. Des.* 86(11): 1243-1252, 2008b.

Elliot A., Buxton G. Temperature dependence of the reactions OH + O²⁻ and OH + HO₂ in water up to 200 °C. *J. Chem. Soc.* 88: 2465-2470, 1992.

Florea M. New use of size exclusion chromatography in kinetics of mechanical degradation of polymers in solution. *J. Appl. Poly. Sci.* 50: 2039, 1993.

Getoff N. Radiation-induced degradation of water pollutants-state of the art. *Radiat. Phys. Chem.* 47, 581-593, 1996.

Ghafoori S., Mehrvar M., Chan P. Free-radical-induced degradation of aqueous polyethylene oxide by UV/H₂O₂: experimental design, reaction mechanisms, and kinetic modeling. *J. Ind. Eng. Chem. Res.* 51: 14980-14993, 2012a.

Ghafoori S., Mehrvar M., Chan P. Kinetic study of photodegradation of water-soluble polymers. *Iranian Polym. J.* 21: 869-876, 2012.

Ghafoori S., Mehrvar M., Chan P. Photoreactor scale-up for degradation of polyvinyl alcohol in aqueous solution using UV/H₂O₂ process. *Chem. Eng. J.* 245: 133-142, 2014.

Hamad D., Mehrvar M., Dhib R. Experimental study of polyvinyl alcohol degradation in aqueous solution by UV/H₂O₂ process. *Polym. Degrad. Stab.* 103: 75-82, 2014.

Hamad D., Dhib R., Mehrvar M. Degradation of aqueous polyvinyl alcohol in a continuous UV/H₂O₂ photoreactor: Experimental and statistical analysis. *J. Polym. Environ.* (submitted April 2015a).

Hamad D., Mehrvar M., Dhib R. Photochemical kinetic modeling of polyvinyl alcohol degradation by UV/H₂O₂ process. *Polym. Degrad. Stab.* (submitted August 2015b).

Hamad D., Dhib R., Mehrvar M. Effects of hydrogen peroxide feeding strategies on the photochemical degradation of water soluble polymers. (submitted to *Chem. Eng. J* September 2015c).

Ito S., Okada Y., Hirai H., Nishida T. Degradation of polyacrylic acids with phenolic side-chains by manganese peroxidase from white rot fungi, *J. Polym. Environ.* 13(4): 357-363, 2005.

Jacob S., Dranoff J. Light intensity profiles in a perfectly mixed photoreactor. *AIChE J.* 16: 359-363, 1970.

Kaczmarek H., Kaminska A., Swiatek M., Rabek J. F. Photo-oxidative degradation of some water-soluble polymers in the presence of accelerating agents. *Angew. Makromol. Chem.* 4622: 109-121, 1998.

Kang S., Liao C., Po S. Decolorization of textile wastewater by photo-Fenton oxidation technology. *Chemosphere.* 41: 1287-1294, 2000.

Kavanaugh M., Chowdhury Z., Kommineni S. Removal of MTBE with advanced oxidation processes. IWA Publishers, Inc. Chapter 3: 111-207, 2004.

Khemani K., Scholz C. Degradable polymers and materials: Principles and practice. New York: Nova Science, 1981.

Kim S., Kim T., Park C., Shin E. Electrochemical oxidation of polyvinyl alcohol using a RuO₂/Ti anode. *Desalination.* 155(1): 49-57, 2003.

Koda S., Yamashita K., Matsumoto K., Nomura H. Characterization of polyvinylchloride by means of sound velocity and longitudinal modulus measurements. Japanese J. Appl. Phys. Part 1. 32(5 B): 2234-2237, 1993.

Kodera Y., McCoy B. Distribution kinetics of radical mechanisms: Reversible polymer decomposition. AIChE J. 3205-3214, 1997.

Koppenol W., Butler J., Van Leeuwen J. The Haber–Weiss cycle. Photochem. Photobio. 28: 655-658, 1978.

Kosaka K., Yamada H., Matsui S., Echigo S., Shishida K. Comparison among the methods for hydrogen peroxide measurements to evaluate advanced oxidation processes: application of a spectrophotometric method using copper (II) ion and 2,9-dimethyl-1,10-phenanthroline. Environ. Sci. Technol. 32: 3821–3824, 1998.

Kostoglou M. Mathematical analysis of polymer degradation with chain-end scission. Chem. Eng. Sci. 55(13): 2507-2513, 2000.

Liao C., Gurol M. Chemical oxidation by photolytic decomposition of hydrogen peroxide. Environ. Sci. Technol. 29: 3007-3014, 1995.

Linden K., Sharpless C., Andrews S., Atasi K., Koratogere V., Stefan M., Suffet I. Innovative UV Technologies To Oxidize Organic And Organoleptic Chemicals. IWA Publishing, London, 2005.

Liua W., Andrewsa S. A., Stefan M. I., Bolton J. R. Optimal methods for quenching H₂O₂ residuals prior to UFC testing. Water Res. 37:3697–3703, 2003.

Lu M., Wu X., Wei X. Chemical degradation of polyacrylamide by advanced oxidation processes. Environ. Technol. 33(9): 1021-1028, 2012.

Madras G. Molecular weight effect on the dynamics of polystyrene degradation. Ind. Eng. Chem. Res. 36(6): 2019-2024, 1997.

Madras G., McCoy B. Oxidative degradation kinetics of polystyrene in solution. Chem. Eng. Sci. 52(16): 2707-2713, 1997.

Madras G., Smith S., McCoy B. Degradation of poly (methyl methacrylate) in solution. Eng. Chem. Res. 35(6): 1795-1800, 1996.

Malik M., Ilyas M., Khan Z. Kinetics of permanganate oxidation of synthetic macromolecule poly(vinyl alcohol). Indian J. Chem. 48A: 189-193, 2009.

McCoy B., Madras G. Degradation kinetics of polymers in solution: Dynamics of molecular weight distributions. AIChE J. 43(3): 802-810, 1997.

McCoy B. Continuous kinetics of cracking reactions: Thermolysis and pyrolysis. Chem. Eng. Sci. 51(11): 2903-2908, 1996.

McCoy B., Wang M. Continuous-mixture fragmentation kinetics: Particle size reduction and molecular cracking. Chem. Eng. Sci. 49(22): 3773-3785, 1994.

Mehrvar M., Anderson W.A., And Moo-Young M. Photocatalytic degradation of aqueous organic solvents in the presence of hydroxyl radical scavengers, Int. J. Photoenergy. 3(4): 187-191, 2001.

Mehrvar M., Tabrizi B. Combined photochemical and biological processes for the treatment of linear alkylbenzene sulfonate in water. Environ. Sci. Health. Part A. 41(4): 581-597, 2006.

Mehrvar M., Tabrizi B. Combined photochemical and biological processes for the treatment of linear alkylbenzene sulfonate in water. J. Environ. Sci. Health. Part A. Toxic/Hazardous Substances and Environmental Engineering. 41(4): 581-597, 2006.

Mehrvar M., Tabrizi G.B., Abdel-Jabbar N. Effects of pilot-plant photochemical pretreatment (UV/H₂O₂) on the biodegradability of aqueous linear alkylbenzene sulfonate (LAS), Int. J. Photoenergy. 7(4): 169-174, 2005.

Metha K., Madras G. Dynamics of molecular weight distributions for polymer scission. Am. Inst. Chem. Eng. J. 47: 2539-2545, 2001.

Modarress H., Nia M.M., Mostafa R. Viscosity measurements and modelling of aqueous polyvinyl alcohol mixtures. Iranian Polym. J. 14 (2), 181-184, 2005.

Mohajerani M., Mehrvar M., Ein-Mozaffari F. An overview of the integration of advanced oxidation technologies and other processes for water and wastewater treatment. Int. J. Eng. 3: 120-146, 2009.

Mohajerani M., Mehrvar M., Ein-Mozaffari F. Recent achievements in combination of ultrasonolysis and other advanced oxidation processes for wastewater treatment. Int. J. Chem. React. Eng. 8(R2): 1-78, 2010.

Moulaya S., Boukherissab M., Abdounea F., Benabdelmoumene F. Low molecular weight poly(acrylic acid) as a salt scaling inhibitor in oilfield operations. J. Iranian Chem. Soc. 2(3): 212-219, 2005.

Nair A., Makwana A., Ahmed M. The use of response surface methodology for modeling and analysis of water and wastewater treatment processes: A review. Water Sci. Technol. 69 (3), 464-478, 2014.

Nakamiya K., Ooi T., Kinoshita S. Degradation of synthetic water-soluble polymers by hydroquinone peroxidase. J. Ferment. Bioengin. 84: 213-218, 1997.

Nigam, Abhash, Fake, Dean M., Klein, Michael T. Simple approximate rate law for both short and long chain Rice Herzfeld kinetics. *AIChE J.* 40(5): 908-910, 1994.

Nita L., Chiriac A., Popescu C., Neamtu I., Alecu L. Possibilities for poly(aspartic acid) preparation as biodegradable compound. *J. Optoelectron. Adv. Mater.* 8(2): 663-666, 2006.

Odian G. *Principle of Polymerization*, 3rd Edition. Wiley. New York, 1991.

Othmer K. *Encyclopaedia of Chemical Technology*, 3rd Edition. *Vinyl Polymers*, John Wiley and Sons. New York, 1984.

Paik Y., Simon E., Swift G. A review of synthetic approaches to biodegradable polymeric carboxylic acids for detergent applications. *Adv. Chem.* 248: 79-98, 1996.

Perry R., Green D., Maloney J. *Perry's Chemical Engineer's Handbook*. McGraw-Hill, New York, 1981.

Poyatos J., Munio M., Almecija M., Torres J., Hontario E., Osorio F. Advanced oxidation process: State of art. *Water. Air Soil Pollute.* 205: 187-204, 2010.

Premraj R., Mukesh D. Biodegradation of polymers. *Indian J. Biotech.* 4:186-193, 2004.

Price G. J., Smith P. F. Ultrasonic degradation of polymer solutions: 1. Polystyrene Revisited. *Polym. Inf.* 24: 159, 1991.

Ranby B. Photodegradation and photo-oxidation of synthetic polymers. *J. Anal. Appl. Pyrolysis.* 15: 237-247, 1989.

Rangaraj A., Vangani V., Rakshit A. Synthesis and characterization of some water-soluble polymers. *J. Appl. Polym. Sci.* 66(1): 45-56, 1997.

Rezaee R., Maleki A., Jafari A., Mazloomi S., Zandsalimi Y., Mahvi A. Application of response surface methodology for optimization of natural organic matter degradation by UV/H₂O₂ advanced oxidation process. *J. Environ. Health Sci. Eng.* 12, 67-75, 2014.

Romero R., Alfano O., Cassano A. Cylindrical photocatalytic reactors: radiation absorption and scattering effects produced by suspended fine particles in an annular space. *Ind. Eng. Chem. Res.* 36: 3094-3109, 1997.

Rudin A. Elements of Polymer Science & Engineering, 2nd Edition, Academic Press, 1998.

Santos L.C., Poli A.L., Cavalheiro C.C.S., Neumann M.G. The UV/H₂O₂ photodegradation of poly (ethylene glycol) and model compounds. *J. Braz. Chem. Soc.* 20: 1467-1472, 2009.

Schulze-Hennings U., Pinnekamp J. Response surface method for the optimization of micro pollutant removal in municipal wastewater treatment plant effluent with the UV/H₂O₂ advanced oxidation process. *Water Sci. Technol.* 67 (9), 2075-2082, 2013.

Scott J., Ollis D. Integration of chemical and biological oxidation processes for water treatment: review and recommendations. *Environ. Prog.* 14(2): 88-103, 1995.

Sezgi A., Cha S., Smith J., McCoy B. Polyethylene pyrolysis: theory and experiments for molecular weight distribution kinetics. *Ind. Eng. Chem. Res.* 37(7): 2582-2591, 1998.

Shonberger H., Baumann A., Keller W. Study of microbial degradation of polyvinyl alcohol (PVA) in wastewater treatment plants. *Am. Dyest. Report.* 18(86): 9-18, 1997.

Shukla N., Darabonia N., Madras G. Ultrasonic degradation of poly (acrylic acid). *J. Appl. Polym. Sci.* 112(2): 991-997, 2009.

- Smagala T., McCoy B. Mechanisms and approximations in macromolecular reactions: reversible initiation, chain scission, and hydrogen abstraction. *Ind. Eng. Chem. Res.* 42: 2461-2469, 2003.
- Solaro R., Corti A., Chiellini E. Biodegradation of poly(vinyl alcohol) with different molecular weights and degree of hydrolysis. *Polym. Adv. Technol.* 11: 873-878, 2000.
- Sonntag C. Free-radical-induced chain scission and cross-linking of polymers in aqueous solution - An overview. *Radiat. Phys. Chem.* 67: 353-359, 2003.
- Sonntag C., Bothea E., Ulanski P., Adhikarya A. Radical transfer reactions in polymers radiation. *Phys. Chem.* 55: 599-603, 1999.
- Staggs J. Modeling random scission of linear polymers. *Polym. Degrad. Stab.* 76(1): 37-44, 2002.
- Stefan M., Hoy A., Bolton J. Kinetics and mechanism of the degradation and mineralization of acetone in dilute aqueous solution sensitized by the UV photolysis of hydrogen peroxide. *Environ. Sci. Technol.* 30: 2382-2390, 1996.
- Sterling J., McCoy B. Distribution kinetics of thermolytic macromolecular reactions. *AIChE J.* 47: 2289-2303, 2001.
- Sun W., Tian J., Chen L., He S., Wang J. Improvement of biodegradability of PVA-containing wastewater by ionizing radiation pre-treatment. *Environ. Sci. Pollut. Res.* 19: 3178-3184, 2012.
- Swaim P., Royce A., Smith T., Maloney T., Ehlen D., Carter B. Effectiveness of UV advanced oxidation for destruction of micro-pollutants. Proceedings of the World Congress on Ozone and Ultraviolet Technologies. IOA/IUVA. Los Angeles, USA, 2007.

Swift G. Requirements for biodegradable water-soluble polymers. *Polym. Degrad. Stab.* 59: 19-24, 1997.

Swift G., Creamer M., Wei X., Yocom K. Water-soluble biodegradable polymers: Synthetic or natural based raw materials? *Macromol. Symp.* 130: 379-391, 1998.

Tabrizi G., Mehrvar M. J. Integration of advanced oxidation technologies and biological processes: Recent developments, trends, and advances. *Environ. Sci. Heal. A* 39(11-12): 3029-3081, 2004.

Tarr M.A. *Chemical Degradation Methods for Wastes and Pollutants: Environmental and Industrial Applications*. New York, NY: Marcel Dekker, 2003.

Tayal A., Khan S. Degradation of a water-soluble polymer: Molecular weight changes and chain scission characteristics. *Macromol.* 33: 9488-9493, 2000.

Vinu R., Madras G. Photocatalytic degradation of polyacrylamide-coacrylic acid. *J. Phys. Chem.* 112: 8928-8935, 2008.

Watanabea M., Kawaib F. Numerical Simulation for Enzymatic Degradation of polyvinyl alcohol. *Polym. Degrad. Stab.* 81: 393-399, 2003.

Weast R., Astle M. *Handbook of Data on Organic Compounds, I and II*. Boca Raton, Florida. CRC Press Inc., 1985.

Weinstein J., Bielski B. Kinetics of the interaction of HO₂ and O²⁻ radicals with hydrogen peroxide: The Haber-Weiss Reaction. *Am. Chem. Soc.* 101: 58-62, 1979.

Whittmann G., Horvath I., Dombi A. UV-induced decomposition of ozone and hydrogen peroxide in the aqueous phase at pH 2-7. *Ozone Sci. Eng.* 24: 281-291, 2002.

Won L., Han S., Choi J., Ghim H., Yoo S., Lee J., Hong S. Preparation of high molecular weight polyvinyl alcohol with high yield using low-temperature solution polymerization of vinylacetate. *J. Appl. Polym. Sci.* 80(7): 1003-1012, 2001.

Xei L., Yue P., Bossmann S., Gob S., Braun A. Oxidative degradation of polyvinyl alcohol by the photochemically enhanced Fenton reaction. *J. Photochem. Photobiol.* 116: 159-166, 1998.

Zhang S.J., Yu H.Q. Radiation-induced degradation of polyvinyl alcohol in aqueous solutions. *Water Res.* 38: 309-316, 2004.

Zhang Y., Rong W., Fu Y., Ma X. Photocatalytic degradation of polyvinyl alcohol on pt/TiO₂ With Fenton Reagent. *J. Polym. Environ.* 19: 966-970, 2011.

LIST OF APPENDICES

APPENDIX A: Calibration Curves

TOC Calibration Curve

The TOC was measured by a Tekmar Dohrmann's Apollo 9000 TOC analyzer. TOC Analyzer is directly and specifically measures the carbon dioxide generated by the oxidation of the organic carbon in the sample. Any potential interference is removed by in-line scrubbers or filters as the sample gas is swept to the detector. The TOC standards employed for TOC calibration was KPH. The TOC standard calibration analysis was carried out using the working standard solutions (10, 25, 50, 100, 250, 500, 750, 1000 ppm). The steps during the TOC analysis (Apollo 9000 TOC Analyzer Operation Manual, 2009) are described as follows:

Inorganic Carbon (IC) detection: 20% phosphoric acid was added to lower the pH so that inorganic carbon was sparged off as CO₂. This was measured to get IC content and to ensure that it was not carried over into the TOC.

Sampling: Samples were injected into the analyzer with the help of an automated syringe from the sampling bottle. The sample injection valve automatically selects the appropriate sample volume for the optimum measuring range.

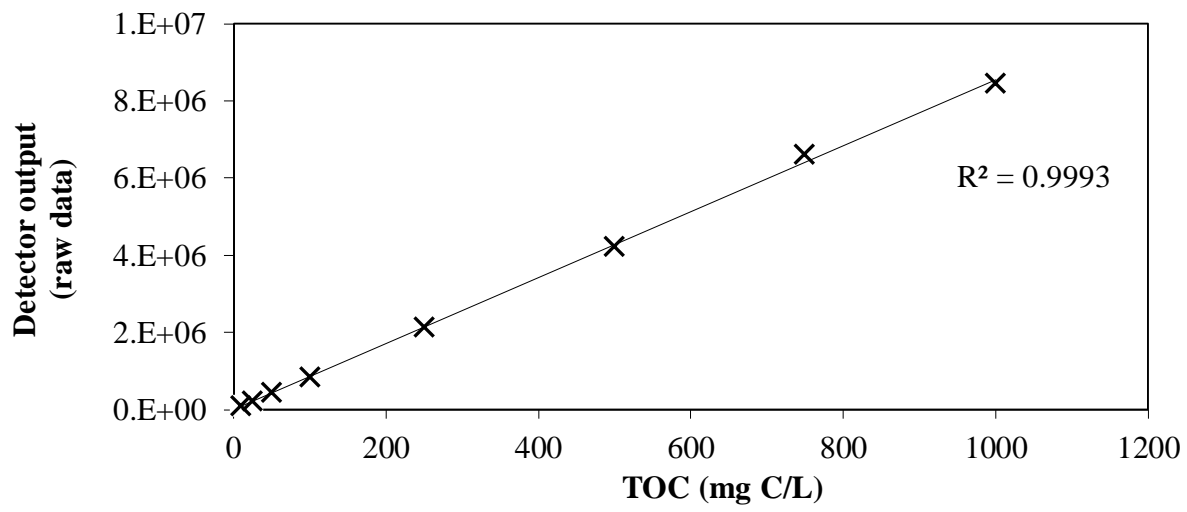
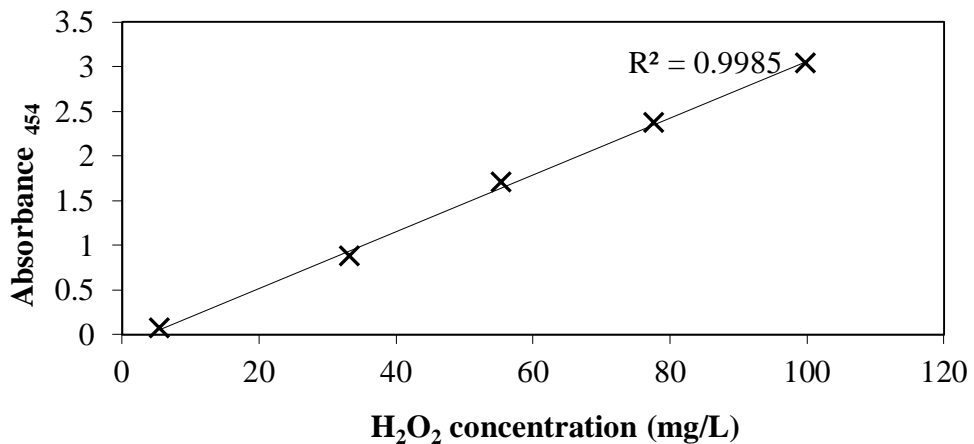


Figure A.1. Calibration curve for measuring total organic carbon by TOC analyzer, plotted for output raw data from the detector versus the amount of organic carbon present, TOC range of 1-1,000 mgC/L.

Hydrogen Peroxide Calibration Curves

The concentration of hydrogen peroxide was determined using DMP method by UV-vis spectrophotometer (Ultrospec 1100 pro, Amersham Biosciences) at 454 nm as discussed in Section 3.6.3.

(a)



(b)

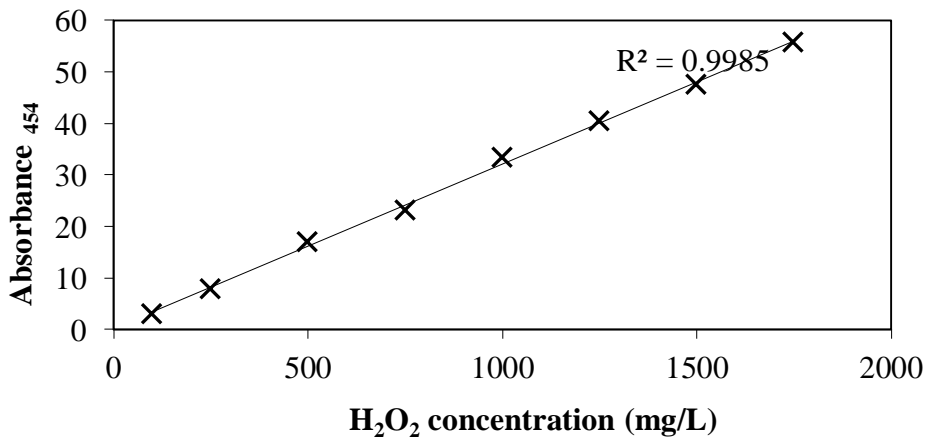


Figure A.2. Calibration curve for determination of hydrogen peroxide concentration based on DMP method; concentration range: (a) 5 -100mg/L, (b) 100-1750 mg/L.

PVA Absorptivity Calibration Curve

The molar extinction of PVA was determined by measuring the absorbance of several concentrations of the PVA in distilled water by means of a spectrophotometer. The spectrophotometer used was Ultrospec 1100 *pro* UV-Visible Spectrophotometer, with the ability to measure the absorbance, percent transmission, and concentration values (discussed in Section 3.6.5).

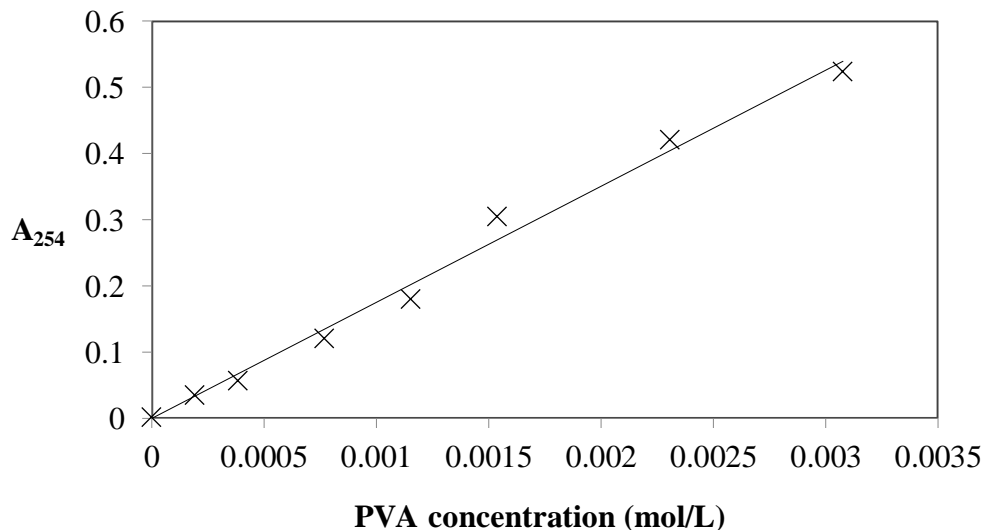


Figure A.3. Absorptivity of PVA at 254 nm by spectrophotometer; PVA concentration range 25-500 mg/L.

APPENDIX B: UV Dosage Calculation

UV Dose (mJ/cm^2) = Intensity \times time

Intensity (UV-C lamp, 254 nm) = 17,900 $\mu\text{W/cm}^2$

Residence time = photoreactor volume/volumetric flow rate

Output power = Intensity \times area

Effective surface area of the lamp = 200 cm^2

Output power = Intensity \times area = 3.6 W

Input power = 14 W (UV-C lamp, 254 nm, model LP4130, Siemens)

Lamp efficiency = 26%

Power density = power/arc length = 0.18 W/cm

Radiometer measurements

The light intensity was measured using Spectroline Digital Radiometer (DRC-100X) (Section 3.6.7).

Table A.1 Light intensity of UV-C lamp (254 nm, model LP4130, Siemens).

For the period of September 2012- December 2013

Date	Reading ($\mu\text{W/cm}^2$)
September 2012	17,278
October 2012	17,597
December 2012	16,901
March 2013	16,800
May 2013	16,500
August 2013	16,002
October 2013	12,360
December 2013	12,100
January 2014*	17,900
March 2014	17,970
May 2014	17,100
August 2014	16,800
October 2014	16,500
December 2014	16,088

*The UV lamp has been replaced with a new one for the period of Jan 2014 -December 2014

APPENDIX C: Error Analysis

Table C.1. Sample of error bars calculation for fed-batch system (data are represented in Figure 4.1, $[PVA]_0 = 500 \text{ mg/L}$).

$[H_2O_2]/[PVA]$ mass ratio	TOC removal %			Mean TOC removal %	Standard deviation % (σ)
	Replicate#1*	Replicate#2*	Replicate#3*		
1	59.65	58.932	57.98	58.64	0.84
5	70.41	72.52	71.39	71.44	1.05
10	87.19	87.89	86.4	87.16	0.74
15	65.13	62.06	62.99	63.73	1.55

The experiments were conducted three times with three replicates in measurements as discussed Section 3.7.

*Each TOC value for each replicate has been measured three times by TOC analyzer, the mean value is provided.

$$\sigma = \sqrt{\frac{1}{n' - 1} \sum_{n'=1}^3 (x - \mu)^2}$$

Where n' is number of data point of the sample, x is the TOC reading, μ is the mean value

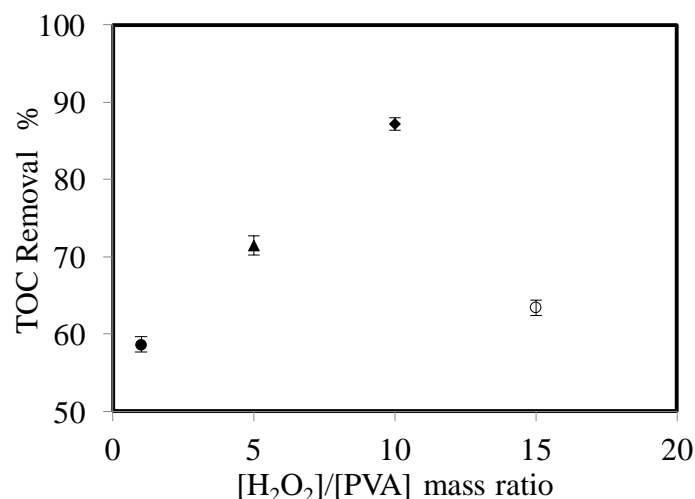


Figure C.1. TOC removal versus $[H_2O_2]/[PVA]$ mass ratio. $[PVA]_0 = 500 \text{ mg/L}$, H_2O_2 dripped into the system, under fed-batch mode of operation.